台灣農業研究
JOURNAL OF TAIWAN AGRICULTURAL RESEARCH
Vol.73 No.2 2024

Research Articles

ISSN 2790-086X

Published by Taiwan Agricultural Research Institute, Ministry of Agriculture

台灣農業研究 JOURNAL OF TAIWAN AGRICULTURAL RESEARCH Vol.73 No.2 2024

ISSN 2790-086X
DOI:10.6156/JTAR

台灣農業研究
JOURNAL OF TAIWAN AGRICULTURAL RESEARCH
Vol.73 No.2 2024

研究報告

農業部農業試驗所出版

Vol.73 No.2 2024

《台灣農業研究》編審會

台灣農業研究

第七十三卷　第二期　　中華民國一一三年六月三十日

出版者　農業部農業試驗所
發行人　林學詩
總編輯　石憲宗
地址　413008 臺中市霧峰區萬豐里中正路 189 號
網址　https://www.tari.gov.tw/jtar
電話　(04)2331-7236
E-mail　jtar@tari.gov.tw
線上投審稿系統　https://www.ipress.tw/J0042
台灣農業研究之稿約格式內容，詳自農業部農業試驗所首頁下列路徑下載：文宣出版 > 台灣農業研究 > 出版品稿約

編印　華藝學術出版部
地址　234634 新北市永和區成功路一段 80 號 18 樓
電話　(02)2926-6006
E-mail　press@airiti.com

定價　新臺幣一七五元
展售門市　1. 國家書店 / 104472 臺北市松江路 209 號 1 樓 / 電話 : (02)2518-0207
國家網路書店 http://www.govbooks.com.tw
2. 五南文化廣場 / 400002 臺中市中山路 6 號 / 電話 : (04)2226-0330

台灣農業研究 (J. Taiwan Agric. Res.) 73(2):71–87 (2024)
https://doi.org/10.6156/JTAR.202406_73(2).0001

Research Article

Taxonomic Review of the Genus *Asiophrida* Medvedev, 1999 in Taiwan (Insecta: Coleoptera: Chrysomelidae: Galerucinae: Alticini), with Notes on Biology

Chi-Feng Lee[1,*], Su-Fang Yu[2], and Mei-Hua Tsou[2]

Abstract

Lee, C. F., S. F. Yu, and M. H. Tsou. 2024. Taxonomic review of the genus *Asiophrida* Medvedev, 1999 in Taiwan (Insecta: Coleoptera: Chrysomelidae: Galerucinae: Alticini), with notes on biology. J. Taiwan Agric. Res. 73(2):71–87.

Asiophrida Medvedev and *Podontia* Dalman belonging to the *Blepharida*-genus group could be found in Taiwan. *Asiophrida scaphoides* (Baly) and *A. spectabilis* (Baly) are redescribed and the illustrations of the penises, gonocoxae, spermathecae, abdominal ventrites VIII in females, and tarsomres I–III and the abdominal ventrites V of both sexes are provided. Detailed biological information, including larval and adult feeding behaviors, host plants, and life cycles is provided. Lectotypes are designated for *Podontia scaphoides* Baly, 1865, *Ophrida binduta* Maulik, 1926, and *P. spectabilis* Baly, 1862.

Key words: Flea beetles, Taxonomy, Anacardiaceae, *Rhus succedanea* var. *succedanea*, *Rhus chinensis* var. *roxburghii*.

INTRODUCTION

The genus *Asiophrida* Medvedev includes large-sized species within the *Blepharida*-genus group. Members of the group are recognized easily by the following combination of characters: emarginate anterior margin of the metatibial apex; elongate-oval eye shape, converging dorsally (except *Podontia*); the convex, chrysomeline appearance of the body; *Blepharida* morpho-group form of the hind femoral spring; and closed procoxal cavities in adults. These genera are also well defined by their biology, especially their shared host plant families, Anacardiaceae and Burseraceae, and their larval feeding habits (external leaf-feeding) (Furth & Lee 2000). Genera of the Oriental region were revised by Medvedev (1999), and 3 new genera were described: *Blepharella*, *Furthia*, and *Asiophrida*. *Asiophrida* comprises 18 species, most of which were originally grouped in *Ophrida* Chapuis. Two of these, *O. scaphoides* (Baly, 1865) and *O. spectabilis* (Baly, 1862), were recorded from Taiwan. Medvedev's definition of *Asiophrida* in a Russian journal is insufficiently detailed, and a number of subsequent papers overlooked or did not follow his nomenclatural acts, including Lee & An (2001), Park & Lee (2001), Lee & Cho (2006), Lee & Cheng (2007), Zhang & Yang (2008), and Aston (2009).

Both *Asiophrida scaphoides* and *A. spectabilis* were described from North China and were recorded from Taiwan during the 1930s (see below). They were briefly redescribed by Kimoto & Takizawa (1997) and Lee & Cheng (2007). In the current study, we provide additional infor-

Received: January 14, 2024; Accepted: February 17, 2024.
* Corresponding author, e-mail: chifeng@tari.gov.tw
[1] Contract Research Fellow, Applied Zoology Division, Taiwan Agricultural Research Institute, Taichung City, Taiwan, ROC.
[2] Citizen Scientists, Taipei, Taiwan, ROC.

mation regarding generic delimits and species identities of both species and describe their feeding biology and life cycles in Taiwan.

MATERIALS AND METHODS

For rearing studies, larvae were placed in small glass containers (diameter 142 mm × height 50 mm) with cuttings from host plants. When mature larvae began searching for pupation sites, they were transferred to smaller plastic containers (diameter 90 mm × height 57 mm) filled with moist soil to about 80% of container volume.

We examined morphology of over 200 dry-mounted adult specimens. For delimiting the variability of diagnostic characters, at least one pair from each locality was examined. Length was measured from the anterior margin of the eye to the elytral apex, and width at the greatest width of the elytra. Type specimens available for study and voucher specimens were deposited at The Natural History Museum, London, UK (BMNH), the National Museum of Natural Science, Taichung, Taiwan (NMNS), and the Applied Zoology Division, Taiwan Agricultural Research Institute, Taichung, Taiwan (TARI). Terminology of the grooves on pronota follows Medvedev (1999).

Exact label data are cited for all type specimens of described species; a double slash (//) divides the data on different labels and a single slash (/) divides the data in different rows. Other comments and remarks are in square brackets: [p]- preceding data are printed, [h]- preceding data are handwritten, [w]- white label, and [b]- blue label.

RESULTS

Genus *Asiophrida* Medvedev

Asiophrida Medvedev, 1999:180 (type species: *Ophrida marmorea* Wiedemann, 1819); Löbl & Smetana 2011:51 (catalogue).

Diagnosis. Pronotum (Fig. 1A) with anterolateral area (AL) centrally depressed, delimited by longitudinal (LAL) and transverse (TAL) punctures; LAL basally connecting with longitudinal punctures (AAL); basal margin with longitudinal lateral grooves (LG); central longitudinal line (CL) reduced except basally; additional groove (PG) near lateral margin behind middle. Prosternal process widely rounded. Mesoventrite (Fig. 1B) with saddle-like process for reception of metasternal process. Hind femora with angular processes at posterior margins near apices. Claws bifid. Tarsomeres I of front and middle legs more swollen in males than in females.

Remarks. Adults of *Asiophrida* differ from those of *Podontia* (Lee & Yu 2021) by their pronotal LAL, TAL, and AAL consisted of punctures (lacking punctures in *Podontia*), widely rounded prosternal process (bifurcate prosternal process in *Podontia*), basal margin of at least abdominal ventrite V in males expanded posteriorly (basal margins of abdominal ventrites not modified in males of *Podontia*), posterior margin of hind tibia smooth and without angular process (posterior margin of hind tibia with one angular process in *Podontia*), spermatheca with spermathecal duct and gland (lacking spermathecal duct and gland in *Podontia*), receptacle apically connected with spermathecal duct (receptacle subapically connected with spermathecal duct), gonocoxae well developed, lobe-like (gonocoxae less developed, usually consisted of one process with dense setae in *Podontia*). Immature stages of *Asiophrida* also display significant differences from those of *Podontia*: egg mass covered by faecal material (egg mass exposed in *Podontia*), old instar larvae dark brown or purple (old instar larvae yellow in *Podontia*).

Asiophrida scaphoides (Baly)

Podontia scaphoides Baly, 1865:430 (China); Gemminger & Harold 1876:3522 (catalogue).

Ophrida scaphoides: Miwa 1931:192 (Taiwan); Chen 1933:216 (Vietnam; key); Chen 1934:271 (redescription; China: Gansu, Jiangsu, Zhejiang, Sichuan, Yunnan, Guizhou); Chûjô 1935:465 (Taiwan); Gressitt & Kimoto

1963:787 (China: Hubei, Guangdong); Kimoto 1970:214 (Taiwan); Kimoto 1987:191 (Taiwan); Kimoto 1989:262 (Taiwan); Kimoto 1991:19 (Taiwan); Takizawa *et al*. 1995:14 (Taiwan); Kimoto & Takizawa 1997:519 (larval morphology, host plant); Kimoto 2000:227 (Thailand); Lee & Cheng 2007:142 (host plant); Aston 2009:4 (China: Hong Kong).

Ophrida binduta Maulik, 1926:233 (India); synonymized by Scherer (1969). **Synonym confirmed.**

Asiophrida scaphoides: Medvedev 1999: 182; Löbl & Smetana 2011:51 (catalogue); Yang *et al*. 2015:354 (China; catalogue).

Types. *Podontia scaphoides* (Figs. 2A–D). Lectotype ♀ (BMNH), here designated to preserve stability of nomenclature since synonyms exist, labeled: "Type / H. T [p, w, circle label with red border] // N. China [h, w] // Baly Coll. [p, w] // SYN- / TYPE [p, w, circle label with blue border] // *Podontia* / *scaphoides* / Baly / N. China [h, b] // Type [h, underside of the previous card] // MNBH(E) / #1024879 [p, w]". Paralectotype: 1♂ (BMNH): "Baly Coll. [p, w] // SYN- / TYPE [p, w, circle label with blue border]".

Ophrida binduta (Figs. 2E–H). Lectotype ♀ (BMNH), here designated to preserve stability of nomenclature since synonyms exist, labeled: "Type [p, w, circle label with red border] // Assam. / W. F. Badgley. / 1906—185. [p, w] // *Ophrida* / *binduta*, M. [h] / Det. Maulik. [p] / Type. 1925 [h, w]". There should be 3 syntypes based on the original description, but only one was found at the BMNH.

Specimens examined (*n* = 136). CHINA. Fujian: 1♂ (BMNH), Foochow (= Fuzhou, 福州), 1923, leg. C. R. Kallogg; **Guangxi:** 1♀ (TARI), Dayaoshan (大瑤山), 17.VI.2016, leg. I. T. Zhao; 1♂ (TARI), same but with "25.VII.2016"; 1♀ (TARI), same but with "14.IX.2017"; 1♀ (TARI), Laoshan Forest Farm (老山林場), 9.IX. 2020, leg. I. T. Zhao; **Sichuan:** 3♀ (BMNH), Gongga Shan mts. (貢嘎山), 14–19.VI.1999, leg. V. Siniaev & A. Plutenko; **Yunnan:** 2♀ (TARI), Luteshan (綠德山), 10.V.2019, leg. Y. T. Wang; 1♂ (TARI), Wudian (武甸), 20.IX.2018, leg. Y. T. Wang; **LAOS. Hua Phan:** 3♂, 4♀ (BMNH), Ban Saleui, Phou Pan (Mt.), 3–30. IV.2014, leg. C. Holzschuh; **TAIWAN. Chiayi:** 1♂, 2♀ (NMNS), Tapu (大埔), 25.III.1998, leg. W. T. Yang; **Hsinchu:** 2♂ (TARI), 1♀ (BMNH), Shinchiku (= Hsinchu, 新竹), 1–30.VII.1918, leg. J. Sonan & K. Miyake; 1♀ (TARI), Tahunshan (大混山), 24.II.2009, leg. M. H. Tsou; 3♂ (TARI), same but with "1.III.2009"; 1♀ (TARI), Talu trail (大鹿林道), 21.V.2011, leg. Y. L. Lin; 1♀ (TARI), same locality, 16. II.2023, leg. Y. F. Hsu; **Kaohsiung:** 2♂ (TARI), Rokkiri (= Liukuei, 六龜), 14.V.1941, leg. Y. Yano; 1♂ (TARI), Tengchih (藤枝), 6. VIII.2013, leg. B. X. Guo; 1♀ (TARI), Tienchih (天池), 1.IV.2015, leg. C. F. Lee; 4♂, 2♀ (TARI), Tou Noo (多納), 3.VI.1989, leg. K. Baba; 4♂, 3♀ (TARI), same locality (= Tona), 7.VII.2016, leg. B. X. Guo; 2♀ (TARI), same locality, 24.VII.2016, leg. U. Ong; **Miaoli:** 1♂ (TARI), Hsuehchien (雪見), 12.X.2021, leg. C. F. Lee; **Nantou:** 1♀ (TARI), Aowanta (奧萬大), 10.VII.2010, leg. Y. T. Wang; 1♂ (NMNS), Chunyang (春陽), 23–24.IX.1997, leg. C. S. Lin & W. T. Yang; 1♂, 3♀ (TARI), same but with "12.VIII.–8.IX.1998"; 1♀ (NMNS), same but with "11.VI.–9.VII.2002"; 1♀ (NMNS), same but with "15.X.–12.XI.2002"; 1♀ (NMNS), same but with "11.VI.–8.VII.2003"; 1♀ (NMNS), same but with "5.VIII.–9.IX.2003"; 1♂, 2♀ (NMNS), same but with "9.IX.–7. X.2023"; 1♂, 1♀ (NMNS), same but with "4.XI.–15.XII.2003"; 1♂ (NMNS), same but with "10.VIII.–8.IX.2004"; 2♀ (NMNS), same but with "8.VI.–14.VII.2017"; 1♂, 2♀ (TARI), same locality, 25.X.2009, leg. Y. T. Wang; 1♀ (TARI), same locality, 20.IV.2011, leg. W. T. Liu; 1♂ (NMNS), same locality but with "No: II Sampling plots, 9.I.–6.II.2007"; 1♂, 1♀ (NMNS), same but with "6.VI.–14.VII.2007"; 1♂, 1♀ (NMNS), same but with "14.VII.–7.VIII.2007"; 1♀ (NMNS), Huisun Forest (惠蓀林場), 17–19. I.1996, leg. W. T. Yang; 1♂ (NMNS), same locality, 11.XI.1998, leg. M. L. Chan; 1♀ (NMNS), same locality, 6.VI.2011, leg. Liang, Tang, Shen; 1♂ (NMNS), same locality, 1.X.2011, leg. H. H. Liang; 1♂ (TARI), 17.XI.2008, same

locality, leg. M. H. Tsou; 2♀ (NMNS), Jiantai Forest District (尖台林區), 17.VII.2019, leg. J. F. Tsai; 1♂, 1♀ (BMNH), Lushan (廬山), 8.VIII. 2008, leg. H. Mendel, U. Ong, M. V. L. Barclay & R. Ewers; 1♀ (TARI), Musha (= Wushe, 霧社), V.18.–VI.15.1918, leg. T. Okuni; 1♀ (NMNS), Nanshanchi (南山溪), 17.VI.1965, leg. B. S. Chang; 1♂ (NMNS), same but with "21. VI.1965"; 1♂ (NMNS), Sungkang (松崗), 10. VII.2000, leg. C. C. Lo; 1♂ (TARI), Tungpu (東埔), 19–23.VII.1982, leg. L. Y. Chou & T. Lin; 1♂ (NMNS), Yuanfeng (鳶峰), 2.VIII.–8.IX.2005, leg. C. S. Lin & W. T. Yang; **New Taipei City:** 1♀ (TARI), Fushan (福山), 17.VI.2008, leg. W. H. Hu; **Pingtung:** 2♂, 1♀ (TARI), Tahanshan (大漢山), 24.VI.2007, leg. C. F. Lee; 1♀ (TARI), same locality, 22.I.2009, leg. M. H. Tsou; 4♂, 6♀ (TARI), same but with "18–21. IV.2009"; 1♂, 1♀ (TARI), same locality, 17.VII.2007, leg. S. F. Yu; 1♀ (TARI), same but with "8.II.2008"; 1♂ (TARI), same but with "22.I.2009"; 1♀ (TARI), same locality, 3.IV.2013, leg. Y. T. Chung; 1♀ (TARI), same but with "10.V.2013"; 1♂ (TARI), same but with "6.VI.2015"; 1♂ (TARI), same locality, 25.X.2014, leg. W. C. Liao; 1♂ (TARI), same but with "22.III.2015"; **Taichung:** 1♂, 2♀ (NMNS), Bojinjiashan (波津加山), 8.X.1987, leg. I. C. Hsu; 1♀ (NMNS), Chungchemg Campsite (中正露營區), 24.V.2010, leg. H. H. Liang; 1♂, 1♀ (NMNS), Guguan (谷關), Shaolai Trail (捎來步道), 25.IX.2021, leg. J. F. Tsai; 1♂ (NMNS), Tachien (達見), 2.IX.1987, leg. I. C. Hsu; 1♂, 3♀ (NMNS), Tangmatanshan (唐麻丹山), 4.X.1987, leg. I. C. Hsu; **Taitung:** 1♂, 4♀ (TARI), Wulu trail (霧鹿林道), 26.IX.2007, J. F. Tsai; **Taoyuan:** 2♀ (NMNS), Junghua (榮華), 2.V.1971, leg. B. S. Chang; 1♂ (NMNS), Paling (巴陵), 23.IV.1972, leg. B. S. Chang; 1♂ (NMNS), Szuling (四稜), 17.IX.2011, leg. Y. T. Wang.

Redescription. Length 8.5–10.0 mm, width 4.2–5.3 mm. General color (Figs. 3A–C) yellowish-brown to reddish-brown; antenna apically and gradually darkened from antennomere V; mesothoracic ventrite blackish-brown or black; tibiae and base of hind femur black, tarsi yellow; elytra with white dots between strial punctures arranged regularly and characteristically. Antennae filiform in males (Fig. 4A), but antennomere I moderately bent, length ratios of male antennomeres I–XI 1.0 : 0.4 : 0.5 : 0.5 : 0.6 : 0.6 : 0.6 : 0.6 : 0.6 : 0.5 : 0.7, length to width ratios of antennomeres I–XI 4.1 : 1.8 : 2.4 : 2.5 : 2.6 : 2.4 : 2.7 : 2.8 : 2.8 : 2.3 : 2.9; shorter in females (Fig. 4B), antennomeres III–X straight, length ratios of female antennomeres I–XI 1.0 : 0.4 : 0.5 : 0.5 : 0.5 : 0.5 : 0.5 : 0.5 : 0.5 : 0.5 : 0.7, length to width ratios of antennomeres I–XI 3.5 : 1.8 : 2.4 : 2.6 : 2.9 : 2.6 : 2.2 : 2.3 : 2.3 : 2.1 : 2.8. Pronotum transverse, 1.8–1.9× wider than long, lateral margin moderately rounded from apex to middle, then parallel-sided from middle to base; apical margin medially and moderately concave, basal margin medially and slightly convex. Elytra parallel-sided, 1.4–1.5× longer than wide. Tarsomeres I of front and middle legs strongly swollen in males (Fig. 4H); less swollen in females (Fig. 4I). Apical margin of abdominal ventrite V in males trilobed (Fig. 4J), notches shallow, basal margins of all abdominal ventrites not modified; apical margin of abdominal ventrite V broadly rounded in females, basal margin not modified. Penis (Figs. 4C–D) elongate, 4.8× longer than wide; parallel-sided, apically narrowed from apical 3/10, apex rounded; slightly bent at middle at lateral view; ostium membranous with one median elongate sclerite. Gonocoxae (Fig. 4G) well developed, combined with deep median notch on apical margin, dense, long setae along apical margin, basal membranous with median basally pointed sclerotization. Ventrite VIII (Fig. 4E) membranous except apical margin and spiculum, with one cluster of short setae at sides of apical margin; spiculum extremely elongate. Receptacle of spermatheca (Fig. 4F) strongly swollen, apically connected with distal spermathecal duct and basally connected with pump, inseparable between distal spermathecal duct, receptacle, and pump; pump strongly curved, apex with one small process; distal spermathecal duct long and apically connected with receptacle.

Variation. Specimens from populations in mainland China are larger and have entirely black hind femora.

Diagnosis. Adults of *Asiophrida scaphoides* are separated easily from those of *A. spectabilis* by their distinct color patterns. In addition, genitalic characters are also diagnostic for species identities. The ventral surface of the penis is flat (Fig. 4D) in *A. scaphoides*, but convex at apical 1/3 (Fig. 6D) in *A. spectabilis*. The apical margin of the gonocoxae is widely rounded in *A. scaphoides* (Fig. 4G), but bilobed in *A. spectabilis* (Fig. 6G). Abdominal ventrite VIII in females of *A. scaphoides* possesses an elongate spiculum, with apical marginal setae restricted to the central part (Fig. 4E). In females of *A. spectabilis* abdominal ventrite VIII has the spiculum subapically widened, and the entire apical margin bears setae (Fig. 6E).

Host plants. Anacardiaceae: *Rhus verniciflua* Stokes (Aston 2009); *R. succedanea* var. *succedanea* L. (Kimoto & Takizawa 1997; Lee & Cheng 2007).

Biology. Although the larval morphology of *Asiophrida scaphoides* was studied by Kimoto & Takizawa (1997), its life history was previously unknown. Based on our observations, this species is univoltine in Taiwan. Overwintered females started depositing egg masses on February 20, 2009, as observed by the senior author. Each egg mass contained ten eggs and was covered with faeces (Fig. 5A). Egg masses were deposited on twigs in the field (Fig. 5B). Larvae hatched after 10 d. Neonate larvae were pale yellow with black heads (Fig. 5C). They cut leaf veins first to stop fluid transport in the veins. Later instar larvae turned purple and fed by scraping the abaxial surface of the lamina (Fig. 5D), while older larvae fed by cutting the leaf lamina. They appeared sticky and coated with faeces (Fig. 5E). Larval durations varied from 14–16 d. Mature larvae crawled into the soil and constructed underground chambers for pupation. Pupal stage (Fig. 5F) duration was approximately 30 d (Fig. 5G). Adults fed by cutting the leaf lamina. They jumped promptly when disturbed. Unlike larvae, adults preferred to remain on the adaxial side of leaves (Fig. 5H).

Distribution. China, India, Laos (new record), Taiwan, Thailand, and Vietnam. This species is widespread in lowlands of Taiwan.

Asiophrida spectabilis (Baly)

Podonita spectabilis Baly, 1862:452 (China).

Ophrida spectabilis: Gemminger & Harold, 1876:3523 (catalogue); Chen 1933:216 (key); Chen 1934:270 (redescription; China: Zhejiang, Jiangsu, Guizhou, Yunnan; Taiwan); Chen 1939:34 (China: Guangxi); Chûjô 1935:465 (Taiwan); Chûjô 1963:400 (Taiwan); Gressitt & Kimoto 1963:787 (China: Tibet, Sichuan, Hubei); Kimoto 1965:489 (Taiwan); Kimoto 1970:214 (Taiwan); Wang *et al*. 1998:26 (biology and control); Lee & An 2001:146 (South Korea); Park & Lee 2001:257 (larval morphology, biology); Lee & Cho 2006:57 (host plants); Lee & Cheng 2007:140 (biology).

Podontia rufoflava Fairmaire, 1889:73 (China); synonymized by Gressitt & Kimoto (1963).

Asiophrida spectabilis: Medvedev 1999:183; Yang *et al*. 2015:354 (China; catalogue); Cho & An 2020:15 (Korea; catalogue); Löbl & Smetana 2011:51 (catalogue).

Types. *Podolia spectabilis* (Figs. 2I–L). Lectotype ♀ (BMNH), here designated to preserve stability of nomenclature since synonyms exist, labeled: "Type / H. T. [p, w, circle with red border] // Baly Coll. [p, w] // SYN- / TYPE [p, w, circle label with blue border] // Podonita / spectabilis / Baly / N. China [h, b] // Type [h, underside of the previous card] // BMNH(E) / #1024845 [p, w]". Paralectotype: 1♀ (BMNH): "Baly Coll. [p, w] // SYN- / TYPE [p, w, circle label with blue border]".

Podontia rufoflava. Fairmaire's collection is at the Muséum national d'Histoire naturelle (MNHN) in Paris. Nonetheless, a recent search through both the MNHN general collection and Fairmaire's collection for types has been unsuccessful (A. Mantilleri, in litt.).

Specimens examined (*n* = 56). CHINA. Fujian: 1♀ (BMNH), Foochow (= Fuzhou, 福州), 2.IX.??, leg. M. S. Yang; **Guanxi:** 1♂ (TARI), Cenwanglaoshan (岑王老山), 27.VII.2020, leg. Y. Q. Lu; **Zhejiang:** 1♀ (BMNH), Hangchow (= Hangzhou, 杭州), 3.VI.1928, leg. P. H. Tsai; 1♂ (TARI), same locality, 14.VIII.1928, leg. C. C. Tao; **KOREA.** 1♀ (TARI), Keizyo, Keikido, 3.VIII.1937, leg. T. Kusanagi; 1♀ (TARI), Keizyo, Keikido, Mt. Hokugaku-zan, 7.VIII.1937, leg. M. Yamada; **TAIWAN. Chiayi:** 1♀ (TARI), Arisan (= Alishan, 阿里山), VI.1914, leg. M. Maki; 1♀ (TARI), 2–23.X.1918, same locality, leg. J. Sonan & M. Yoshino; 1♂, 1♀ (TARI), Taihorin (= Talin, 大林), VI.1908, leg. T. Shiraki; **Hsinchu:** 1♂ (TARI), Litungshan (李棟山), 6.VI.2010, leg. Y. L. Lin; **Hualien:** 2♀ (BMNH), Costal Range (海岸山脈), SE of Fuli (富里), 12–16.XI.2008, leg. L. Dembický; **Hualien:** 2♂, 3♀ (NMNS), Hsipao (西寶), 5.XII.1991, leg. Y. C. Shiau; **Ilan:** 1♀ (TARI), Piyahau (= Pihau, 碧猴), 16.X.1937, leg. Y. Miwa; 1♀ (TARI), Riyohen (= Chinyuehtsun, 金岳村) – Rato (= Lotung, 羅東), 5.IX.1929, leg. R. Takahashi; 1♀ (TARI), Taiheizan (= Taipingshan, 太平山), VII.1930, leg. Y. Minowa; **Nantou:** 1♀, Horisha (= Puli, 埔里), 20.V.1919, leg. H. Kawamura; 1♂, 1♀ (TARI), same locality (= Hori), VII.1937, leg. K. Nakamura; 3♂, 1♀ (NMNS), Nanshanchi (南山溪), 21.V.1965, leg. B. S. Chang; 1♀ (NMNS), same but with "1.VI.1965"; 2♂ (NMNS), same but with "8.VI.1965"; 2♂ (NMNS), same but with "17.VI.1965"; 1♂ (TARI), Takeya (= Chienchityu, 乾溪子), 8.VII.1940, leg. M. Chujo; **New Taipei City:** 1♀ (NMNS), crossroads between Beiyi Highway (北宜公路) and Shuangfeng Road (雙峰路), 4.X.1992, leg. W. I. Chou; 2♂ (TARI), Shinten (= Hsintien, 新店), 24.X.1929, leg. M. Chujo; **Taichung:** 2♀ (TARI), Hakumo (= Paimao, 白毛), 12.VI.1926, leg. R. Takahashi; **Taipei:** 1♂, 1♀ (TARI), Peitou (北投), 2.X.2006, leg. S. F. Yu; 1♂, 3♀, Sozan (= Yangmingshan, 陽明山), 25.X.1936, leg. M. Chujo; 1♂, 4♀, same locality, 13.VI.1943, collector unknown; 1♀ (TARI), Sishoushan (四獸山), 19.VIII.2014, leg. H. T. Cheng; 1♀ (TARI), Taihoku (= Taipei, 臺北), IX.1911, leg. I. Nitobe; **Taitung:** 1♂ (TARI), Lichia (利嘉), 9.V.2010, leg. M. L. Jeng; **Taoyuan:** 1♂, 1♀ (TARI), Kalaho (嘎拉賀), 20.IX.2009, leg. Y. T. Wang.

Redescription. Length 13.8–15.0 mm, width 6.9–8.0 mm. General color (Figs. 3D–F) yellowish-brown; antenna black, but four basal antennomeres yellowish-brown; elytra with white stripes arranged regularly and characteristically. Antennae filiform in males (Fig. 6A), but antennomere I moderately bent, length ratios of male antennomeres I–XI 1.0 : 0.3 : 0.5 : 0.6 : 0.7 : 0.6 : 0.6 : 0.6 : 0.6 : 0.5 : 0.6, length to width ratios of antennomeres I–XI 3.4 : 1.7 : 2.9 : 2.8 : 2.8 : 2.7 : 2.8 : 2.6 : 3.0 : 2.4 : 2.9; similar in females (Fig. 6B), antennomeres III–X straight, length ratios of female antennomeres I–XI 1.0 : 0.3 : 0.5 : 0.6 : 0.6 : 0.5 : 0.6 : 0.5 : 0.5 : 0.5 : 0.6, length to width ratios of antennomeres I–XI 3.6 : 1.6 : 2.7 : 2.9 : 3.0 : 2.6 : 2.5 : 2.6 : 2.6 : 2.2 : 3.0. Pronotum transverse, 1.7–1.8× wider than long, lateral margin moderately rounded from apex to middle, then parallel-sided from middle to base; apical margin medially and moderately concave, basal margin medially and slightly convex. Elytra parallel-sided, 1.5–1.6× longer than wide. Tarsomeres I of front and middle legs strongly swollen in males (Fig. 6H); less swollen in females (Fig. 6I). Apical margin of abdominal ventrite V in males trilobed (Fig. 6J), notches shallow, basal margins of all abdominal ventrites unmodified; apical margin of abdominal ventrite V broadly rounded in females, basal margin unmodified. Penis (Figs. 6C–D) elongate, 4.5× longer than wide; parallel-sided, apically narrowed from apical 3/10, apex rounded; slightly bent at middle at lateral view, ventral surface convex at apical 1/3; ostium membranous with one median elongate sclerite and one pair of lateral curved sclerites. Gonocoxae (Fig. 6G) well developed, lobe-like and combined, apical margin weakly emarginate on either side of middle, several

long setae along apical margin, and short setae near apices, base membranous with median basally pointed sclerotized area, and two pair of elongate weakly margined sclerotized areas. Ventrite VIII (Fig. 6E) membranous except apical margin and speculum, with short setae along apical margin, much denser at central part; spiculum extremely elongate and subapically widened. Receptacle of spermatheca (Fig. 6F) strongly swollen, apically connected with distal spermathecal duct and basally connected with pump, inseparable between distal spermathecal duct, receptacle, and pump; pump strongly curved, apex with one small process; distal spermathecal duct long and apically connected with receptacle.

Diagnosis. Adults of *Asiophrida spectabilis* are separated easily from those of *A. scaphoides* by their distinct color patterns. In addition, genitalic characters are diagnostic for species identities. The ventral surface of the penis is convex at the apical 1/3 in *A. spectabilis* (Fig. 6D) but flat in *A. scaphoides* (Fig. 4D). The apical margin of the gonocoxae is bilobed in *A. spectabilis* (Fig. 6G) but is widely rounded in *A. scaphoides* (Fig. 4G). In females of *A. spectabilis* abdominal ventrite VIII possesses a spiculum that is subapically widened, and an entire apical margin bearing setae (Fig. 6E). In females of *A. scaphoides* the spiculum is elongate, and setae of the apical margin are restricted to central part (Fig. 4E).

Host plants. Anacardiaceae: *Rhus verniciflua* Stokes (Park & Lee 2001); *R. trichocarpa* Miq. (Park & Lee 2001); *R. chinensis* Mill. (Wang *et al*. 1998; Park & Lee 2001); *R. chinensis* var. *roxburghii* (DC.) Rehder (Lee & Cheng 2007; = *R. javanica*, recorded by Lee & Cho 2006); *R. punjabensis* Stewart (Wang *et al*. 1998).

Biology. The larval morphology of *Asiophrida spectabilis* was studied by Park & Lee (2001). Its observed life history was similar in China (Hubei) (Wang *et al*. 1998), South Korea (Park & Lee 2001), and Taiwan (Lee & Cheng 2007). This species is univoltine and larvae from overwintered eggs started to hatch during mid-March in Taiwan but mid-April in South Korea. Egg mass contain approximately 15 eggs and are covered with faeces (Fig. 7B). Egg masses are deposited on twigs in the field (Fig. 7C). In the laboratory, larvae hatched in 5 d after being splashed with water. Neonate larvae are pale yellow with black heads (Fig. 7D). Later instar larvae turned purple and fed by scraping the adaxial surface of the lamina (Fig. 7E), while older larvae feed by cutting the leaf lamina. They appeared sticky and were coated with faeces (Fig. 7F). Larval durations varied from 25–30 d. Mature larvae crawled into the soil and constructed underground chambers for pupation. Larvae turned yellow inside the underground chambers. Pupal duration (Fig. 7G) was approximately 35 d in Taiwan and 45–50 d in China. Adults feed by cutting the leaf lamina. They jump promptly while disturbed. Adults (Fig. 7H) appear during middle June to early October in China and Taiwan but early August to late October in South Korea. Females start depositing egg masses during early September in China, middle September to middle October in South Korea, and late October in Taiwan (Fig. 7A).

Distribution. China, South Korea, Taiwan. This species is widespread in lowlands of Taiwan.

CONCLUSION

Medvedev (1999) proposed diagnostic characters of pronotum, pro- and mesosterna, hind femora, and claws for generic delimitation between *Podontia* and *Asiophrida*. More diagnostic characters can be observed on genitalic structures and immature stages. However, adults of *Asiophrida* are more similar to those of *Ophrida*, differing from the latter only by the well-developed Al area on the pronotum. The genus *Ophrida* require detailed study, especially of genitalic morphology and immatures to determine if the two genera are distinct or synonyms.

ACKNOWLEDGMENTS

We thank the Taiwan Chrysomelid Research Team for collecting materials, including Hsing-Tzung Cheng, Yi-Ting Chung, Bo-Xin Guo, Su-Fang Yu, and Mei-Hua Tsou; for taking photographs of specimens and live individuals in the field, including Hsing-Tzung Cheng, Su-Fang Yu, Mei-Hua Tsou, and Hseuh Lee. We thank Jan Bezděk and Yongying Ruan for providing valuable literature. We especially thank Chang Chin Chen for assisting our study in various ways. We thank Chris Carlton for reading the draft and editing for the American English style. This study was supported by the National Science and Technology Council NSTC 112-2313-B-055-001-MY3.

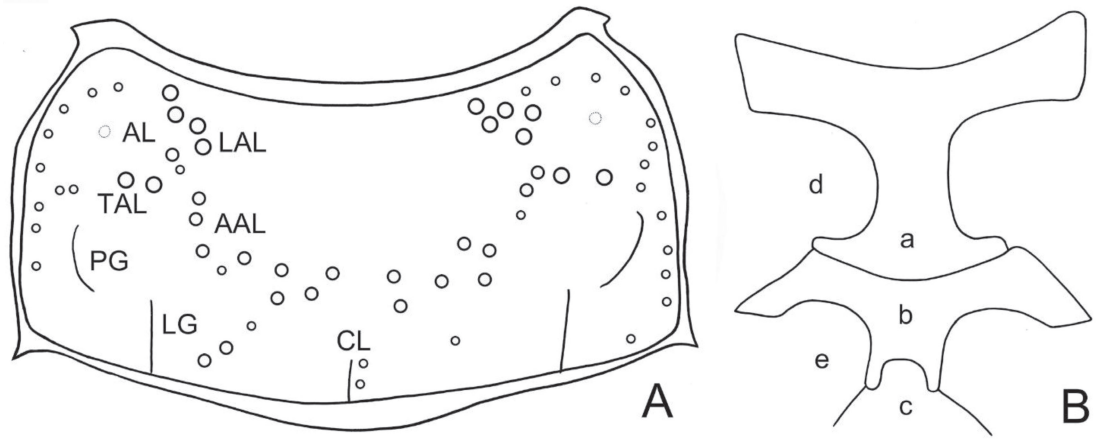

Fig. 1. Diagnostic characters of pronotum and thoracic ventrites, *Asiophrida scaphoides*. A. Pronotum, AAL: longitudinal groove behind middle, AL: anterolateral area, CL: central line, LAL: longitudinal groove above middle, LG: basal longitudinal groove, PG: posterior groove, TAL: transverse groove; B. Thorax, a: prosternum, b: mesoventrite, c: metaventrite, d: anterior coxa, e: middle coxa.

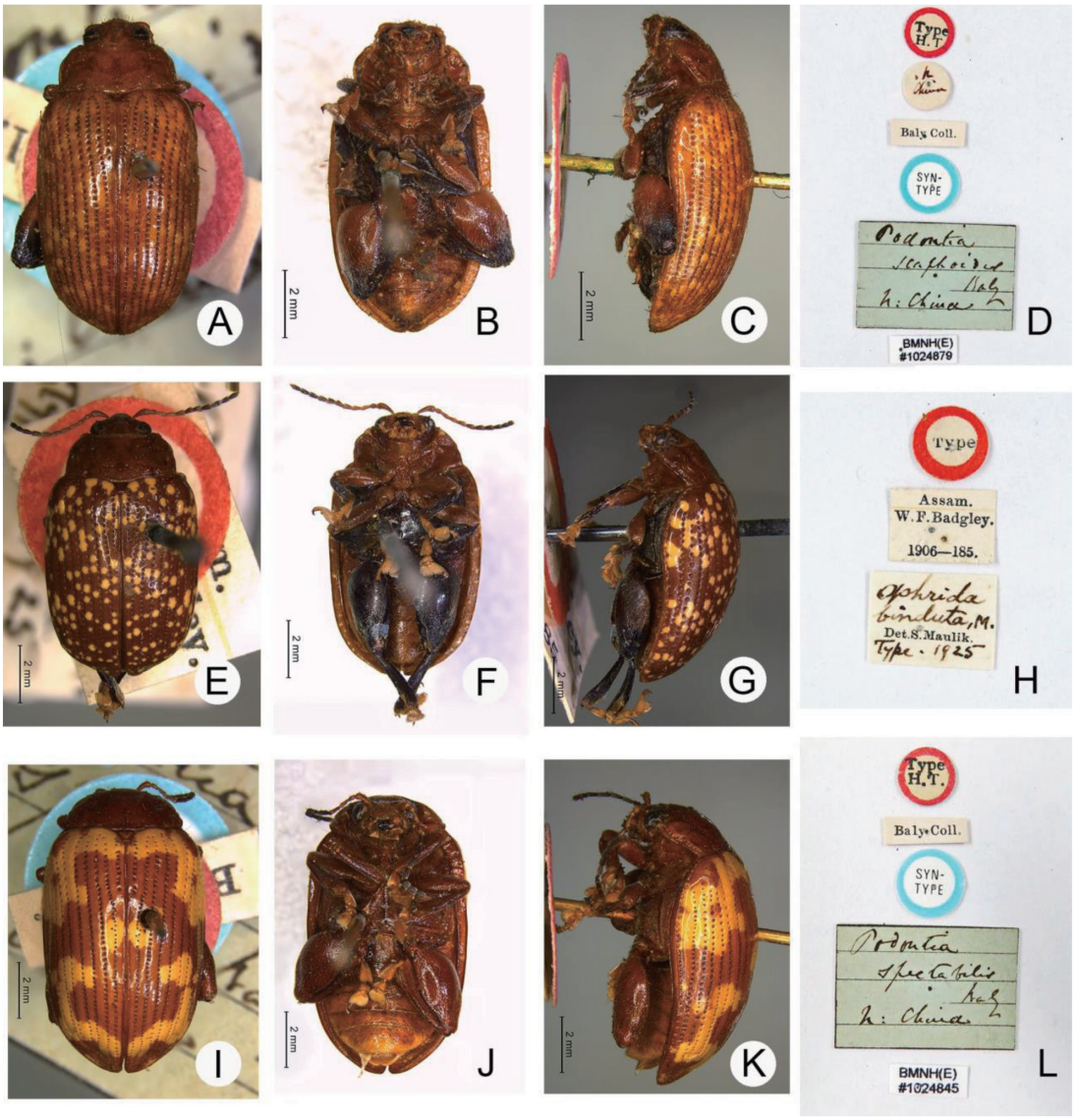

Fig. 2. Type specimens and labels of *Podontia scaphoides*, *Ophrida binduta*, and *P. spectabilis*. A–D: *P. scaphoides*, A. lectotype, dorsal view; B. ditto, ventral view; C. ditto, lateral view; D. labels; E–H: *O. binduta*, E. lectotype, dorsal view; F. ditto, ventral view; G. ditto, lateral view; H. labels; I–L: *P. spectabilis*, I. lectotype, dorsal view; J. ditto, ventral view; K. ditto, lateral view; L. labels.

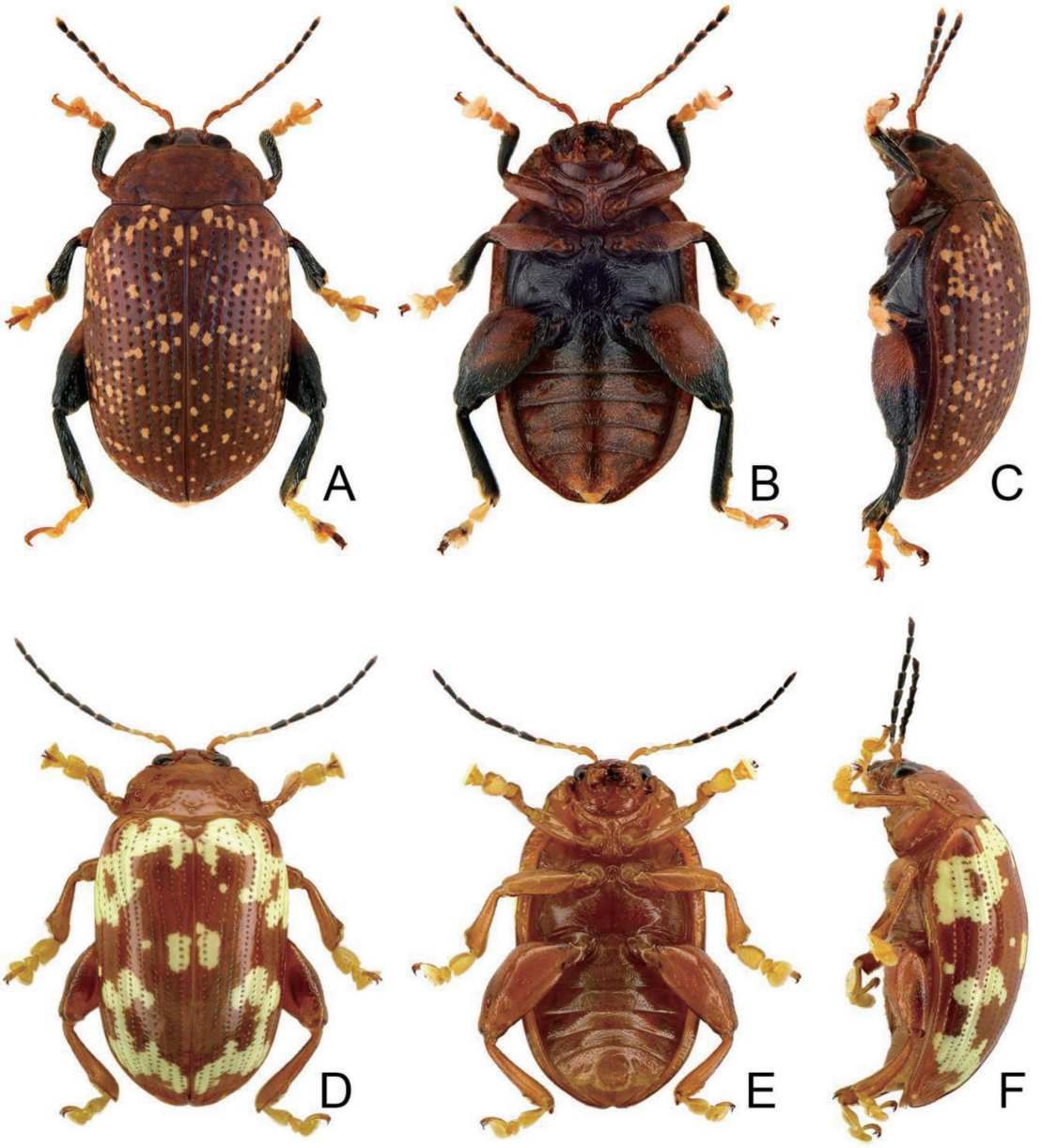

Fig. 3. Habitus of adult *Asiophrida scaphoides* and *A. spectabilis*. A. *A. scaphoides*, female, dorsal view; B. Ditto, ventral view; C. Ditto, lateral view; D. *A. spectabilis*, male, dorsal view; E. Ditto, ventral view; F. Ditto, lateral view.

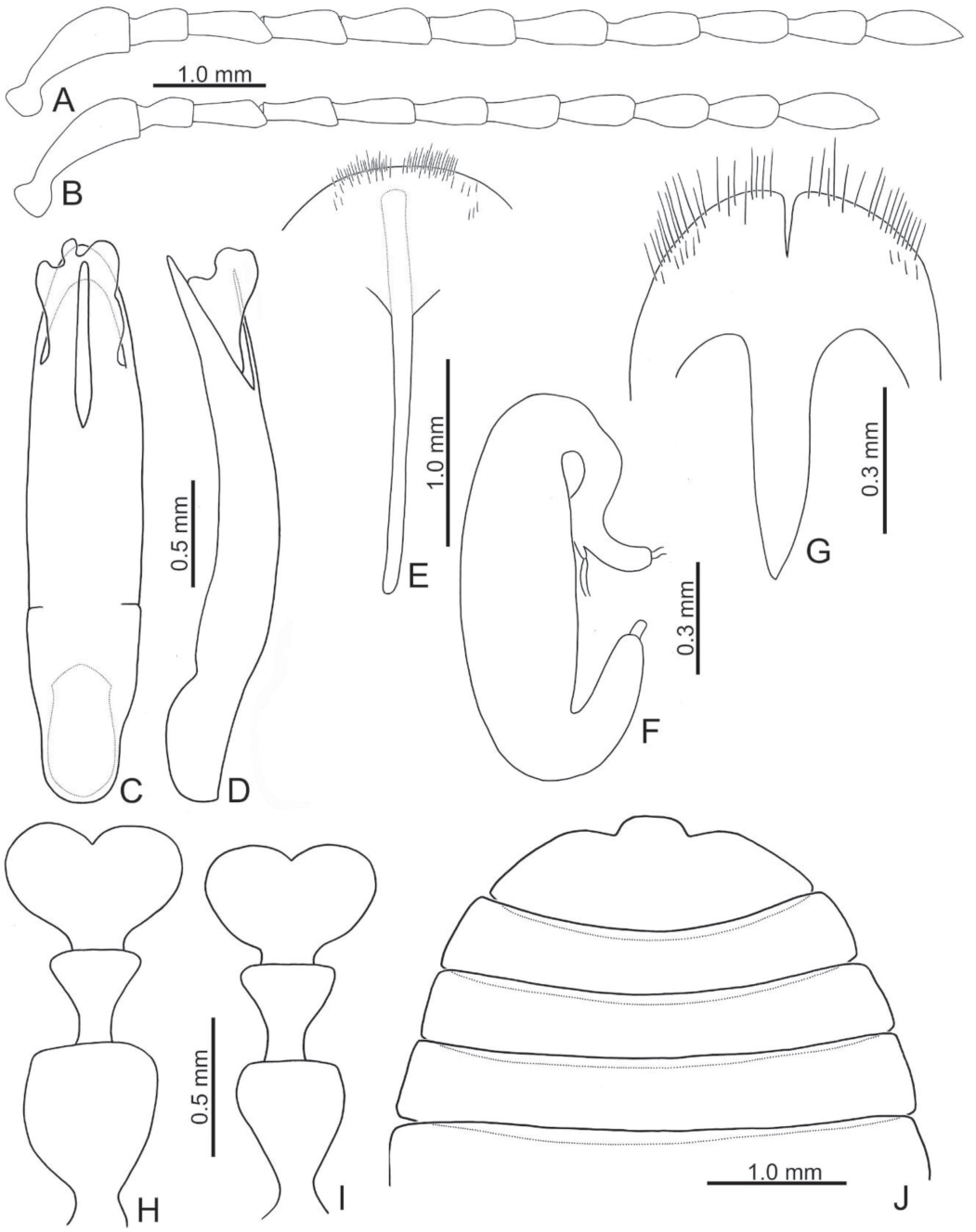

Fig. 4. Diagnostic characters of *Asiophrida scaphoides*. A. Antenna, male; B. Antenna, female; C. Penis, dorsal view; D. Penis, lateral view; E. Ventrite VIII, female; F. Spermatheca; G. Gonocoxae; H. Tarsomeres I–III, male; I. Tarsomeres I–III, female; J. Ventrite I–V, male.

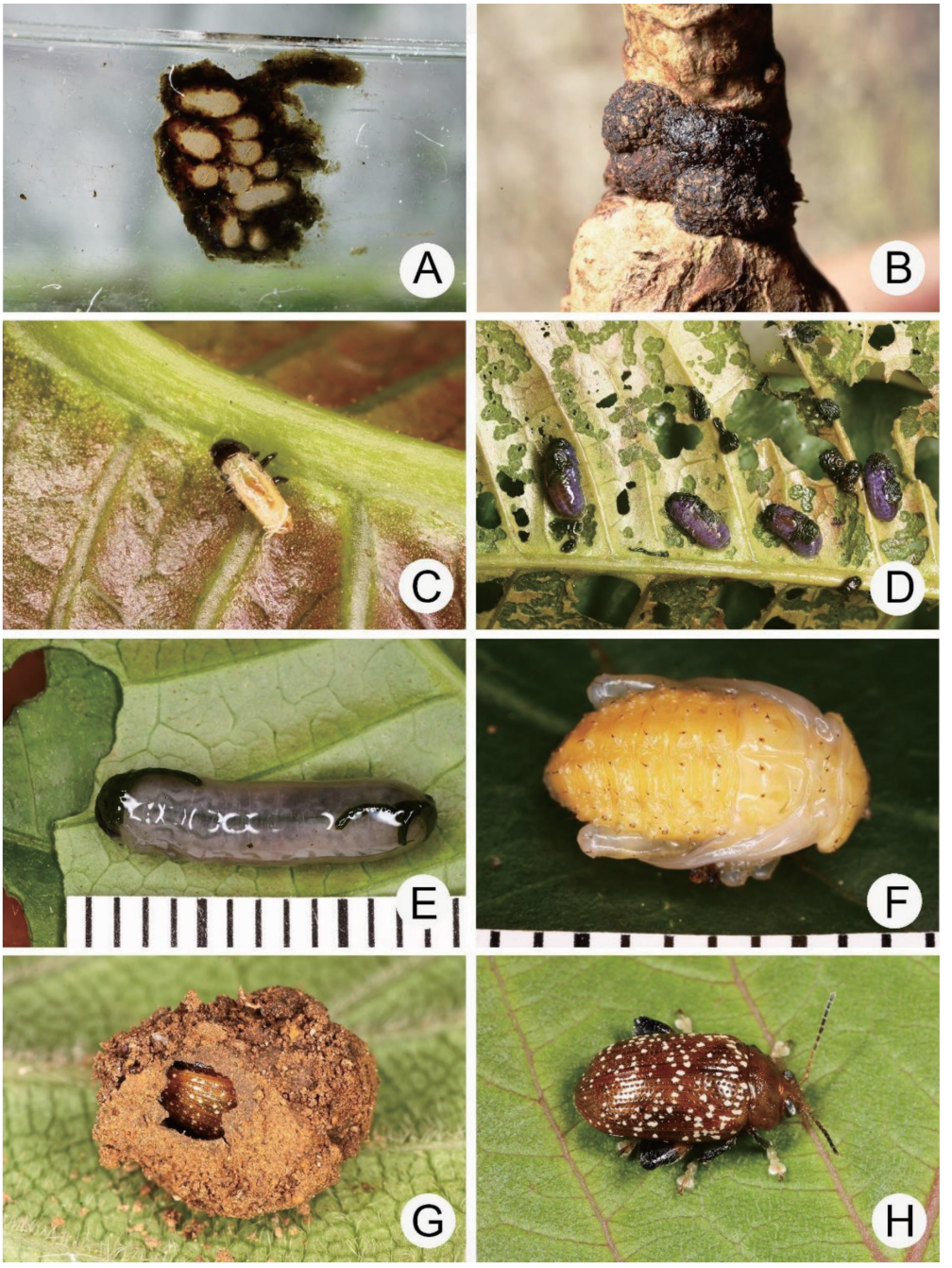

Fig. 5. Life stages of *Asiophrida scaphoides*. A. The egg mass deposited inside a glass container at the laboratory; B. Egg masses deposited on the twigs in the field; C. First-instar larva; D. Second-instar larva; E. Third-instar larva; F. Pupa; G. Adult within underground chamber; H. Alert adult.

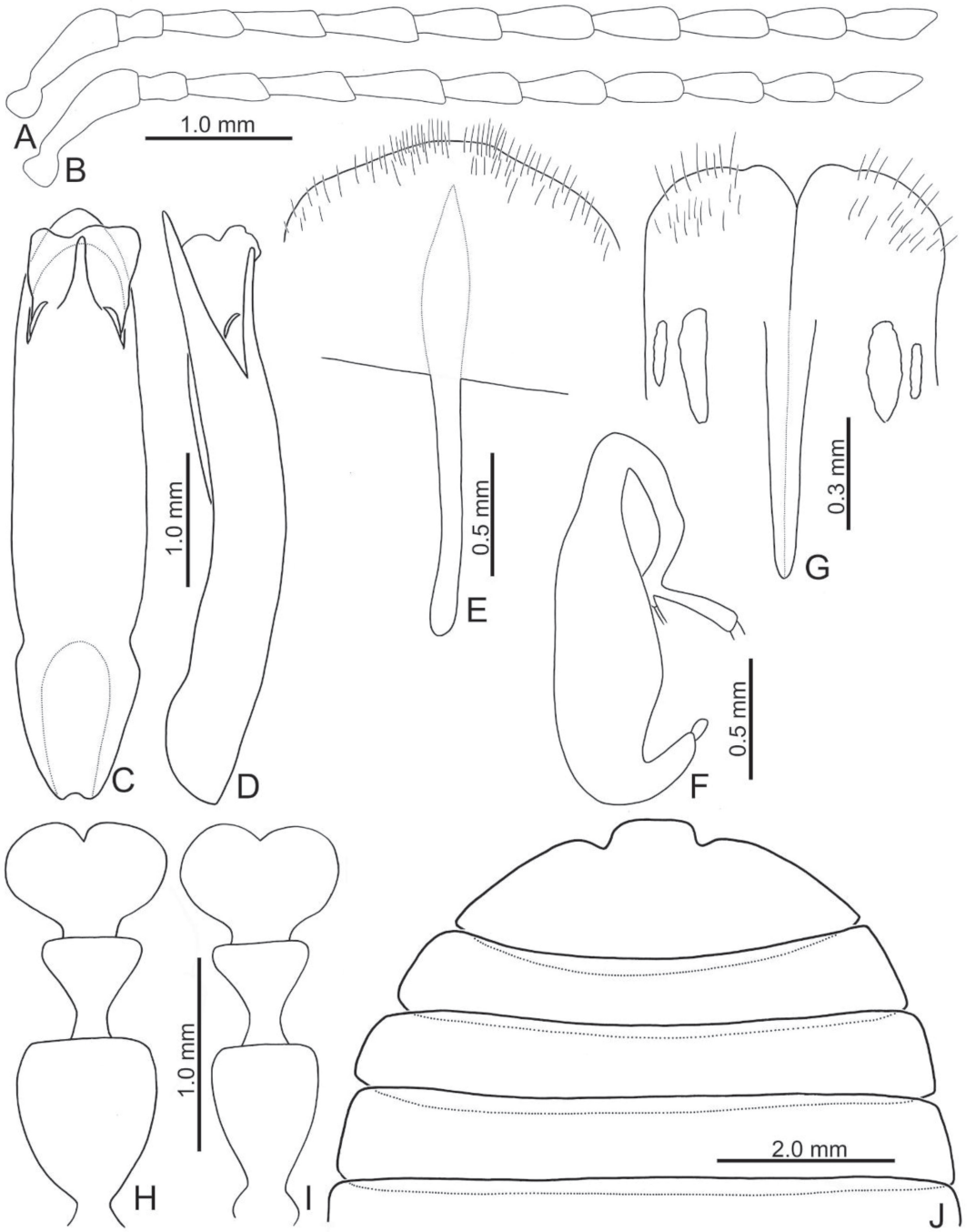

Fig. 6. Diagnostic characters of *Asiophrida spectabilis*. A. Antenna, male; B. Antenna, female; C. Penis, dorsal view; D. Penis, lateral view; E. Ventrite VIII, female; F. Spermatheca; G. Gonocoxae; H. Tarsomeres I–III, male; I. Tarsomeres I–III, female; J. Ventrite I–V, male.

Fig. 7. Life stages of *Asiophrida spectabilis*. A. Female depositing egg masses on twig; B. Eggs exposed in egg mass; C. Egg masses deposited on twigs in the field; D. First-instar larva; E. Second-instar larva; F. Third-instar larva; G. Pupa; H. Alert adult.

REFERENCES

Aston, P. 2009. Chrysomelidae of Hong Kong part 2 subfamily Alticinae. Hong Kong Entomol. Bull. 1:1–13.

Baly, J. S. 1862. Descriptions of new genera and species of phytophaga. J. Entomol. 1:450–459.

Baly, J. S. 1865. Descriptions of new genera and species of phytophaga. Trans. Entomol. Soc. London, ser. 3. 2:427–440.

Chen, S. H. 1933. Study of Chinese Halticinae beetles with descriptions of some exotic new species. Sinensia 3:211–254.

Chen, S. H. 1934. Revision of the Halticinae (Col. Chrysomelidae) of Yunnan and Tonkin. Sinensia 5:225–416.

Chen, S. H. 1939. Flea beetles collected at Kwangsi. Sinensia 10:20–55.

Cho, H. W. and S. L. An. 2020. An annotated checklist of leaf beetles (Coleoptera: Chrysomelidae) of Korea, with comments and new records. Far East. Entomol. 404:1–36. doi:10.25221/fee.404.1

Chûjô, M. 1935. Studies on the Chrysomelidae in the Japanese empire (VIII). Subfamily Halticinae (3). Trans. Nat. Hist. Soc. Formosa 25:459–476.

Chûjô, M. 1963. Chrysomelid-beetles from Formosa, preserved in the Hungarian Natural History Museum, Budapest. Ann. Hist. Nat. Mus. Natl. Hung. 55:379–402.

Fairmaire, L. 1889. Coléoptères de l'intérieur de la Chine, 5^{e} partie. Ann. Soc. Enotomol. Fr. 6(9):5–84.

Furth, D. G. and J. E. Lee. 2000. Similarity of the *Blepharida*-group genera using larval and adult characters (Coleoptera: Chrysomelidae: Alticinae). J. N. Y. Entomol. Soc. 108:26–51. doi:10.1664/0028-7199(2000)108[0026:SOTBGG]2.0.CO;2

Gemminger, M. and E. von Harold. 1876. Catalogus Coleopterorum hucusque descriptorum synonymicus et systematicus. Tom XII. Chrysomelidae (Par II.). Languriidae, Erotylidae, Endomychidae, Coccinellidae, Corylophidae, Platypsyllidae. E. H. Gummi. Monachii. 344 pp.

Gressitt, J. L. and S. Kimoto. 1963. The Chrysomelidae (Coleopt.) of China and Korea, part 2. Pac. Ins. Mon. 1B:301–1026.

Kimoto, S. 1965. A list of specimens of Chrysomelidae from Taiwan preserved in the Naturhistorisches Museum/Wien (Insecta: Coleoptera). Ann. Naturhist. Mus. Wien 68:485–490.

Kimoto, S. 1970. Notes on the Chrysomelidae from Taiwan IV. Kontyû 38:205–221.

Kimoto, S. 1987. The Chrysomelidae (Insecta: Coleoptera) collected by the Nagoya University Scientific Expedition to Taiwan in 1986. Kurume Univ. J. 36:183–194.

Kimoto, S. 1989. The Taiwanese Chrysomelidae (Insecta: Coleoptera) collected by Dr. Kintaro Baba, on the occasion of his entomological survey in 1983 and 1986. Kurume Univ. J. 38:237–272.

Kimoto, S. 1991. The Taiwanese Chrysomelidae (Insecta: Coleoptera) collected by Dr. Kintaro Baba, on the occasion of his entomological survey in 1987, 1988 and 1989. Kurume Univ. J. 40:1–27.

Kimoto, S. 2000. Chrysomelidae (Coleoptera) of Thailand, Cambodia, Laos and Vietnam. VIII. Alticinae. Bull. Inst. Comp. Stud. Intl. Cult. Soc. 26:103–299.

Kimoto, S. and H. Takizawa. 1997. Leaf Beetles (Chrysomelidae) of Taiwan. Tokai University Press. Tokyo, Japan. 581 pp.

Lee, C. F. and H. T. Cheng. 2007. The Chrysomelidae of Taiwan 1. Sishou-Hills Insect Observation Network. Taipei County, Taiwan. 199 pp. (in Chinese)

Lee, C. F. and S. F. Yu. 2021. Redescription of *Podontia lutea* (Olivier, 1790) and *P. dalmani* Baly, 1865 (Insecta: Coleoptera: Chrysomelidae: Galerucinae: Alticini), with Notes on the Biology of *P. lutea*. J. Taiwan Agric. Res. 70:157–169. doi:10.6156/JTAR.202109_70(3).0001

Lee, J. E. and S. L. An. 2001. Family Chrysomelidae. Economic Insects of Korea 14. Insecta Koreana Supplement 21. National Institute of Agricultural Science and Technology. Suwon, Korea. 231 pp. (in Korean)

Lee, J. E. and H. W. Cho. 2006. Leaf Beetles in the Crops (Coleoptera: Chrysomelidae). Economic Insects of Korea 27. Insecta Koreana Supplement 34. National Institute of Agricultural Science and Technology. Suwon, Korea. 127 pp. (in Korean)

Löbl, I. and A. Smetana. 2011. Catalogue of Palaearctic Coleoptera, Vol. 7. Apollo Books. Stenstrup, Denmark. 373 pp.

Maulik, S. 1926. The Fauna of British India, Including Ceylon and Burma. Coleoptera. Chrysomelidae (Chrysomelinae and Halticinae). Taylor & Francis. London, UK. 442 pp.

Medvedev, L. N. 1999. A revision of the group Blepharidini (Chrysomelidae: Alticinae) from the Oriental region. Russian Entomol. J. 8:175–184.

Miwa, W. 1931. A Systematic Catalogue of Formosan Coleoptera. Department of Agriculture, Government Research Institute, Rep. No. 55. Taihoku, Taiwan. 359 pp. (in Japanese)

Park, J. Y. and J. E. Lee. 2001. Biology and immature stages of *Ophrida spectabilis* (Baly) from Korea (Coleoptera: Chrysomelidae: Alticinae). Korean J.

Entomol. 31:257–260.

Scherer, G. 1969. Die Alticinae des indischen Subkontinentes (Coleoptera-Chrysomelidae). Pac. Ins. Mon. 22:1–251.

Takizawa, H., S. Nakamura, and K. Kojima. 1995. The Taiwanese chrysomelid beetles preserved in Hiwa Museum for Natural History (Chrysomelidae: Coleoptera). Misc. Rep. Hiwa Mus. Nat. Hist. 33:1–16. (in Japanese with English abstract)

Wang, B. Q., X. R. Ai, Z. J. Chen, Y. F. He, and T. W. Song. 1998. Biology of *Ophrida spectabilis* (Baly) and its control. Entomol. Know. 35(1):26–28. (in Chinese with English abstract)

Yang, X., S. Ge, R. Nie, Y. Ruan, and W. Li. (eds.) 2015. Chinese Leaf Beetles. Science Press. Beijing, China. 507 pp.

Zhang, L. J. and X. K. Yang. 2008. Description of the immature stages of *Ophrida xanthospilota* (Baly) (Coleoptera: Chrysomelidae). Proc. Entomol. Soc. Wash. 110:693–700. doi:10.4289/07-041.1

臺灣產斑碩葉蚤屬 *Asiophrida* Medvedev 種類的分類回顧及其生物學注解 (鞘翅目：金花蟲科：螢金花蟲亞科：葉蚤族)

李奇峰 [1,*]　余素芳 [2]　曹美華 [2]

摘要

李奇峰、余素芳、曹美華。2024。臺灣產斑碩葉蚤屬 *Asiophrida* Medvedev 種類的分類回顧及其生物學注解 (鞘翅目：金花蟲科：螢金花蟲亞科：葉蚤族)。台灣農業研究 73(2):71–87。

碩葉蚤屬 (*Podontia* Dalman) 與斑碩葉蚤屬 (*Asiophrida* Medvedev) 為 *Blepharida*-group 當中，有分布到臺灣的兩個屬。斑碩葉蚤屬包含白斑大葉蚤 (*A. scaphoides* (Baly)) 與白紋大葉蚤 (*A. spectabilis* (Baly))，本文重新描述此兩物種，並針對雄性生殖器、雌蟲生殖突基節、雌蟲受精囊、雙性的第一至第三跗節與第五腹節及雌蟲的第八腹節腹板加以描繪；同時提供此兩種葉蚤其幼蟲與成蟲取食行為、寄主植物及生活史等生物學之詳細資料。本研究同時指定 *Podontia scaphoides* Baly, 1865, *Ophrida binduta* Maulik, 1926 及 *P. spectabilis* Baly, 1862 的選模標本。

關鍵詞：葉蚤、分類學、漆樹科、木蠟樹、羅氏鹽膚木。

投稿日期：2024 年 1 月 14 日；接受日期：2024 年 2 月 17 日。
* 通訊作者：chifeng@tari.gov.tw
[1] 農業部農業試驗所應用動物組聘用研究員。臺灣 臺中市。
[2] 公民科學家。臺灣 臺北市。

台灣農業研究 (J. Taiwan Agric. Res.) 73(2):89–99 (2024)
https://doi.org/10.6156/JTAR.202406_73(2).0002

Research Article

Using Multiplex RT-PCR Assay for Detection and Differentiation of Three Pepper-Infecting Viruses

Cheng-Ping Kuan[1,*], Chung-Jen Hsiao[2], Ying-Huey Cheng[3], and Shu Chen[4]

Abstract

Kuan, C. P., C. J. Hsiao, Y. H. Cheng, and S. Chen. 2024. Using multiplex RT-PCR assay for detection and differentiation of three pepper-infecting viruses. J. Taiwan Agric. Res. 73(2):89–99.

A multiplex reverse transcription-polymerase chain reaction (multiplex RT-PCR) method was developed to enable the simultaneous detection and differentiation of three tobamoviruses infecting peppers, namely pepper mild mottle virus (PMMoV), tobacco mosaic virus (TMV), and tomato mosaic virus (ToMV). The differentiation was achieved using 3 optimized specific oligonucleotide primer pairs, including 1 universal primer for detecting all tobamoviruses and 3 virus-specific primers as forward in the multiplex RT-PCR. The amplification of these three target viruses was finely tuned by analyzing the PCR primer ratios. The multiplex RT-PCR products generated distinct fragments: 519 base pairs (bp) for PMMoV, 228 bp for TMV, and 177 bp for ToMV. Importantly, this method exhibits a high level of specificity, as no products were amplified from non-target pepper virus RNAs as templates. Additionally, it has been demonstrated that multiplex RT-PCR is a virus-specific, sensitive, and cost-effective method for the multiple detection of pepper-infecting tobamoviruses in the field.

Key words: Tobamoviruses, Pepper mild mottle virus, Tobacco mosaic virus, Tomato mosaic virus, Detection.

INTRODUCTION

Pepper (*Capsicum annuum* L.), a member of the Solanaceae family, is widely cultivated in Taiwan. However, viral diseases can result in severe symptoms and cause epidemics and significant economic losses (Jones 2021). Among the various viruses affecting peppers, aside from insect-transmitted ones, mechanical and seed-born tobamoviruses, as highlighted by Moury & Verdin (2012), are particularly prevalent. Tobamoviruses lack insect vectors but can easily be transmitted through plant saps and mechanical tools. Tobamoviruses are highly infectious through mechanical means and can be found in seeds and plant debris (Spence *et al*. 2001), and even in wastewater (Rosario *et al*. 2009). Traditionally, tobacco mosaic virus (TMV) and tomato mosaic virus (ToMV) are the predominant tobamoviruses in pepper fields, but their management has been successful through resistance breeding utilizing resistance genes. Tobamovirus genomes consist

Received: December 12, 2023; Accepted: March 14, 2024.
* Corresponding author, e-mail: pcr123@tari.gov.tw
[1] Associate Research Fellow, Crop Genetic Resources and Biotechnology Division, Taiwan Agricultural Research Institute, Taichung City, Taiwan, ROC.
[2] Project Assistant, Crop Genetic Resources and Biotechnology Division, Taiwan Agricultural Research Institute, Taichung City, Taiwan, ROC.
[3] Research Fellow and Division Director, Department of Plant Protection and Utilization, Fengshan Tropical Horticultural Experiment Branch, Taiwan Agricultural Research Institute, Kaohsiung, Taiwan, ROC.
[4] Research Fellow and Division Director, Crop Genetic Resources and Biotechnology Division, Taiwan Agricultural Research Institute, Taichung City, Taiwan, ROC.

of single-stranded RNA (ssRNA) encapsulated in stable, rod-shaped particles, approximately 300 nm long, known for their remarkable stability (Knapp & Lewandowski 2001). Generally, TMV-infected pepper plants exhibit chlorotic mosaic leaves, and stunted growth with distortion of younger leaves and fruits. In the case of pepper mild mottle virus (PMMoV) infection of pepper, leaf symptoms are typically mild, and may remain asymptomatic, but the virus causes striking symptoms on the fruit. These tobamovirus epidemics significantly reduce both the yield and quality of pepper production. ToMV has a broad host range, including members of the Solanaceae family such as tomatoes and peppers (Broadbent 1976).

Multiplex reverse transcription-polymerase chain reaction (multiplex RT-PCR) is a widely adopted technique known for its speed, reliability, and cost-effectiveness in simultaneously detecting multiple viruses (Viganó & Stevens 2007; Deb & Anderson 2008; Wei *et al*. 2009). In this study, we present a specific and sensitive multiplex RT-PCR method capable of simultaneously detecting and differentiating three tobamoviruses, PMMoV, TMV, and ToMV in pepper crops.

MATERIALS AND METHODS

Virus sources and cDNA clones

Virus isolates of PMMoV, TMV, ToMV, potato virus Y (PVY), pepper mottle virus (PepMoV), potato virus X (PVX), and cucumber mosaic virus (CMV) were kindly provided by Dr. Ting-Ching Deng (former virus specialist in Plant Pathology Division, Taiwan Agricultural Research Institute), and were maintained in tobacco (*Nicotiana benthamiana*) in the greenhouse (Cheng *et al*. 2013). The experiments were conducted at the Virus and Bacteria Laboratory, Division of Plant Pathology, Taiwan Agricultural Research Institute, Taiwan. The viruses were introduced to tomato or bell pepper plants (*Capsicum annuum*) by grinding with ten times the amount (w/v) of potassium phosphate buffer (0.01 M $KHPO_4$, pH 7.0). Disease symptoms were observed, and leaves were collected 6 wk after virus inoculation and used for confirmation via RT-PCR. RT-PCR products that were amplified using primers designed for the detection of PMMoV, ToMV, and TMV (Table 1, referred to as tobamo3/tobamo2 or tobamo2.1R) underwent purification. This purification step was carried out using a PCR DNA Purification Kit (Promega, Madison, WI, USA), following the manufacturer's instructions. Subsequently, these purified products were cloned into the pGEM-T vector (Promega, Madison, WI, USA). The generated plasmids were named pEASY-PMMoV, pEASY-ToMV, and pEASY-TMV. Each plasmid contained inserts of the expected size corresponding to PCR products PMMoV, TMV, and ToMV. These plasmids were used in multiplex PCR experiments.

RNA extraction

One hundred milligrams of fresh tomato or bell pepper leaves were ground in liquid nitrogen and used to extract total RNA according to the operation manual (Trizol reagent, Invitrogen, Carlsbad, CA, USA). The extracted total RNA was resuspended in 50 μL of diethyl pyrocarbonate (DEPC)-treated water and stored at -80℃ and was used for subsequent experiments.

Table 1. Nucleotide sequences of primers use in this study[z].

Primer/probe	Sequence (5′-3′)	Product (bp)	Tm (℃)	Reference
Tobamo3 (F)	5′-CAR ACN ATW GTB TAY CA-3′	540	50	Gibbs *et al*. 2004
Tobamo2 (R)	5′-TTB GCYTCR AAR TTC CA-3′	540	50	Gibbs *et al*. 2004
Tobamo2.1R	5′-TTB GCY TCA AAA TTC CA-3′	540	50	This study
PMMoV-Rp-0521-F	GCTTTTTGGTCCTGTATTTTCAGAAT			This study
ToMV-Rp-0521-F	TACAACTTTTATCGGTAATACC			This study
TMV-Rp-0521-F	TACCGCAGGTATAAAAACTTGCATC			This study

[z] bp: base pairs; PMMoV: pepper mild mottle virus; ToMV: tomato mosaic virus; TMV: tobacco mosaic virus.

Primer selection and optimization of multiplex RT-PCR

To ensure the specificity and efficiency of the multiplex RT-PCR method, previously published tobamovirus primers, tobamo2, and tobamo3 (Gibbs *et al*. 2004), were initially utilized. However, for increasing specificity, new species-specific primers, PMMoV-Rp-0521-F, TMV-Rp-0521-F, and ToMV-Rp-0521-F, were designed based on the alignment of the RNA-dependent RNA polymerase (RdRp) gene sequences of PMMoV, TMV, and ToMV obtained from the National Center for Biotechnology Information (NCBI) GenBank (Fig. 1, Fig. 2, and Fig. 3). These primers were combined with tobamo2.1, modified from tobamo2, for multiplex RT-PCR

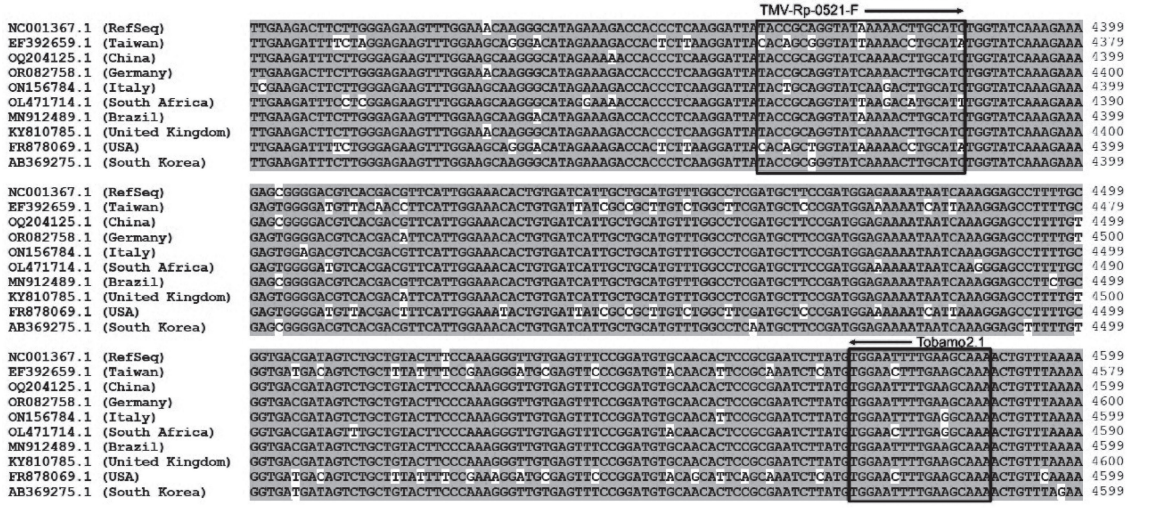

Fig. 1. Sequences alignment of tobacco mosaic virus and the position of the designed primers (shown in black box). Accession numbers for the virus isolates (top to bottom) are NC001367.1, EF392659.1, OQ204125.1, OR082758.1, ON156784.1, OL471714.1, MN912489.1, KY810785.1, FR878069.1, and AB369275.1. The design of the primers was based on the conserved sequences within the RNA-dependent RNA polymerase (RdRp) gene.

Fig. 2. Sequences alignment of tomato mosaic virus and the position of the designed primers (shown in black box). Accession numbers for the virus isolates (top to bottom) are NC002692.1, KJ207374.1, KR537870.1, ON156781.1, OL652662.1, MW848529.1, MW012409.1, LC650928.1, and KU321698.1. The design of the primers was based on the conserved sequences within the RNA-dependent RNA polymerase (RdRp) gene.

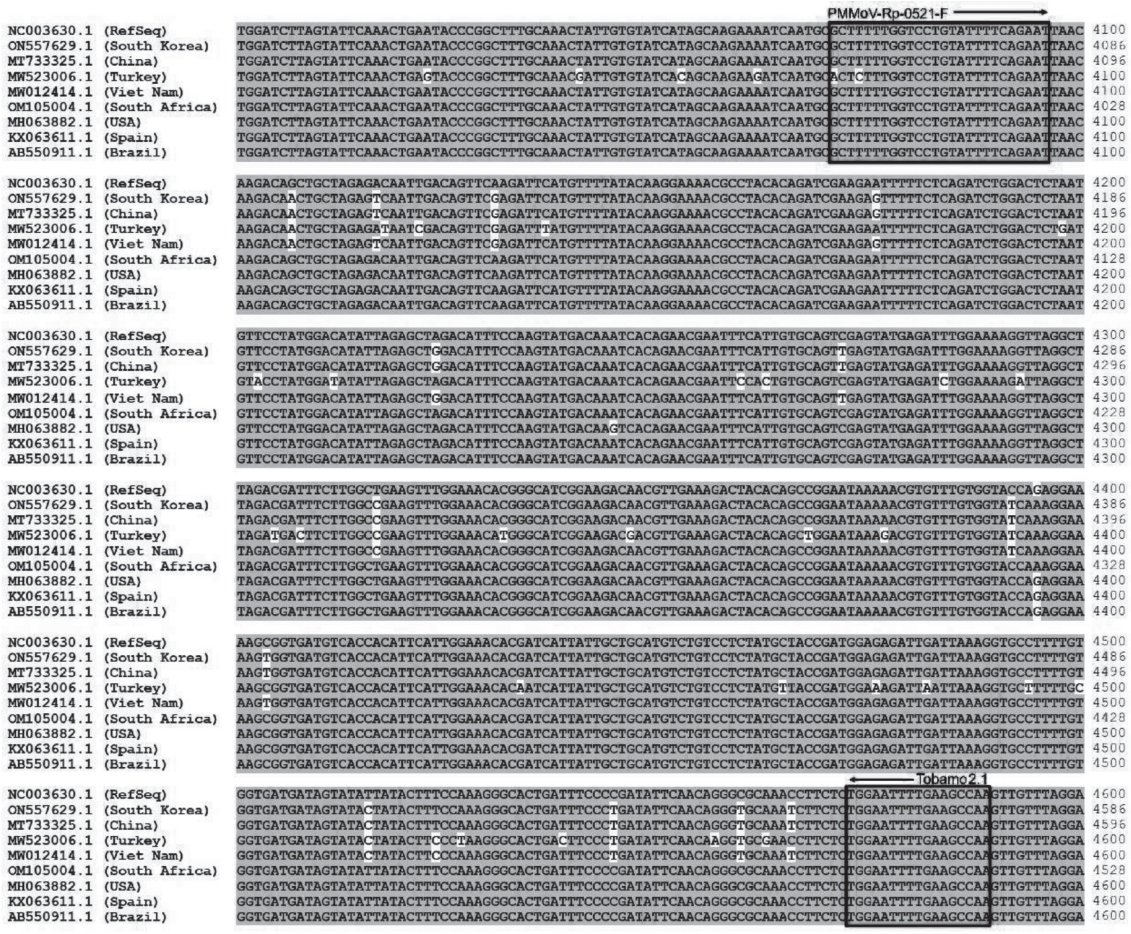

Fig. 3. Sequences alignment of pepper mild mottle virus and the position of the designed primers (shown in black box). Accession numbers for the virus isolates (top to bottom) are NC003630.1, ON557629.1, MT733325.1, MW523006.1, MW012414.1, OM105004.1, MH063882.1, KX063611.1, and AB550911.1. The design of the primers was based on the conserved sequences within the RNA-dependent RNA polymerase (RdRp) gene.

(Fig. 4). To optimize the multiplex PCR reaction, different combinations of primer ratios and concentrations were tested. The concentration ranges for each primer were as follows: 0.1–0.15 μM of PMMoV-Rp-0521-F, 0.2–0.4 μM of TMV-Rp-0521-F, 0.1–0.4 μM of ToMV-Rp-0521-F, and 0.4 μM of tobamo2.1R. In a 25 μL RT reaction, 2 μg of total RNA extracted from bell pepper or tomato leaves and 1 μL of random hexamer primers (50 μM) were mixed thoroughly and incubated at 70℃ for 5 min, then placed on ice. Subsequently, 5 μL of 5× first-strand buffer (Promega, Madison, WI, USA), 5 μL of 10 mM dNTPs, 1 μL of Moloney murine leukemia virus (MMLV) reverse transcriptase (200 U) (Promega), and 1 μL of recombinant ribonuclease (RNasin) ribonuclease inhibitor (25 U) (Promega) were added. Make up the volume to 25 μL with sterile water, and allow the reaction to proceed for 60 min at 42℃. In the PCR reaction, 2.5 μL of 10× PCR buffer (Protech, Taipei, Taiwan), 0.5 μL of 10 mM dNTPs, 0.5 μL each of the primers: PMMoV-Rp-0521-F (0.1–0.15 μM), TMV-Rp-0521-F (0.2–0.4 μM), ToMV-Rp-0521-F (0.1–0.4 μM), and tobamo2.1R (0.4 μM), and 2 μL of the cDNA template were mixed, and adjust the volume to 25 μL with ddH_2O. The PCR reaction

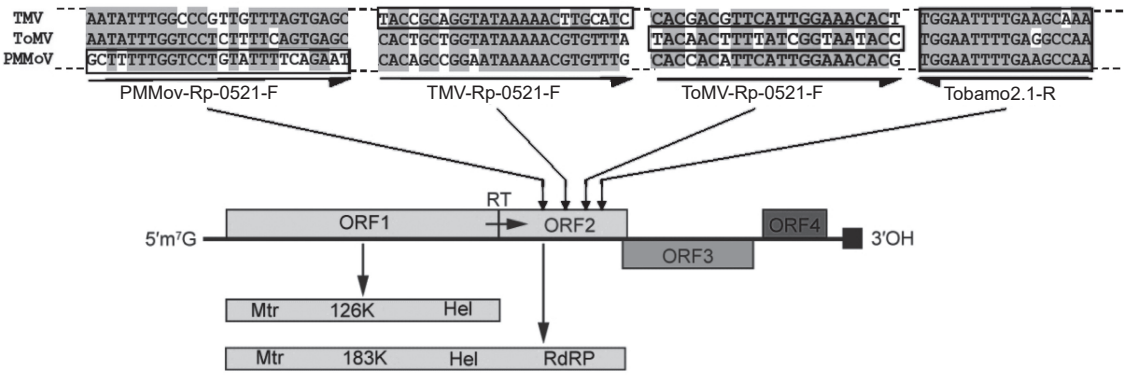

Fig. 4. A schema showing the genome organization of the four predicted open reading frames (ORFs) of a tobamovirus and the positions of the designed primers. RT: reverse transcription.

conditions are set as initial denaturation at 95℃ for 5 min, followed by 30 cycles of denaturation at 95℃ for 30 s, annealing at 55℃ for 30 s, and extension at 72℃ for 30 s. Finally, the reaction was extended at 72℃ for 5 min and held at 16℃ to complete the reaction. To analyze the PCR products, 5 μL of the reaction mixture was subjected to 1.5% agarose gel electrophoresis. A gel imaging system (Bio-Rad, Hercules, CA, USA) was used to visualize and document the electrophoresis results.

Specificity assay of multiplex RT-PCR

To assess the specificity of multiplex RT-PCR for PMMoV, ToMV, and TMV, samples collected from bell pepper or tomato plants infected with PMMoV, ToMV, TMV, PVY, PepMoV, PVX, or CMV, along with samples from healthy bell pepper or tomato plants were tested. Total RNA extracted from these samples was subjected to RT-PCR using mixed primers under the same reaction conditions as described above.

Sensitivity assay of multiplex PCR

To evaluate the sensitivity of multiplex RT-PCR in detecting PMMoV, TMV, and ToMV, this study employed a methodology involving cloned plasmid DNA containing fragments of these viral genes. The plasmids were mixed in equal proportions, and sensitivity was assessed using a series of 10× dilutions ranging from 1 × 10^2 to 1 × 10^{10} copies. These dilutions were created by combining the viral gene-selected plasmids with pEASY-PMMoV, pEASY-ToMV, and pEASY-TMV at individual concentrations of 50 ng μL^{-1}. Subsequently, 5 μL of the PCR product was extracted for analysis through 1.5% agarose gel electrophoresis. The electrophoresis results were visualized using a gel imaging system (Bio-Rad, Hercules, CA, USA).

Evaluation of mixed viruses in pepper samples using multiplex RT-PCR

Bell peppers infected with PMMoV and TMV, and tomatoes infected with ToMV were utilized in this study. Approximately 0.1 g of leaf tissue from each infected sample was collected and subjected to RNA extraction following the total RNA purification described above. These extracted total RNAs were divided into 3 sets: one for each virus (PMMoV, TMV, and ToMV), another set combining 2 viruses (PMMoV + TMV, TMV + ToMV, and ToMV + PMMoV), and the third set containing all 3 viruses (PMMoV + TMV + ToMV). These RNA sets were subjected to RT-PCR reactions as described above.

RESULTS

Optimization of the RT-PCR assay

To assess the suitability of the newly designed species-specific primers (PMMoV-Rp-

0521-F, TMV-Rp-0521-F, and ToMV-Rp-0521-F) in combination with the universal *Tobamovirus* primer (tobamo2.1), a series of experiments were conducted. Initially, it was confirmed that PMMoV, TMV, and ToMV could be all amplified by PCR using the universal *Tobamovirus* primer pair tobamo2/tobamo3 (data not shown) (Gibbs *et al*. 2004). Subsequently, the newly designed species-specific primers were tested in combination with tobamo2.1 for multiplex RT-PCR. Several primer ratios at different mixing concentrations were explored to optimize the PCR reaction conditions (Fig. 5). The optimal primer concentration combination for multiplex RT-PCR was determined to be PMMoV : ToMV : TMV : tobamo2.1 = 0.15 : 0.2 : 0.3 : 0.4. Using this combination, the PCR products for PMMoV, ToMV, and TMV were specifically amplified, resulting in amplicon sizes of 519 base pairs (bp) for PMMoV, 228 bp for TMV, and 177 bp for ToMV (Fig. 5).

Specificity of the RT-PCR for tobamovirus detection

The findings indicated that the merged primers could generate a 519-bp product when subjected to PCR with PMMoV. Additionally, a 228-bp product was yielded when employed in PCR with TMV, and a 177-bp product was obtained when utilized in PCR with ToMV. Each multiplex RT-PCR did not react with PVY, PepMoV, PVX, or CMV as well as healthy bell

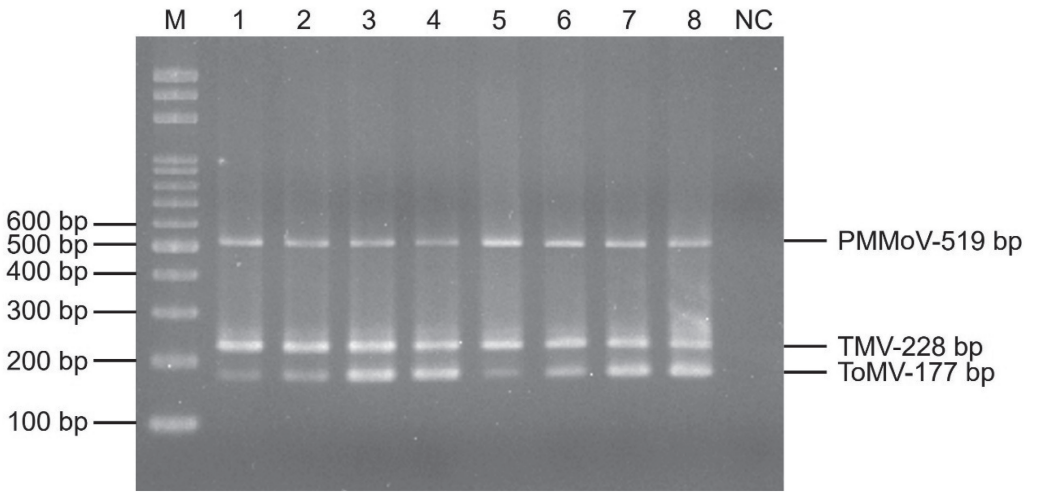

	1	2	3	4	5	6	7	8
PMMoV	0.1	0.1	0.1	0.1	0.15	0.15	0.15	0.15
TMV	0.4	0.4	0.4	0.4	0.2	0.2	0.2	0.2
ToMV	0.1	0.2	0.3	0.4	0.1	0.2	0.3	0.4
Tobamo 2.1	0.4	0.4	0.4	0.4	0.4	0.4	0.4	0.4

Fig. 5. Optimization of multiplex reverse transcription-polymerase chain reaction (multiplex RT-PCR) with different concentration ratios of primer set. Total RNA of mix-infected sweet pepper plants was used for multiplex RT-PCR amplification. The primer concentration ratio of each treatment is shown at the lower panel of the figure. The number indicates the concentration (μM) of each primer pair in a PCR reaction. The RT-PCR products of tobamoviruses identified by 1.5% agarose gel electrophoresis are indicated by arrows. Lane M: 100 base pairs (bp) DNA ladder (Invitrogen, Carlsbad, CA, USA); Lane NC: no template control.

peppers and tomatoes. Furthermore, no primer dimers were formed in the nucleic acid amplification products (Fig. 6).

Sensitivity of the multiplex PCR

To determine the detection limit of multiplex PCR, the products of PMMoV, TMV, and ToMV amplified by PCR were cloned into plasmid DNA. A plasmid mix containing these clones was prepared, and a 10× serial dilution, ranging from 10^9 to 10^0 copies in 10 sets, along with a no template control (NC), was used to assess the sensitivity of the multiplex PCR. Sensitivity was tested using the PCR method, and the results showed that the sensitivity could reach as low as 10^4 copies (Fig. 7).

Detection of the three tobamoviruses in plant samples

To evaluate the performance of the established multiplex RT-PCR, artificially mixed viral RNAs extracted from infected plants

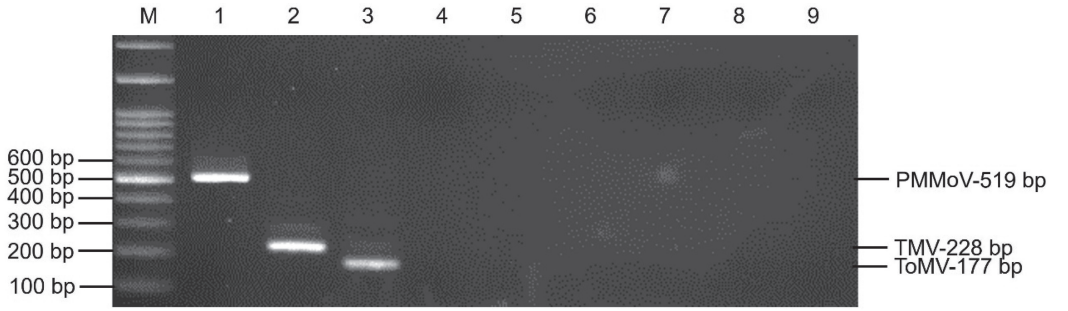

Fig. 6. Specificity of multiplex reverse transcription-polymerase chain reaction (multiplex RT-PCR) for detection of pepper mild mottle virus (PMMoV), tomato mosaic virus (ToMV) and tobacco mosaic virus (TMV). Lane M: 100 base pairs (bp) DNA ladder; Lane 1: PMMoV; Lane 2: ToMV; Lane 3: TMV; Lane 4: potato virus Y (PVY); Lane 5: pepper mottle virus (PepMoV); Lane 6: potato virus X (PVX); Lane 7: cucumber mosaic virus (CMV); Lane 8: healthy bell pepper; Lane 9: healthy tomato.

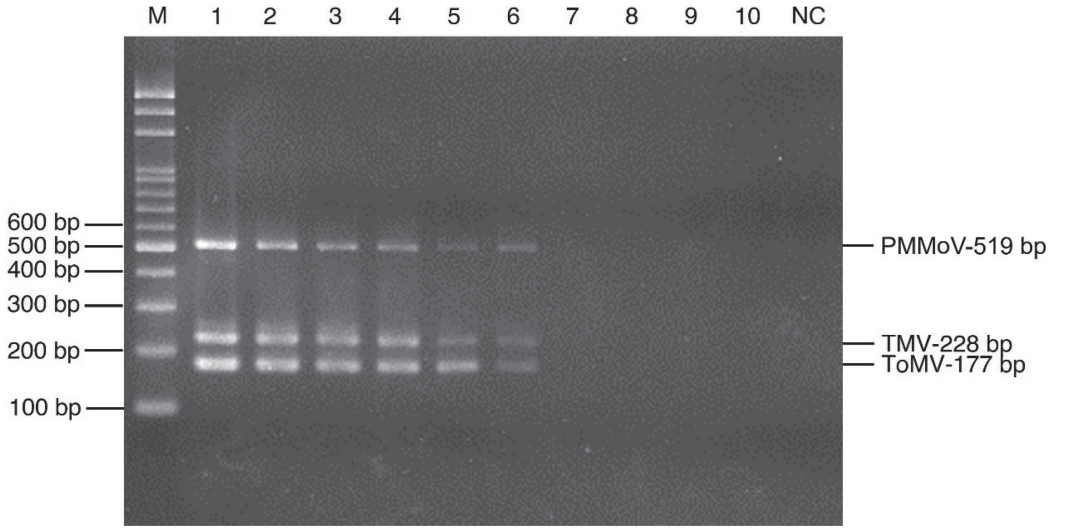

Fig. 7. Estimation of the detection limit of multiplex PCR for pepper mild mottle virus (PMMoV), tobacco mosaic virus (TMV), and tomato mosaic virus (ToMV) using 10× serial dilutions of viral clones. Lane M: 100 base pairs (bp) DNA ladder; Lane NC: no template control; Lane 1–10: 10^9–10^0 copies of viral RNA-dependent RNA polymerase (RdRp) genes.

were tested. The results demonstrated that the multiplex RT-PCR could detect various combinations of mixed virus RNA extracts. Specifically, it successfully detected the presence of PMMoV RNA, TMV RNA, ToMV RNA, PMMoV + TMV RNAs, TMV + ToMV RNAs, and ToMV + PMMoV RNAs, as well as the combination of PMMoV + TMV + ToMV RNAs. These detections resulted in the generation of target fragments of 519 bp (PMMoV), 228 bp (TMV), and 177 bp (ToMV). Importantly, no false-positive reactions were observed when healthy bell pepper plants were tested (Fig. 8).

DISCUSSION

The PCR-based method has become a general and routine virus diagnostic method, capable of confirming specific viral infections. If combined with multiplex RT-PCR, it can be used to detect multiple viruses at the same time, offering advantages of speed, reliability, cost reduction, and shorter processing time (Viganó & Stevens 2007; Deb & Anderson 2008; Wei *et al*. 2009). Our study marks the first instance of using the RdRp gene to identify three different tobamoviruses. In general, detecting multiple viruses simultaneously requires 6 primers (3 primer pairs), but our assay only requires 4 primers while maintaining specificity for distinguishing and identifying these three viruses.

Gibbs *et al*. (1998) developed an RT-PCR detection method using a pair of RdRp region-specific primers based on the conservative RNA sequence of tobacco mosaic virus. However, their evaluation was limited to the use of a hybridization-based method. Vinayarani *et al*. (2011) previously established a multiplex RT-PCR detection method for distinguishing TMV and ToMV in chili varieties. Nemes & Salánki (2020) simultaneously detected five viruses (CMV, TMV, PMMoV, PVY, and tomato spot wilt virus (TSWV)) in sweet peppers, but they did not simultaneously detect PMMoV, TMV, and ToMV. Moreover, their results could only detect 2 tobamovirus-related viruses. Currently, differentiating these three viruses by conventional methods remains challenging, except through nucleic acid sequencing.

Another approach employs a universal RT-PCR assay using 2 degenerate primers (Letschert *et al*. 2002), but it can only detect members of tobamoviruses (i.e., TMV, ToMV, PMMoV, Odontoglossum ringspot virus, and tobacco mild green mosaic virus). Dovas *et al*. (2004) described a point-nested reverse transcriptase-polymerase chain reaction-restriction fragment length polymorphism (RTPCR-RFLP) method for TMV detection. However, this

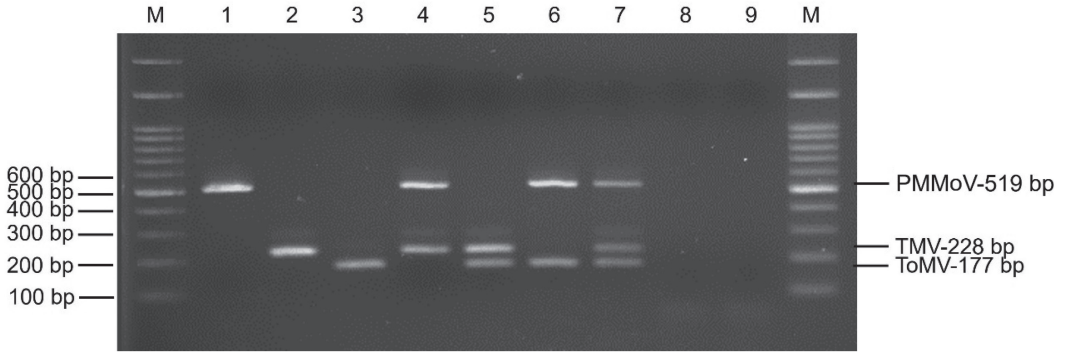

Fig. 8. Multiplex RT-PCR detection of pepper-infecting viruses, pepper mild mottle virus (PMMoV), tobacco mosaic virus (TMV), or tomato mosaic virus (ToMV) from pepper leaves in artificial combinations of infections using mixed RNAs. Lane M: DL2000 DNA Marker; Lane 1: PMMoV RNA; Lane 2: TMV RNA; Lane 3: ToMV RNA; Lane 4: PMMoV + TMV RNAs; Lane 5: TMV + ToMV RNAs; Lane 6: ToMV + PMMoV RNAs; Lane 7: PMMoV + TMV + ToMV RNAs; Lane 8: healthy bell pepper RNA; Lane 9: no template control (NC).

method is time-consuming, labor-intensive, and costly due to the repeated PCR amplification and restriction enzyme digestion. Therefore, new primer designs were tested for multiplex RT-PCR. Primer ratios are crucial factors affecting PCR specificity and amplification efficiency (Ma & Michailides, 2007; Wei *et al*. 2009). Hence, primer ratios were optimized, and our results indicated that well-designed primers can avoid the generation of primer dimers. From the above results, it can be concluded that the minimum detectable virus concentration using RT-PCR is 10^4 copies in a 25 uL reaction.

In our study, the newly developed multiplex RT-PCR can simultaneously detect and differentiate PMMoV, TMV, and ToMV using three specific forward primers PMMoV-Rp-0521-F, TMV-Rp-0521-F, and ToMV-Rp-0521-F, combining a universal reverse primer tobamo2.1R. This multiplex RT-PCR method could be used for virus detection in single virus infection as well as in mixed infection. This indicates that the multiplex RT-PCR is capable of accurately identifying various mixed virus infection scenarios. In addition, the use of artificially infected bell peppers with three viruses also showed that this combination of primer pairs can simultaneously detect the three viruses. The method we developed offers a simple and convenient approach to developing multiplex assays based on previously published primers and can be supplemented with newly designed primers when necessary. This specific and sensitive method for detecting multiple tobamoviruses in the Solanaceae family is suitable for large-scale sampling efforts to study the distribution of tobamoviruses in Taiwan and other regions worldwide. This detection technique can facilitate research in tobamovirus epidemiology, outbreak monitoring, and the study of interactions between viruses, hosts, and vectors.

REFERENCES

Broadbent, L. 1976. Epidemiology and control of Tomato mosaic virus. Annu. Rev. Phytopathol. 14:75–96. doi:10.1146/annurev.py.14.090176.000451

Cheng, Y. H., T. C. Deng, C. C. Chen, C. P. Kuan, and C. A. Chang. 2013. Identification and occurrence of Pepper mottle virus isolated from peppers in Taiwan. J. Taiwan Agric. Res. 62:360–371. (in Chinese with English abstract) doi:10.6156/ JTAR/2013.06204.06

Deb, M. and J. M. Anderson. 2008. Development of a multiplexed PCR detection method for *Barley* and Cereal yellow dwarf viruses, Wheat spindle streak virus, Wheat streak mosaic virus and Soil-borne wheat mosaic virus. J. Virol. Methods 148:17–24. doi:10.1016/j.jviromet.2007.10.015

Dovas, C. I., K. Efthimiou, and N. I. Katis. 2004. Generic detection and differentiation of tobamoviruses by a spot nested RT-PCR-RFLP using dI-containing primers along with homologous dG-containing primers. J. Virol. Methods 117:137–144. doi:10.1016/j.jviromet.2004.01.004

Gibbs, A., J. Armstrong, and M. Gibbs. 2004. A type of nucleotide motif that distinguishes tobamovirus species more efficiently than nucleotide signatures. Arch. Virol. 149:1941–1954. doi:10.1007/s00705-004-0346-3

Gibbs, A., J. Armstrong, A. M. Mackenzie, and G. F. Weiller. 1998. The GPRIME package: Computer programs for identifying the best regions of aligned genes to target in nucleic acid hybridisation-based diagnostic tests, and their use with plant viruses. J. Virol. Methods 74:67–76. doi:10.1016/s0166-0934(98)00070-6

Jones, R. A. C. 2021. Global plant virus disease pandemics and epidemics. Plants 10:233. doi:10.3390/plants10020233

Knapp, E. and D. J. Lewandowski. 2001. Tobacco mosaic virus, not just a single component virus anymore. Mol. Plant Pathol. 2:117–123. doi:10.1046/j.1364-3703.2001.00064.x

Letschert, B., G. Adam, D. E. Lesemann, P. Willingmann, and C. Heinze. 2002. Detection and differentiation of serologically cross-reacting tobamoviruses of economical importance by RT-PCR and RT-PCR-RFLP. J. Virol. Methods 106:1–10. doi:10.1016/S0166-0934(02)00135-0

Ma, Z. and T. J. Michailides. 2007. Approaches for eliminating PCR inhibitors and designing PCR primers for the detection of phytopathogenic fungi. Crop Prot. 26:145–161. doi:10.1016/j.cropro.2006.04.014

Moury, B. and E. Verdin. 2012. Viruses of pepper crops in the Mediterranean basin: A remarkable stasis. Adv. Virus Res. 84:127–162. doi:10.1016/B978-0-12-394314-9.00004-X

Nemes, K. and K. Salánki. 2020. A multiplex RT-PCR

assay for the simultaneous detection of prevalent viruses infecting pepper (*Capsicum annuum* L.). J. Virol. Methods 278:113838. doi:10.1016/j.jviromet.2020.113838

Rosario, K., C. Nilsson, Y. W. Lim, Y. Ruan, and M. Breitbart. 2009. Metagenomic analysis of viruses in reclaimed water. Environ. Microbiol. 11:2806–2820. doi:10.1111/j.1462-2920.2009.01964.x

Spence, N. J., I. Scaly, P. R. Mills, and G. D. Foster. 2001. Characterization of a tobamovirus from trailing petunias. Eur. J. Plant Pathol. 107:633–638. doi:10.1023/A:1017980712521

Viganó, F. and M. Stevens. 2007. Development of a multiplex immunocapture-RT-PCR for simultaneous detection of BMYV and BChV in plants and single aphids. J. Virol. Methods 146:196–201. doi:10.1016/j.jviromet.2007.06.018

Vinayarani, G., K. N. Madhusudhan, S. A. Deepak, S. R. Niranjana, and H. S. Prakash. 2011. Detection of mixed infection of tobamoviruses in tomato and bell pepper by using RTPCR and duplex RT-PCR. Intl. J. Plant Pathol. 2:89–95. doi:10.3923/ijpp.2011.89.95

Wei, T., G. Lu, and G. R. G. Clover. 2009. A multiplex RT-PCR for the detection of Potato yellow vein virus, Tobacco rattle virus and Tomato infectious chlorosis virus in potato with a plant internal amplification control. Plant Pathol. 58:203–209. doi:10.1111/j.1365-3059.2008.01979.x

使用多重 RT-PCR 檢測和區分 3 種感染甜椒病毒

關政平[1,*]　蕭崇仁[2]　鄭櫻慧[3]　陳述[4]

摘要

關政平、蕭崇仁、鄭櫻慧、陳述。2024。使用多重 RT-PCR 檢測和區分 3 種感染甜椒病毒。台灣農業研究 73(2):89–99。

本研究利用多重反轉錄聚合酶鏈鎖反應 (multiplex reverse transcription-polymerase chain reaction; multiplex RT-PCR) 方法，同時檢測與區分感染甜椒的 3 種 tobamoviruses，分別是辣椒輕斑駁病毒 (pepper mild mottle virus; PMMoV)、菸草嵌紋病毒 (tobacco mosaic virus; TMV) 及番茄嵌紋病毒 (tomato mosaic virus; ToMV)。使用 1 種用於檢測所有 tobamoviruses 的通用引子與 3 種病毒專一性引子透過分析 PCR 引子比率，對這 3 種目標病毒的擴增進行調整。產生的 PCR 產物由不同的片段組成：PMMoV 為 519 base pairs (bp)，TMV 為 228 bp 及 ToMV 為 177 bp。本方法表現出高度的專一性，沒有與其他非目標甜椒病毒擴增產生特定的產物。此外，multiplex RT-PCR 已被證明是對檢測甜椒植物中多種 tobamoviruses，為一種特異性、靈敏且經濟有效的方法。

關鍵詞：辣椒輕斑駁病毒、菸草嵌紋病毒、番茄嵌紋病毒、偵測。

投稿日期：2023 年 12 月 12 日；接受日期：2024 年 3 月 14 日。
* 通訊作者：pcr123@tari.gov.tw
[1] 農業部農業試驗所遺傳資源及生物技術組副研究員。臺灣 臺中市。
[2] 農業部農業試驗所遺傳資源及生物技術組計畫助理。臺灣 臺中市。
[3] 農業部農業試驗所鳳山熱帶園藝試驗分所植物保護及園產品加工系研究員兼系主任。臺灣 高雄市。
[4] 農業部農業試驗所遺傳資源及生物技術組研究員兼組長。臺灣 臺中市。

台灣農業研究 (J. Taiwan Agric. Res.) 73(2):101–111 (2024)
https://doi.org/10.6156/JTAR.202406_73(2).0003

研究報告

檬果果實套袋防治炭疽病效果之預測技術開發

莊再揚[1] 呂理燊[2] 高清文[3] 楊宏仁[4] 蔡志濃[5,*] 楊秀珠[2] 安寶貞[6,*]

摘要

莊再揚、呂理燊、高清文、楊宏仁、蔡志濃、楊秀珠、安寶貞。2024。檬果果實套袋防治炭疽病效果之預測技術開發。台灣農業研究 73(2):101–111。

炭疽病與蒂腐病為檬果果實的重要病害，也是外銷上重要的限制因子，因此能早期預測病害發生情形，有利於外銷檬果的品質保證，避免造成損失。利用益收生長素 (Ethephon, 2-chloro-ethylphosphonic acid) (39.5% 溶液) 3,000 倍稀釋液噴霧或浸漬硬核期「愛文」檬果果實 5 min，再將果實置於 30℃密閉環境下，果實若已經被炭疽病菌感染，將於處理後 3–5 d 開始陸續出現炭疽病之病斑，再調查處理後第 9 天與 12 天之發病果實率，用此方法可以預估一個果園中套袋果實成熟後之大約罹病率。使用此法時，果實必須生長至其最大體積 (硬核期) 之後 (大約在果實成熟前 1 mo 左右)，否則果實不易轉色，病斑不會出現。果實經生理落果期結束後套袋，而調查之果實於成熟前 15–30 d 再採收，再經益收生長素處理 9–12 d 後，再調查完全轉色之果實發病率，如果單果炭疽病平均發病病斑數在 2 個以下 (發病率在 20% 以下)，且蒂腐病病斑數平均在 1 個以下 (罹病率在 10% 以下)，但合計發病率須在 20% 以下，該果園才可被選為合格之外銷供果園，檬果果實可於 9 分熟時採收，進行外銷處理作業。

關鍵詞：檬果炭疽病、潛伏感染、益收生長素、病害預測、非農藥防治。

前言

炭疽病 (anthracnose) (由 *Colletotrichum* spp. 引起) 為蔬果花卉的重要病害，尤其在熱帶與亞熱帶地區為造成儲藏期果實腐敗重要原因之一 (Cook 1975)。在臺灣，炭疽病為經濟果樹檬果的最重要病害 (Ann *et al*. 1994, 2013)，尤其「愛文」品種十分感病 (Leu *et al*. 1996)，病菌自開花至果實成熟期均可侵染寄主，罹病組織經常出現黑點與黑斑及落花、落果情形，嚴重影響檬果之結實率；更有甚者，病菌經常行『潛伏感染』(Simmonds 1941; Verhoeff 1974)，在果實採收後熟後才陸續出現病斑 (Baker *et al*. 1940; Simmonds 1963)，造成果實腐敗，嚴重影響檬果果實之櫥架壽命與經濟價值，也是當時 (1990 年代之前) 臺灣檬果外銷的限制因子。而套袋對檬果炭疽病確實有良好之防治效果，且以愈早套袋之防治效果愈佳 (Ann *et al*. 1994, 1996, 2013)，幼果期即予以套袋之處理在採果後 12 d 之發病率為 0–5%，生理落果時套袋者為 27%，落果停止時套袋者為 42%，採果前 2 wk 者為 68%，無套袋者 (全期施藥) 則為 72%。但是，檬果在開花期與幼果期無法套袋，生理落果期終止後才開始套袋，無法預知病菌是否已經侵入而行潛伏感染。因此，如能預先偵測外觀健康之果實於採

投稿日期：2023 年 11 月 14 日；接受日期：2024 年 1 月 19 日。
* 通訊作者：tsaijn@tari.gov.tw, pjann@tari.gov.tw, pjann5039@gmail.com
[1] 前國立臺灣大學植物病理與微生物學系教授。臺灣 臺北市。
[2] 農業部農業藥物試驗所前研究員。臺灣 臺中市。
[3] 農業部農業藥物試驗所前所長。臺灣 臺中市。
[4] 農業部農業試驗所嘉義農業試驗分所前研究員兼分所長。臺灣 嘉義市。
[5] 農業部農業試驗所植物病理組研究員兼組長。臺灣 臺中市。
[6] 農業部農業試驗所植物病理組前研究員兼組長。臺灣 臺中市。

收後熟後可能出現病斑數目的有無與多寡，則可預估該果園檬果果實成熟後之發病情形，進而篩選出優良的外銷供果園採果外銷，亦為一可行之途 (Ann *et al*. 1996)。

乙烯 (ethylene, C_2H_2) 有促進果實後熟的效果，El-Kazzaz *et al*. (1983) 報告乙烯有促進貯藏期果實病原菌生長之能力，誘發病害。而 39.5% 益收生長素 (Ethephon, 2-chloro-ethylphosphonic acid) 為乙烯之先驅物，在臺灣廣泛推廣於香蕉、番茄、鳳梨、葡萄及梨等果樹果實之催熟使用 (Fei & Wang 2007)。本研究經多年試驗發現益收生長素可以使用於檬果套袋果實炭疽病的預先偵測，特此報告。

材料與方法

檬果果園管理、果實套袋及採果

試驗地點選擇臺南市玉井地區 5–20 年生之「愛文」檬果果園，且需初選田間清潔而葉部病害較少者為『外銷初選供果園』，並於果粒生長約為姆指大時進行疏果，而於果實生理落果期終止時 (果實寬度約3–5 cm) 進行套袋。將果實套白色防水紙袋 (25 cm × 15 cm)，並注意將袋口封好，避免病菌與害蟲的再侵入感染。選定試驗日期，果實於成熟前 (硬核期 (green mature)) 15–30 d 採果，每個果園隨機採收約 20–25 粒果實，套袋不可去除，需一併採回實驗室，於浸藥處理前拆除。

益收生長素處理濃度對檬果果實罹病率之影響調查

初步試驗以達硬核期 (即達果實最大生長期，約成熟前 30–45 d) 的套袋果實進行測試，而益收生長素溶液檢測的使用濃度為 1,000、2,000 及 3,000 倍稀釋液，檬果果實在浸漬益收生長素溶液 5 min 後或噴布處理後，覆蓋報紙，並置於溫度 30℃密閉空間，進行果實催熟作業，病斑調查則在生長素溶液處理後 3、6、9、12 d 進行。

益收生長素對不同成熟度檬果果實潛伏感染病害的偵測效果

以稀釋 3,000 倍益收生長素來測試不同果齡之檬果果實在處理後出現炭疽病病斑的情形，因此套袋後之檬果果實每隔 15 d 採收 1 次進行偵測，至果實成熟時為止。採收後的果實經益收生長素處理催熟後，於 3、6、9、12 d 調查果實的轉色與炭疽病、蒂腐病 (fruit stem end rot，亦稱果腐病) 的發病情形。

益收生長素處理與檬果果實病害調查

預先試驗之結果顯示稀釋 3,000 倍的 39.5% 益收生長素溶液處理為最適合使硬核期的綠色「愛文」檬果果皮轉為紅色。故每單一供試果園配製稀釋 3,000 倍的益收生長素溶液 10 L 供試驗，當果實生長達硬核期後，每果園採集 20–25 果實，浸漬前才將果實除去紙袋，果實直接浸漬於益收溶液中 5 min，撈起後，放置於鋪有 3 層報紙的塑膠籃內 (40 × 60 × 30 cm)。容器內鋪有 4–5 層報紙，上置處理後的檬果果實，其上再覆蓋 4–5 張報紙。處理後的果實放置於室溫下 (以 30℃為佳)，於翌日開始每隔 3 d 調查炭疽病與蒂腐病 (該病害的病菌並非潛伏感染病菌，可能為病菌已侵入果梗或附著於套袋上) 的發病情形，至 12 d 為止。並按下列公式計算果實炭疽病之發病果實率 (%) 與發病度 (%) (參考用)。蒂腐病以發病果實率 (%) 表示。果實以出現 1 個病斑 (大於 0.5 cm) 即算發病。炭疽病發病度之調查方法，每次調查果實上之病斑數： 0 代表未罹病；1 代表 1–5 病斑；2 代表 6–10 病斑；3 代表 11–15 病斑；4 代表 15 病斑以上者。

果實發病率 = 發病果實數/調查果實數 × 100%；果實發病度 = [(Σ 指數 × 該指數發病果實數)/4 × 全部調查果實數] × 100% (參考用)；果實成熟度之調查分為 3 級，0：未轉色、1：部分轉色、2：完全轉為紅色；果實成熟度 = [(Σ 指數 × 該指數果實數)/2 × 全部調查果實數] × 100%。

在正式實驗時，果實於生理落果期終止時套袋，套袋前噴灑甲基鋅乃浦可濕性粉劑 (Propineb 400 倍稀釋液) 與撲克拉錳可濕性粉劑 (Prochloraz-Manganese 6,000 倍稀釋液)，至果實表面藥液乾燥後，於當日或翌日 (如果施藥後未降雨) 將果實套白色紙袋，並注意將袋口封好。果實於 8 分熟時採收 (已達硬核期)，

當日即以益收生長素 3,000 倍稀釋液浸漬處理 5 min，並於採後第 3 天開始調查炭疽病與蒂腐病之發生情形。爾後，每隔 3 d 繼續調查果實上炭疽病與蒂腐病之病斑數目 1 次，至 12 d 為止。並計算果實炭疽病與蒂腐病之果實發病率 (%) 與發病度 (參考用)。

結果

套袋與病害防治

本試驗亦顯示套袋對檬果炭疽病確實有良好之防治效果 (Ann *et al*. 1998)，本試驗測試玉井李農友 1992 年之套袋果園之已達硬核期的檬果果實於益收生長素溶液處理 12 d 後，炭疽病發病率為 10%，蒂腐病為 0%，無病果實率為 90%，可供外銷；反之當年其未套袋果園之檬果於益收處理 12 d 後，炭疽病發病率為 20%，蒂腐病為 40%，無病果實率僅有 50%，外銷 (無病果實率須在 80% 以上) 即不合格。尤其配合早期套袋與田間管理之果園 (含自動進行套袋地區)，炭疽病在所有臺南市「愛文」檬果主要生產區 (包括玉井、南化及左鎮) 之發生均較往年降低。

益收生長素對不同成熟度檬果果實潛伏感染病害的偵測效果

以益收生長素 3,000 倍稀釋液處理不同生長期之「愛文」檬果果實 5 min，發現果實在生長至硬核期 (此時已達其最大體積，約在採收前 30–45 d) 以後，於室溫下 (約 30℃) 經 3–5 d，果實便會開始轉色，並且逐漸出現病斑 (圖 1)。然而，果實之果齡如果太年輕，或未達硬核期，益收生長素處理後之果實完全不能轉色，或有部分果實不能轉色 (圖 2)，一般不轉色之果實亦不出現病斑，而延後轉色的果實的病斑出現亦較晚，因而嚴重影響預測結果。

益收生長素處理對潛伏感染病害的偵測效果評估

利用益收生長素溶液處理已達硬核期之檬

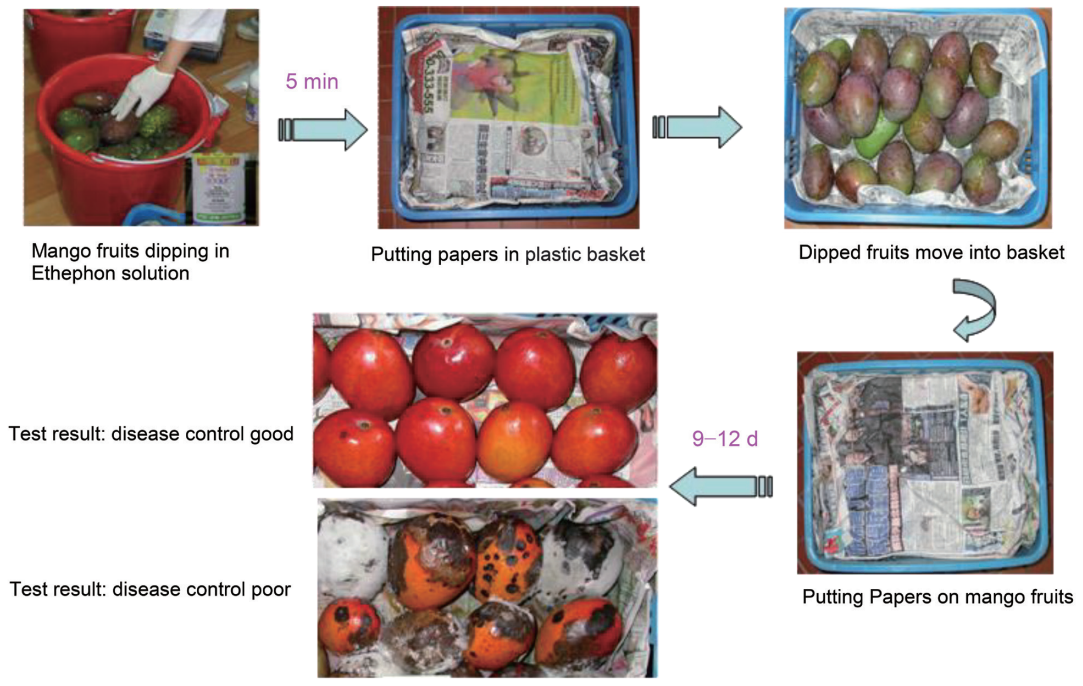

圖 1. 「愛文」檬果經稀釋 3,000 倍之益收生長素處理，9 d 後轉色果實出現炭疽病之情形。

Fig. 1. Nine days after Ethephon (3,000×) treatment, green mature fruits of 'Irwin' mango turned red and appeared anthracnose spots.

圖 2. 未達硬核期之「愛文」檬果經益收生長素處理 9 d 後仍未能轉色 (綠色果實部分) 或僅部分轉色之情形。
Fig. 2. Nine days after Ethephon treatment, the expending-stage 'Irwin' mango fruits kept green or turned red incompletely.

果果實，發現不同果園果實出現炭疽病病斑之情形差異極大，在處理 9–12 d 後，發病果實率可從 0% (完全健康) 至 100% 不等。計算 1992、1993、1994 及 1995 年調查初選供果果園之果實病害發病率 (表 1–4)，其果實平均發病率列於表 5，除 1992 年較差外，1993、1994 及 1995 年之結果均大致相似，但由於每年均有新果農加入參選，新果農之果實一般發病率較嚴重，整合計算果實發病率有逐年降低之現象。在調查果實經益收生長素溶液催熟處理 12 d 以後，1992 年度初選檬果供果園果實之平均炭疽病罹病率為 22.4%，蒂腐病率為 28.9%，無病果率為 63.3%，合格率約為 36.1%，顯示當時 (1993–1995 年) 農民對檬果果實炭疽病之防治已有顯著之進步。由於每年新增加之供果園為數不少，且有部分果園因管理不佳而退出，因而每年之供果園數變易甚大。此外，果園與果園間之罹病率差異甚大，顯示不同果園在管理上仍有相當之差異。尤其有些果園在不同年度間之發病率差異亦甚大，據農民所言，只要在防治上稍一疏忽 (如一次降雨後延誤或來不及施藥)，就可能使當年之檬果罹患嚴重的炭疽病。

討論

在熱帶與亞熱帶地區，炭疽病目前仍為檬果的最重要病害 (Uddin *et al*. 2018)，由於該病害之病原菌有潛伏感染的特性，病斑經常在果實成熟後才出現，便成為儲藏期果實腐敗之主要原因之一 (Cook 1975)。在臺灣，檬果中最受歡迎的品種「愛文」對炭疽病非常感病，病害非常嚴重，近年來仍建議以早期套袋的方式保護果實 (Ann *et al*. 1998, 2013)，以隔絕病蟲害侵染。由於果實套袋後，病菌無法入侵，病斑數目即不再增加，基於此項原理，本文發表開發『潛伏感染病害的預先偵測技術』，來推測採收後果實的可能出現病斑的情形，以篩選優良的檬果外銷供果園。

有關潛伏感染病害的偵測，Parris & Jones (1941) 曾報告溴化甲烷 (methyl bromide, $BrCH_3$) 可用來偵測豆子的炭疽病，顯示潛伏感染病害可經由某些化學物質之處理與刺激，而提前表現病徵。由於溴化甲烷為一種劇毒物質，較不適宜用於偵測檬果炭疽病，且國際間已禁用溴化甲烷，臺灣亦自 2019 年後只允許檢疫燻蒸處理使用。而 Cerkauskas & Sinclair (1980) 利用殺草劑巴拉刈 (paraquat) 處理來檢測大豆

表 1. 1992 年臺南市玉井地區自檬果外銷初選供果園採收之硬核期「愛文」檬果套袋果實經益收生長素 3,000 倍稀釋液預先處理後，果實炭疽病與蒂腐病的陸續發病情形 (%)。

Table 1. The prediction data of disease incidences of anthracnose and stem end rot of green mature 'Irwin' mango fruits treated with Ethephon solution (3,000× dilution) for 12 d. (The mango fruits were harvested from candidate orchards at Yujing, Tainan in July 1992)[z]

Farmer	Anthracnose (%)[y]						Stem end rot (%)[y]						Healthy fruit at
No.	6[x]	9	12	15	18	No.	6[x]	9	12	15	18	No.	the 12th day (%)
1	0.0	0.0	0.0	0.0	9.8	1	0.0	0.0	0.0	5.0	15.0	1	100.0
2	1.5	1.5	1.5	1.5	4.8	2	0.0	0.0	0.0	4.5	22.7	1	98.5
3	0.0	1.7	3.3	13.3	24.6	4	0.0	0.0	0.0	0.0	5.0	1	96.7
4	0.0	0.0	3.3	8.3	14.8	4	0.0	0.0	0.0	0.0	10.0	1	96.7
5	0.0	1.5	1.5	3.2	5.0	2	0.0	0.0	4.5	9.1	18.2	11	94.0
6	3.3	5.0	6.7	8.3	27.7	7	0.0	0.0	0.0	0.0	10.0	1	93.3
7	3.3	6.7	5.3	16.7	24.4	6	0.0	0.0	5.0	5.0	20.0	13	89.7
8	3.2	4.8	9.5	13.3	21.4	9	0.0	0.0	4.8	33.3	76.2	12	85.7
9	6.7	6.7	16.7	28.3	31.3	17	0.0	0.0	0.0	25.0	35.0	1	83.3
10	0.0	1.7	7.4	7.4	26.1	8	0.0	0.0	10.0	10.0	30.0	17	82.6
11	5.0	6.7	13.3	23.3	37.0	15	0.0	0.0	5.0	10.0	35.0	13	81.7
12	6.6	15.0	19.3	24.6	60.3	19	0.0	0.0	0.0	0.0	10.0	1	80.7
13	0.0	3.5	14.8	31.3	63.3	16	0.0	0.0	5.0	10.0	40.0	13	80.2
14	8.3	15.0	22.8	22.9	28.8	22	0.0	0.0	0.0	5.0	20.0	1	77.2
15	6.3	7.3	9.9	10.0		10	0.9	3.2	14.2	31.7		24	75.9
16	11.1	15.0	25.0	28.3	42.1	24	0.0	0.0	0.0	0.0	5.0	1	75.0
17	4.7	25.0	26.3	31.3	41.0	25	0.0	0.0	0.0	15.0	30.0	1	73.7
18	6.7	6.7	11.7	11.8	23.8	12	0.0	0.0	15.0	30.0	50.0	25	73.3
19	1.7	6.7	19.3	19.3	48.0	19	0.0	5.0	10.0	15.0	25.0	17	70.7
20	4.8	4.8	20.6	29.8	35.7	21	0.0	0.0	9.5	33.3	61.9	16	69.9
21	7.6	9.1	17.5	21.1	31.0	18	0.0	4.5	13.6	36.4	72.2	23	68.9
22	13.3	15.0	22.9	30.6	72.7	23	0.0	0.0	10.0	30.0	55.0	17	67.1
23	6.6	13.3	11.1	44.4	46.7	11	0.0	0.0	25.0	25.0	50.0	31	63.9
24	3.3	8.8	31.5	56.3	78.8	28	0.0	5.0	10.0	15.0	35.0	17	58.5
25	3.3	4.4	11.9	27.3	73.3	13	0.0	25.0	30.0	45.0	70.0	32	58.1
26	3.3	6.7	12.2	19.0	28.6	14	0.0	20.0	30.0	40.0	70.0	32	57.8
27	6.7	31.7	36.8	52.9	78.6	31	0.0	5.0	10.0	20.0	25.0	17	53.2
28	18.3	23.3	29.8	47.1	62.5	26	0.0	10.0	20.0	70.0	85.0	26	50.2
29	14.5	30.3	41.2	45.2	93.3	33	0.0	5.0	10.0	25.0	45.0	17	48.8
30	16.7	21.7	33.3	46.3	66.7	29	0.0	5.0	20.0	60.0	85.0	26	46.7
31	18.3	35.1	38.9	44.4	80.0	32	0.0	10.0	20.0	40.0	60.0	26	41.1
32	10.0	20.0	33.3	37.3	45.5	29	0.0	5.0	30.0	60.0	75.0	32	36.7
33	12.3	17.5	29.8	44.4	60.0	26	0.0	0.0	42.1	84.2	89.5	36	28.1
34	8.3	43.1	61.1	75.0	91.6	34	0.0	15.0	20.0	25.0	45.0	26	18.9
35	8.3	58.3	71.9	88.2	97.6	35	0.0	10.0	30.0	50.0	60.0	32	0.0
36	11.7	63.3	86.7	91.7	93.3	36	0.0	10.0	20.0	20.0	30.0	26	0.0
Check[w]	6.7	28.3	58.8	90.6	97.7		0.0	2.2	13.3	24.4	31.1		72.1

[z] Twenty fruits were taken from each candidate orchard in July 1992 which was about 25–40 d before ripening. Test fruits were dipped in 39.5% Ethephon solution (3,000×) for 5 min.
[y] % of diseased fruit (disease incidences).
[x] Days after treatment with Ethephon.
[w] Mango fruit without bagging.

表 2. 1993 年臺南市玉井地區自檬果外銷初選供果園採收之硬核期「愛文」檬果套袋果實經益收生長素 3,000 倍稀釋液預先處理後，果實炭疽病與蒂腐病的陸續發病情形 (%)。

Table 2. The prediction data of disease incidences of anthracnose and stem end rot of green mature 'Irwin' mango fruits treated with Ethephon solution (3,000× dilution) for 12 d. (The mango fruits were harvested from candidate orchards at Yujing, Tainan from May to June 1993)[z]

Farmer No.	Anthracnose (%)[y]					Stem end rot (%)[y]			Healthy fruit at the 12th day (%)
	3[x]	6	9	12	15	9[x]	12	15	
1	0	0	0	0	-[w]	0	0	-	100
2	0	0	0	0	-	0	0	-	100
3-1	0	0	0	0	0	0	0	4	100
4-1	0	0	0	4	28	0	0	0	96
5	0	0	0	0	-	0	5	-	95
6	0	0	0	0	-	0	5	-	95
7	0	0	0	5	-	0	0	-	95
8	0	0	0	5	-	5	5	-	90
9	0	0	0	0	-	0	10	-	90
10-1	0	8	8	12	16	0	0	0	88
11	0	0	5	15	-	0	0	-	85
12	0	0	10	10	-	0	5	-	85
3-2	0	5	5	10	-	5	10	-	80
10-2	0	5	15	20	-	0	0	-	80
13	0	0	5	15	-	0	5	-	80
14-1	4	8	8	12	12	0	8	12	80
14-2	0	0	20	25	-	0	0	-	75
15	0	0	15	20	-	0	5	-	75
16	12	16	24	24	24	0	4	4	72
17	0	10	10	25	-	0	5	-	70
18	0	0	10	25	-	0	5	-	70
4-2	0	10	30	35	-	0	0	-	65
19	0	0	5	10	-	10	30	-	60
20	0	5	20	30	-	5	10	-	60
21	0	10	20	25	-	10	20	-	55
22	0	10	20	45	-	0	5	-	50
23	0	5	35	50	-	0	5	-	45
24	0	5	30	50	-	10	15	-	35
25	0	0	45	60	-	0	10	-	30
26	5	40	75	80	-	0	5	-	15
27	0	40	65	85	-	0	10	-	15

[z] Twenty fruits were taken from each candidate orchard from May to June 1993 which was about 25–40 d before ripening. Test fruits were dipped in 39.5% Ethephon solution (3,000×) for 5 min.
[y] % of diseased fruit (disease incidences).
[x] Days after treatment with Ethephon.
[w] No data.

表 3. 1994 年臺南市玉井地區自檬果外銷初選供果園採收之硬核期「愛文」檬果套袋果實經益收生長素 3,000 倍稀釋液預先處理後，果實炭疽病與蒂腐病的陸續發病情形 (%)。

Table 3. The prediction data of disease incidences of anthracnose and stem end rot of green mature 'Irwin' mango fruits treated with Ethephon solution (3,000× dilution) for 12 d. (The mango fruits were harvested from candidate orchards at Yujing, Tainan in June 1994)[z]

Farmer No.	Anthracnose (%)[y]			Stem end rot (%)[y]			Healthy fruit at the 12th day (%)
	6[x]	9	12	6[x]	9	12	
1	0	0	5	0	0	0	95
2	0	5	5	0	0	0	95
3	0	0	10	0	0	0	90
4	0	10	10	0	0	0	90
5	0	0	15	0	0	10	80
6	0	0	20	0	5	10	75
7	0	15	25	0	0	5	75
8	0	15	15	5	10	10	75
9	0	10	15	0	5	15	70
10	0	25	25	0	5	10	70
11	0	10	25	0	5	5	70
12	5	10	20	0	10	10	70
13	0	0	20	0	10	25	65
14	0	30	30	0	5	5	65
15	0	15	30	0	10	10	60
16	0	10	35	0	5	5	60
17	10	15	20	0	20	25	55
18	0	45	55	0	5	5	40
19	5	45	50	0	15	15	40
20	0	45	50	0	10	25	30
21	0	45	55	0	10	20	30

[z] Twenty fruits were taken from each candidate orchard in June 1994 which was about 25–40 d before ripening. Test fruits were dipped in 39.5% Ethephon solution (3,000×) for 5 min.
[y] % of diseased fruit (disease incidences).
[x] Days after treatment with Ethephon.

真菌病害之感染。之後，許多學者 (Cerkauskas *et al*. 1983; Hartman *et al*. 1986) 均用該殺草劑來促進作物潛伏感染病菌提早發病，尤其是炭疽病菌，以協助試驗進行。然而，巴拉刈是一種非選擇性接觸性殺草劑，處理後的組織均會死亡，較不能達到病害預測的效果，而且目前該殺草劑已被國際禁用。之後，乙烯亦被報告有促進貯藏期病原菌生長之效果 (El-Kazzaz *et al*. 1983)，39.5% 益收生長素為乙烯之先驅物，在臺灣常用於番茄、鳳梨、葡萄之生長調節及香蕉與鳳梨之催熟 (Fei & Wang 2007)。因此本研究以益收生長素 3,000 倍稀釋液處理不同生長期之「愛文」檬果果實，發現果實在生長至硬核期 (此時已達其最大體積，約在採收前 1–1.5 mo) 以後，於室溫下 (夏天約 30℃) 約經 3–5 d，果實便會開始轉色，並且逐漸出現病斑 (圖 1)。然而，果實之果齡如果太年輕，則果實完全不能轉色，或有部分果實不能轉色，一般不轉色之果實亦不出現病斑，而延後轉色的果實出現病斑亦較晚。利用益收生長素之處理，發現不同果園果實出現炭疽病病斑之情形差異極大，在處理 9–12 d 後，發病果實率可從 0% (完全健康) 至 80% 以上不等 (表 1)。蒂腐病亦為檬果貯藏期病害 (Liao 1975)，該病

表 4. 1995 年臺南市玉井地區自檬果外銷初選供果園採收之硬核期「愛文」檬果套袋果實經益收生長素 3,000 倍稀釋液預先處理後，果實炭疽病與蒂腐病的陸續發病情形 (%)。

Table 4. The prediction data of disease incidences of anthracnose and stem end rot of green mature 'Irwin' mango fruits treated with Ethephon solution (3,000× dilution) for 12 d. (The mango fruits were harvested from candidate orchards at Yujing, Tainan in June 1995)[z]

Farmer No.	Anthracnose (%)[y]			Stem end rot (%)[y]			Healthy fruit at the 12th day (%)
	6[x]	9	12	6[x]	9	12	
1	0	0	0	0	5	5	95
2	0	5	10	0	0	0	90
3	0	7	14	0	0	0	86
4	0	0	0	0	5	15	85
5	0	0	15	0	0	0	85
6	0	0	5	0	5	10	85
7	0	10	15	0	0	0	85
8	0	0	15	0	0	5	80
9	10	15	15	0	5	5	80
10	0	5	15	0	0	10	75
11	0	0	10	0	5	15	75
12	0	7	25	0	0	0	75
13	0	5	15	5	5	10	75
14	10	10	10	0	5	15	75
15	0	20	20	0	0	5	75
16	5	15	30	0	0	0	70
17	15	15	25	0	5	5	70
18	5	5	20	0	5	20	65
19	0	20	35	0	0	0	65
20	0	30	50	0	0	0	50
21	0	25	30	5	15	20	50
22	5	20	45	0	5	10	45
23	0	25	50	0	0	5	45
24	15	35	55	0	0	5	40
25	5	30	45	0	5	15	40
26	15	20	45	0	20	25	30
27	30	50	45	0	10	25	30
28	15	45	45	15	0	30	25

[z] Twenty fruits were taken from each candidate orchard in June 1995 which was about 25–40 d before ripening. Test fruits were dipped in 39.5% Ethephon solution (3,000×) for 5 min.
[y] % of diseased fruit (disease incidences).
[x] Days after treatment with Ethephon.

害亦可經由益收生長素之處理而顯現病徵。由於蒂腐病發病後，病斑擴展迅速，嚴重影響外銷果實品質。因此，本試驗研究建議「愛文」檬果果實在經由益收生長素檢測處理 9–12 d 後，發病果實率 ── 炭疽病在 20% 以下，蒂腐病在 10% 以下，得選為『優良外銷供果園』，其生產之果實可供外銷日本與其他國家。

如今，國產檬果已能成功外銷日本、東南亞各地，洗刷多年來檬果無法外銷之噩夢。由於國產「愛文」檬果的果實炭疽病防治較往日

表 5. 1992、1993、1994 及 1995 年臺南市玉井地區外銷候選供果園檬果病害依預先偵測結果之比較 (果實炭疽病與蒂腐病之發病率) (%)。

Table 5. Comparison of the prediction data of disease incidences (%) of anthracnose and stem end rot of green mature 'Irwin' mango fruits treated with Ethephon solution (3,000× dilution) for 12 d from 1992 to 1995. (The mango fruits were harvested from candidate orchards at Yujing, Tainan)[z]

	Anthracnose (%)[y]			Stem end rot (%)[y]			Healthy fruit (%)		
Year	6[x]	9	12	6[x]	9	12	6	9	12
1992	17.6	26.9	34.8	3.2	15.3	37.6	80	65	32.1
1993	5.6	16.9	24.8	0.0	1.7	6.5	94	82	71.9
1994	0.9	16.8	25.2	0.2	7.3	10.9	99	81	65.0
1995	4.8	13.3	26.1	0.0	3.8	9.5	95	85	69.7

[z] Twenty fruits were taken from each candidate orchard from 1992 to 1995 which was about 25–40 d before ripening. Test fruits were dipped in 39.5% Ethephon solution (3,000×) for 5 min.
[y] % of diseased fruits (disease incidences).
[x] Days after treatment with Ethephon solution.

得宜，內銷檬果之品質亦大幅提升，使櫥架壽命延長。由於預先偵測之結果顯示，檬果果園的果實炭疽病發病率差異甚大 (表 1–4)，可見田間管理對病害嚴重與否影響甚大，農民仍需加強輔導。包括：部分農民的『套袋』方法不正確，嚴重影響果實著色與降低套袋之防病功效。未套袋前，應定期施藥，保護果實不被潛伏感染病菌侵入 (如果病菌已侵入，套袋亦無效，因套袋並無治療病害之功能) (Ann *et al*. 1998, 2013)，套袋的當日或前 1 d (如果未降雨) 必須施藥，不可將病菌與蟲卵包藏在套袋內，套袋內果實上之藥劑亦可因套袋而使藥效延長。

『套袋』為目前防治檬果炭疽病之有效方法 (Ann *et al*. 1998, 2013)，而且果實套袋可提高糖度含量與提早成熟 (Ann *et al*. 1998)。此外，目前許多「愛文」檬果園均以套袋方法防治果實病蟲害，以減少農藥之使用，對發展『永續農業』、降低產銷成本、保護環境免於污染及保障農民與消費者健康，均有助益。但在試驗時，發現如果花期不施藥，於檬果開花著果後立即套袋，果實成熟後仍有許多病斑出現 (Ann *et al*. 1998)，因而在病害防治研究方面，對炭疽病『潛伏感染』之機制仍應加強研究，如能找出對潛伏感染器官有破壞能力之方法，將對解決炭疽病造成之潛伏感染病害有莫大助益。在其他非農藥防治方法 (Leu *et al*. 1988, 1996)，除抗病品種、套袋 (Ann *et al*. 1998, 2013)、地面覆蓋 (Ann *et al*. 1998)、施用土壤添加物 (如 CaO，可降低蘋果果實的罹病率) (Conway *et al*. 1991) 及生物防治 (Chuang & Ann 1997) 外，亦應繼續探討其他可行之道。

誌謝

本文承蒙農業部 (前行政院農業委員會) 科技計畫 (82 科技-2.4-糧-03，83 科技-2.4-糧-27，84 科技 -2.4-糧-23，85 科技 -1.6-糧-28) 補助，謹此致謝！

引用文獻

Ann, P. J., R. C. Huang, and M. F. Chen. 1994. Effects of environmental factors on disease incidence of mango anthracnose. Plant Pathol. Bull. 3:34–44. (in Chinese with English abstract) doi:10.6649/PPB.199403_3(1).0005

Ann, P. J., L. S. Leu, T. Y. Chuang, and C. W. Kao. 1996. Development of a technique for forecasting of mango fruit anthracnose. Plant Prot. Bull. 38:376–377. (abstract in Chinese)

Ann, P. J., L. S. Leu, T. Y. Chuang, and C. W. Kao. 1998. Effect of fruit bagging and mulching on control of mango fruit anthracnose disease. Plant Pathol. Bull. 7:19–26. (in Chinese with English abstract) doi:10.6649/PPB.199803_7(1).0003

Ann, P. J., J. N. Tsai, H. F. Ni, and H. R. Yang. 2013. Current status on occurrence and management of major diseases of mango in Taiwan. Plant Pathol. Bull. 22:67–92. (in Chinese with English abstract) doi:10.6649/PPB.201306_22(2).0001

Baker, R. E. D., S. H. Crowdy, and R. K. Mckee. 1940. A review of latent infection caused by *Colletotrichum gloeosporioides* and allied fungi. Trop. Agric. 17:128–132.

Cerkauskas, R. F., O. D. Dhingra, and J. B. Sinclair. 1983. Effect of three desiccant-type herbicides on fruiting structures of *Colletotrichum truncatum* and *Phomopsis* spp. on soybean stems. Plant Dis. 67:620–622. doi:10.1094/PD-67-620

Cerkauskas, R. F. and J. B. Sinclair. 1980. Use of paraquat to aid the detection of fungi in soybean tissues. Phytopathology 70:1036–1038. doi:10.1094/Phyto-70-1036

Chuang, T. Y. and P. J. Ann. 1997. Biological control of mango anthracnose. Plant Prot. Bull. 39:227−240. (in Chinese with English abstract)

Conway, W. S., C. E. Sams, J. A. Abbott, and B. D. Bruton. 1991. Postharvest calcium treatment of apple fruit to provide broad-spectrum protection against postharvest pathogens. Plant Dis. 75:620–622. doi:10.1094/PD-75-0620

Cook, A. A. 1975. Diseases of Tropical and Subtropical Fruits and Nuts. Hafner Press. New York, NY. 231 pp.

El-Kazzaz, M. K., N. F. Sommer, and A. A. Kader. 1983. Ethylene effects on *in vitro* and *in vivo* growth of certain postharvest fruit-infecting fungi. Phytopathology 73:998–1001. doi:10.1094/Phyto-73-998

Fei, W. C. and Y. C. Wang. (eds.) 2007. Plant Protection Manual (Friuts). Taiwan Agricultural Chemicals and Toxic Substances Research Institute. Taichung, Taiwan. 297 pp. (in Chinese)

Hartman, G. L., J. B. Manandhar, and J. B. Sinclair. 1986. Incidence of *Colletotrichum* spp. on soybean leaves were collected in soybeans and weeds in Illinois and pathogenicity of *Colletotrichum truncatum*. Plant Dis. 70:780–782. doi:10.1094/PD-70-780

Leu, L. S., Z. Y. Chuang, P. J. Ann, H. L. Yang, S. C. Yang, and C. W. Kao. 1996. Control of mango anthracnose without fungicides. Plant Prot. Bull. 38:377. (abstract in Chinese)

Leu, L. S., H. C. Young, G. T. Chien, and H. E. Tzeng. 1988. Screening of resistant varieties to mango anthracnose. Plant Prot. Bull 30:337–348. (in Chinese with English abstract)

Liao, C. H. 1975. Mango disease in Taiwan: Fruit stem-end rot. Scientific Agric. 23:415–416. (in Chinese)

Parris, G. K. and W. W. Jones. 1941. The use of methyl bromide as a means of detecting latent infections by *Colletotrichum* spp. Phytopathology 31:570–571.

Simmonds, J. H. 1941. Latent infection in tropical fruits discussed in relation to the part played by species of *Gloesporium* and *Colletotrichum*. Proc. R. Soc. Queensl. 52:92–120.

Simmonds, J. H. 1963. Studies in the latent phase of *Colletotrichum* species causing ripe rots of tropical fruits. Queensland J. Agric. Anim. Sci. 20:373–424.

Uddin, M. N., S. H. T. Shefat, M. Afroz, and N. J. Moon. 2018. Management of anthracnose disease of mango caused by *Colletotrichum gloeosporioides*: A review. ACTA Scientific Agric. 2(10):169–177.

Verhoeff, K. 1974. Latent infection by fungi. Annu. Rev. Phytopathol. 12:99–110. doi:10.1146/annurev.py.12.090174.000531

Development of a Technique for Forecasting (or Pre-Detection) Anthracnose Disease Incidences of Green Mature Bagging Mango Fruits

Tsai-Young Chuang[1], Lii-Sin Leu[2], Chin-Wen Kao[3], Hong-Ren Yang[4], Jyh-Nong Tsai[5,*], Hsiu-Chu Yang[2], and Pao-Jen Ann[6,*]

Abstract

Chuang, T. Y., L. S. Leu, C. W. Kao, H. R. Yang, J. N. Tsai, H. C. Yang, and P. J. Ann. 2024. Development of a technique for forecasting (or pre-detection) anthracnose disease incidences of green mature bagging mango fruits. J. Taiwan Agric. Res. 73(2):101–111.

Symptoms of anthracnose disease gradually appeared on fruits, when green mature 'Irwin' mango was sprayed with 39.5% 2-chloro-ethylphosphonic acid (Ethephon) solution (3,000×), or dipped in the same solution for 5 min, covered with paper, and kept at 30℃ for 3–5 d. By the mean of Ethephon treatment, the average disease incidences of ripened mango fruits in the same orchards could be predicted. The method was also useful for the prediction of the incidence of stem end rot of mangoes. However, the peel of young mango fruits harvested during expanding stages was not able to turn red after treatment with Ethephon solution. Meanwhile, none of the postharvest disease spots appeared on treated green mango fruits. Stimulation of Ethephon for changing the color of fruits only if mango fruits were about 30–45 d before fully mature. A procedure for the prediction of postharvest mango diseases was developed as follows. Twenty to twenty-five green mature fruits were taken from each candidate orchard, and numbers of diseased and healthy fruits were read on the 9th and 12th day after ripening with Ethephon solution treatment, respectively. Fruits from candidate orchards, with predicted disease incidences of anthracnose < 20% as well as stem end rot < 10%, were acceptable for export.

Key words: Mango anthracnose, Latent infection, Forecasting (pre-detecting) inoculation, Non-pesticide disease control.

Received: November 14, 2023; Accepted: January 19, 2024.

* Corresponding authors, e-mail: tsaijn@tari.gov.tw, pjann@tari.gov.tw, pjann5039@gmail.com

[1] Former Professor, Department of Plant Pathology and Microbiology, National Taiwan University, Taipei, Taiwan, ROC.

[2] Former Research Fellows, Agricultural Chemicals Research Institute, Taichung City, Taiwan, ROC.

[3] Former Director General, Agricultural Chemicals Research Institute, Taichung City, Taiwan, ROC.

[4] Former Research Fellow and Director, Chiayi Agricultural Experiment Branch, Taiwan Agricultural Research Institute, Chiayi, Taiwan, ROC.

[5] Research Fellow and Division Director, Plant Pathology Division, Taiwan Agricultural Research Institute, Taichung City, Taiwan, ROC.

[6] Former Research Fellow and Division Director, Plant Pathology Division, Taiwan Agricultural Research Institute, Taichung City, Taiwan, ROC.

台灣農業研究 (J. Taiwan Agric. Res.) 73(2):113–122 (2024)
https://doi.org/10.6156/JTAR.202406_73(2).0004

研究報告

甘藷羽狀斑駁病毒反轉錄恆溫環狀擴增檢測技術 (RT-LAMP) 之建立與應用

林靜宜[1,*]　倪蕙芳[2]　林慧如[3]

摘要

林靜宜、倪蕙芳、林慧如。2024。甘藷羽狀斑駁病毒反轉錄恆溫環狀擴增檢測技術 (RT-LAMP) 之建立與應用。台灣農業研究 73(2):113–122。

病毒病害為限制甘藷生產的重要因子，其中由馬鈴薯 Y 病毒屬 (*Potyvirus*) 中之甘藷羽狀斑駁病毒 (sweet potato feathery mottle virus; SPFMV) 引起之病害，為全球甘藷栽培區廣泛發生之病毒病害。甘藷健康種苗的生產與早期的病毒診斷鑑定皆需仰賴快速可靠的病毒檢測技術，亦是有效防治病毒病害的重要關鍵。本研究建立單步驟反轉錄恆溫環狀擴增 (reverse transcription loop-mediated isothermal amplification; RT-LAMP) 檢測技術，藉以檢測 SPFMV，並利用比色法，藉 hydroxy naphthol blue 作為指示染劑，以利肉眼辨別反應之結果。以此技術實際檢測罹病甘藷植物總量 RNA，最佳反應條件為 63℃、45–60 min；可檢測的最低 RNA 濃度為 237.9×10^{-5} ng μL^{-1}，相較於反轉錄聚合酵素連鎖反應 (reverse transcription polymerase chain reaction; RT-PCR) 可檢測的最低 RNA 濃度為 237.9×10^{-3} ng μL^{-1}，顯示 RT-LAMP 之檢測靈敏度較 RT-PCR 高 100 倍。此外，該 RT-LAMP 技術亦成功應用於田間甘藷之 SPFMV 檢測，顯示 RT-LAMP 檢測技術是具有快速、專一且靈敏之 SPFMV 檢測方法，未來可優化目前種苗檢定技術與提供給甘藷業者使用。

關鍵詞：甘藷羽狀斑駁病毒、反轉錄恆溫環狀擴增檢測技術、甘藷。

前言

甘藷 (學名：*Ipomoea batatas*，英名：Sweet potato) 為旋花科 (Convolvulaceae)，甘藷屬 (*Ipomoea*) 作物，原產於熱帶美洲墨西哥，隨後傳至熱帶亞洲與非洲，目前為全球五大根莖類作物之一 (Food and Agriculture Organization of the United Nations 2022)。臺灣現行甘藷生產主要提供鮮食，部分用途為食品加工與工業原料。根據農業部 2022 年之統計年報 (https://agrstat.moa.gov.tw/sdweb/public/official/OfficialInformation.aspx) 顯示，臺灣甘藷總栽培面積為 9,154 ha，約 60% 產區集中在雲林縣與彰化縣，分別為 4,137 ha 與 1,467 ha，栽培品種以「台農 57 號」與「台農 66 號」最為常見。

病毒病害為甘藷生產主要的限制因子，由於甘藷利用塊根與莖蔓進行無性繁殖，一旦植株受到病毒感染，將隨後代種苗蔓延而導致產量受到嚴重影響。目前已知可感染甘藷的病毒種類已超過 30 種 (Clark *et al*. 2012)，臺灣文獻記載之甘藷病毒種類則有甘藷捲葉病毒 (sweet potato leaf curl virus; SPLCV) (Chung *et al*. 1985)、甘藷羽狀斑駁病毒 (sweet potato feathery mottle virus; SPFMV) (Liao *et al*. 1979)、甘藷潛伏病毒 (sweet potato latent virus; SPLV) (Liao *et al*. 1979)、甘藷病毒 2 (sweet potato virus 2; SPV2)，又稱甘藷病毒 Y

投稿日期：2023 年 11 月 27 日；接受日期：2024 年 1 月 22 日。
* 通訊作者：eris2024@tari.gov.tw
[1] 農業部農業試驗所植物病理組助理研究員。臺灣 臺中市。
[2] 農業部農業試驗所嘉義農業試驗分所植物保護系副研究員兼系主任。臺灣 嘉義市。
[3] 農業部農業試驗所嘉義農業試驗分所植物保護系計畫助理。臺灣 嘉義市。

(sweet potato virus Y; SPVY) (Wang *et al*. 2014)、甘藷G病毒 (sweet potato virus G; SPVG) (Wang *et al*. 2013)、甘藷褪綠矮化病毒 (sweet potato chlorotic stunt virus; SPCSV) (Cheng *et al*. 2020) 及甘藷褪綠斑點病毒 (sweet potato chlorotic fleck virus; SPCFV) (Chiu 2020)。其中分類上為 *Potyvirus* 屬之 SPFMV 廣泛地發生在世界之甘藷產區，為常見的甘藷病毒 (Ateka *et al*. 2004)，此病毒單獨感染甘藷時病徵輕微，常見罹病植株之葉脈呈現羽狀黃化或是葉片出現輕微嵌紋病徵；然而，於田間常與其他病毒如 SPCSV 與 SPLCV 等複合感染植株，則會造成葉片畸形、加重植株黃化嵌紋及矮化的病徵，對甘藷生長造成明顯危害，造成之產量損失可達 44–95% (Domola *et al*. 2008; Adikini *et al*. 2016; Wanjala *et al*. 2020)。

甘藷病毒病目前尚無防治藥劑，因此以健康種苗作為栽種來源，於甘藷生產上扮演關鍵的角色，能有效降低病毒發生率、維持甘藷產量及品質。為生產健康種苗，須於種苗生產各階段進行病毒檢測，確定無病毒後，才能進入大量繁殖的階段。因此，病毒檢測技術為發展健康種苗產業的重要關鍵。現今甘藷病毒病主要常見之檢測技術為血清檢測法之酵素連結抗體法 (enzyme-linked immunosorbent assay; ELISA) 與分子檢測法中的聚合酶連鎖反應 (polymerase chain reaction; PCR) 及反轉錄聚合酵素連鎖反應 (reverse transcription PCR; RT-PCR) 等 (Opiyo *et al*. 2010; Li *et al*. 2012; Boonham *et al*. 2014)。然而，血清學檢測需要專一性之抗血清，製作過程繁雜、成本高，目前一些重要的甘藷病毒仍缺乏抗血清，如 SPLCV 等 (Wanjala *et al*. 2021)；此外，甘藷組織中含有抑制物質，可影響血清學檢測之正確性，且血清學檢測適用於病毒力價 (titer) 高之樣品，而甘藷罹病株內之病毒力價低，不易檢出病毒 (Kreuze & Fuentes 2008)。現有之 PCR 與 RT-PCR 等分子檢測法，雖具有專一性與靈敏性，但需要特定的實驗室設備儀器與專業的實驗人員才能完成。本研究為優化現行檢測效率，以恆溫環狀擴增法 (loop-mediated isothermal amplification; LAMP) (Notomi *et al*. 2000) 為基礎，發展可在恆溫下反應、操作簡便且快速之單步驟反轉錄恆溫環狀擴增 (reverse transcription loop-mediated isothermal amplification; RT-LAMP) 檢測 SPFMV，以期能應用於甘藷健康種苗生產、田間病毒診斷及鑑定等工作。

材料與方法

供試病毒來源

2018–2019 年自嘉義、雲林及彰化之甘藷田區採集疑似感染病毒之植株，經 RT-PCR 檢測，並將 RT-PCR 產物核酸定序確認為 SPFMV 感染後，利用扦插方式繁殖罹病株，作為病毒來源。

甘藷總量 RNA 之萃取

植物組織利用 Monarch® Total RNA Miniprep 純化套組 (NEW ENGLAND BioLabs Inc., Ipswich, MA, USA) 萃取總量 RNA，依據純化套組所附之操作步驟進行。取 0.1 g 植物組織，於研缽中加入液態氮急速冷凍並研磨成粉狀。將均質之植物組織粉末與 800 µL RNA protection reagent 於 1.5 mL 微量離心管中均勻混合，離心 2 min (1,600× *g*)，吸取上清液至新的微量離心管中，再加入等體積之 RNA lysis buffer 均勻混合後，吸取 800 µL 混合液至過濾管 (column tube)，離心 30 s (1,600× *g*)，收集濾液至新的微量離心管。將濾液加入等體積 95% 酒精，混合均勻後，吸取混合液至純化過濾管，離心 30 s (1,600× *g*)，移除濾液後加入 500 µL RNA priming buffer 至純化過濾管，離心 30 s (1,600× *g*) 後移除濾液。加入 500 µL RNA wash buffer 至純化過濾管，離心 30 s (1,600× *g*) 後移除濾液，並重複此步驟 1 次。最後加入 100 µL TE buffer，離心 30 s，濾出純化 RNA。純化之 RNA 存放於 -20℃ 條件下，供之後試驗使用。

引子設計

自 GenBank 資料庫中收集 SPFMV 臺灣病

毒株與其他地區病毒株之鞘蛋白 (coat protein; CP) 序列，經比對分析後，選擇 CP 序列的高保留區進行引子設計。藉由 PrimerExplorer V5 軟體 (http://primerexplorer.jp/e) 設計引子 (表 1)，核酸引子則委託源資生物科技公司 (臺灣臺北市) 進行合成。

反轉錄恆溫環狀擴增法

利用 Loopamp RNA amplification kit (Eiken Chemical Co., Ltd., Tokyo, Japan) 作為反應試劑。反應總體積為 25 μL，含有 2 μL RNA 模板，12.5 μL 2× reaction mix，1 μL 酵素混合液 (*Bst* DNA polymerase 與 AMV reverse transcriptase)，40 pmol 引子 SPFMV-FIP 與 SPFMV-BIP，5 pmol 引子 SPFMV-F3 與 SPFMV-B3，反應條件為 63℃，30–60 min；85℃，5 min。反應結果以肉眼觀察是否產生白色混濁物並加入 1 μL 染劑 hydroxy naphthol blue (HNB) (3 mM) (Sigma, St. Louis, MO, USA) 觀察呈色變化，必要時取 10 μL RT-LAMP 產物以 1.5% 瓊脂凝膠電泳分析結果。

反轉錄聚合酵素連鎖反應

以供試植株之總量 RNA 作為模板，根據上述設計的引子 (SPFMV-F3/SPFMV-B3) 進行單步驟 RT-PCR (one-step RT-PCR) (SensoQuest LabCycler 011-101, SensoQuest, Göttingen, Germany)，利用 Super 2 RT-PCR Kit (Protech, Taipei, Taiwan) 作為反應試劑，反應總體積 20 μL，含有 2 μL RNA 模板，0.5 μL 10 mM 引子與 10 μL 2× reaction mix。反應條件為 42℃反應 30 min，95℃反應 2 min，重複 35 個循環：93℃ 1 min、55℃ 1 min 及 72℃ 2 min，最終反應於 72℃持續 5 min。取 10 μL RT-PCR 產物以 1.5% 瓊脂凝膠電泳分析結果。

專一性試驗

為分析本研究設計之 RT-LAMP 引子組偵測 SPFMV 之專一性，分別自健康甘藷植株與感染 SPLV、SPCSV 及 SPFMV 之罹病甘藷植株，以上述方法萃取其總量 RNA，作為測試模板來源。取 2 μL RNA 進行 RT-LAMP，反應結果以加入染劑 (3 mM HNB) (Sigma, St. Louis, MO, USA) 觀察呈色變化，並以 1.5% 瓊脂凝膠電泳分析確認結果。

比較 RT-PCR 與 RT-LAMP 偵測 SPFMV 之靈敏度試驗

為分析 RT-LAMP 檢測技術與 RT-PCR 技術之靈敏度差異，將萃取罹病甘藷植株之總量 RNA 濃度自起始經 10 倍系列稀釋後，分別依上述方法進行 RT-LAMP 與單步驟 RT-PCR 試驗。RT-LAMP 之反應結果以加入染劑 (3 mM HNB) (Sigma, St. Louis, MO, USA) 觀察呈色變化並以 1.5% 瓊脂凝膠電泳分析確認結果；RT-PCR 產物以 1.5% 瓊脂凝膠電泳分析結果。

田間罹病株之病毒檢測

自田間採集具有疑似病毒病徵 (黃化與嵌紋等) 之甘藷葉片，依上述方法取約 0.1 g 葉片組織萃取總量 RNA，將純化之 RNA 分別利用上述 RT-LAMP 與 RT-PCR 方法進行 SPFMV 之檢測與分析。

表 1. 本研究中使用之引子。

Table 1. The primers used in this study.

Primer name	Sequence 5′ to 3′	Target region
SPFMV-F3	CAACGTAATTTGACTGATATG	Coat protein
SPFMV-B3	GTCGTGTGCCTCTCCGTATC	
SPFMV-FIP	TCTTTWGCRCGTGYAGGGCGCGATATGCATTTGAT	
SPFMV-BIP	GCACTTAAGAATGCGTCTTGCGTGGAGACGTTTCC	

結果

RT-LAMP 偵測 SPFMV 之反應條件試驗

為建立穩定與有效之 RT-LAMP 反應條件，本研究利用自罹病植株萃取之 RNA 作為模板，進行最佳反應溫度與時間之試驗。有效反應溫度試驗中，結果顯示所設計之 SPFMV 引子組於 60–65℃區間反應後經電泳分析都能觀察到產物之生成，皆為正反應，其中以 63℃時所增幅之產物條帶最為顯著 (圖 1A)。因此，選擇於 63℃時，利用 RT-LAMP 分別進行 30、45 及 60 min 之有效反應時間試驗，電泳分析結果發現反應時間為 45 與 60 min 皆能增幅出產物，但時間長度為 30 min 時，則未觀察到產物生成 (圖 1B)。綜上所述，SPFMV 最佳反應條件為 63℃、45–60 min 後經 85℃、5 min 以停止反應。RT-LAMP 反應結果為正反應時，會生成白色混濁物，可藉由肉眼辨別 (圖 1C)。此外，亦可利用染劑呈色經由肉眼直接判別。本研究利用 HNB 作為指示染劑，建立可視化技術，染劑加入反應液後，正反應時呈現藍色，負反應時則為紫色 (圖 1C)。

引子專一性試驗

本試驗中係對 SPFMV 鞘蛋白序列之高保留區設計引子組，為確認引子組對 SPFMV 之專一性，於 63℃條件下進行 RT-LAMP 反應 60 min，結果顯示僅 SPFMV 之罹病植株 RNA 作為模板時出現正反應，可觀察到指示染劑呈現藍色；其他罹病植株 RNA 如 SPLV、SPCSV、未罹病植株 RNA 及無核酸模板對照組皆為負反應，於加入指示染劑時，呈現紫色 (圖 2)。

RT-PCR 與 RT-LAMP 之靈敏度比較

為瞭解 RT-LAMP 偵測 SPFMV 之靈敏度，同時與 RT-PCR 技術比較兩者間的靈敏度差異，以萃取罹病植株 RNA 作為試驗用模板，RNA 以分光光度計測定其濃度為 237.9 ng μL^{-1}。將 RNA 之起始濃度經系列 10 倍稀釋後分別進

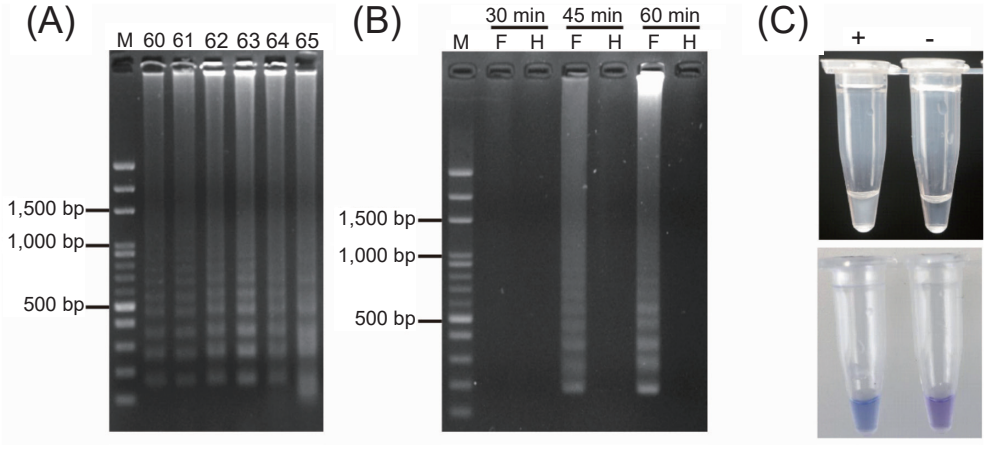

圖 1. 以 RT-LAMP 偵測 SPFMV 之最適條件試驗。(A) 於 60、61、62、63、64 及 65℃測試反應之最適溫度。(B) 於 30、45 及 60 min 測試最適反應時間。F：感染 SPFMV 甘藷葉 RNA；H：健康甘藷葉組織 RNA；M：100 bp DNA ladder。(C) 利用比色法分析 RT-LAMP 產物。上：未加入指示染劑之反應結果；下：加入指示染劑 (HNB) 之反應結果。+：正反應；-：負反應。

Fig. 1. Optimization assays of reverse transcription loop-mediated isothermal amplification (RT-LAMP) for detecting sweet potato feathery mottle virus (SPFMV). (A) The optimal temperature tests at 60, 61, 62, 63, 64 and 65℃. (B) The optimal reaction times for amplification at 30, 45 and 60 min. F: RNA from SPFMV infected sweet potato leaves; H: RNA from healthy sweet potato leaves; M: 100 base pairs (bp) DNA ladder. (C) The colorimetric RT-LAMP assay. Up: the naked-eye visual RT-LAMP assay without indicator dye; down: the naked-eye visual RT-LAMP assay with indicator dye (hydroxy naphthol blue; HNB). +: positive reaction; -: negative reaction.

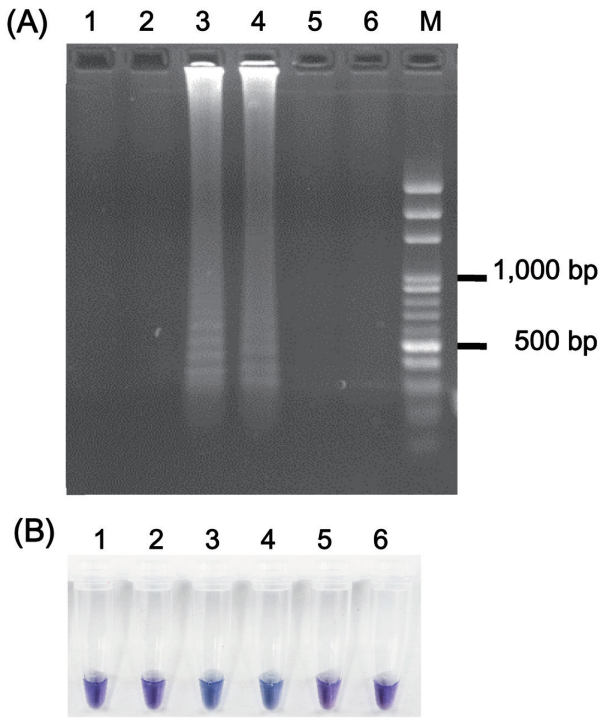

圖 2. 利用 RT-LAMP 偵測 SPFMV 之專一性試驗。(A) 以 1.5% 瓊脂凝膠電泳分析結果；(B) 加入指示染劑 (HNB) 之呈色結果。1：感染 sweet potato latent virus (SPLV) 之病株 RNA；2：感染 sweet potato chlorotic stunt virus (SPCSV) 病株 RNA；3–4 感染 SPFMV 病株 RNA；5：健康甘藷植株 RNA；6：無核酸模板對照組；M：100 bp DNA ladder。

Fig. 2. Specificity of the reverse transcription loop-mediated isothermal amplification (RT-LAMP) assay for detecting the RNA of sweet potato feathery mottle virus (SPFMV). The amplified products were detected by (A) 1.5% agarose-gel electrophoresis and (B) indicator dye (hydroxy naphthol blue; HNB). No.1: RNA from sweet potato latent virus (SPLV) infected plants; No. 2: RNA from sweet potato chlorotic stunt virus (SPCSV) infected plants; No. 3–4: RNA from SPFMV infected plants; No. 5: RNA from healthy sweet potato plants; No. 6: non-templet control; and M: 100 base pairs (bp) DNA ladder.

行 RT-LAMP 與 RT-PCR。反應後之電泳分析結果顯示，RT-LAMP 的偵測最低濃度為 237.9 × 10^{-5} ng μL^{-1} (圖 3A)，以指示染劑進行呈色時，亦可觀察到染劑轉為藍色時之最低濃度為 237.9 × 10^{-5} ng μL^{-1} (圖 3B)。RT-PCR 反應之預期條帶大小為 194 bp (base pair)，經電泳分析結果顯示可偵測最低濃度為 237.9 × 10^{-3} ng μL^{-1} (圖 3C)。

田間植株之病毒檢測

利用 RT-LAMP 與 RT-PCR 法檢測田間疑似病毒感染之甘藷樣品，共採集 14 株田間甘藷葉片，萃取總量 RNA 後進行檢測，結果顯示，RT-LAMP 測得 9 株感染 SPFMV，其檢出率為 64.3%；使用 RT-PCR 則測得 7 株具有 SPFMV，檢出率為 50% (表 2)，顯示 RT-LAMP 與傳統 RT-PCR 法皆可應用於檢測田間受 SPFMV 感染之甘藷植株，但其中以 RT-LAMP 較為靈敏。

討論

病毒為甘藷生產過程中影響產量與品質的重要病原之一，嚴重時產量損失可達 44–95% (Domola *et al*. 2008; Adikini *et al*. 2016; Wanjala *et al*. 2020)。目前防治管理方法主要使用

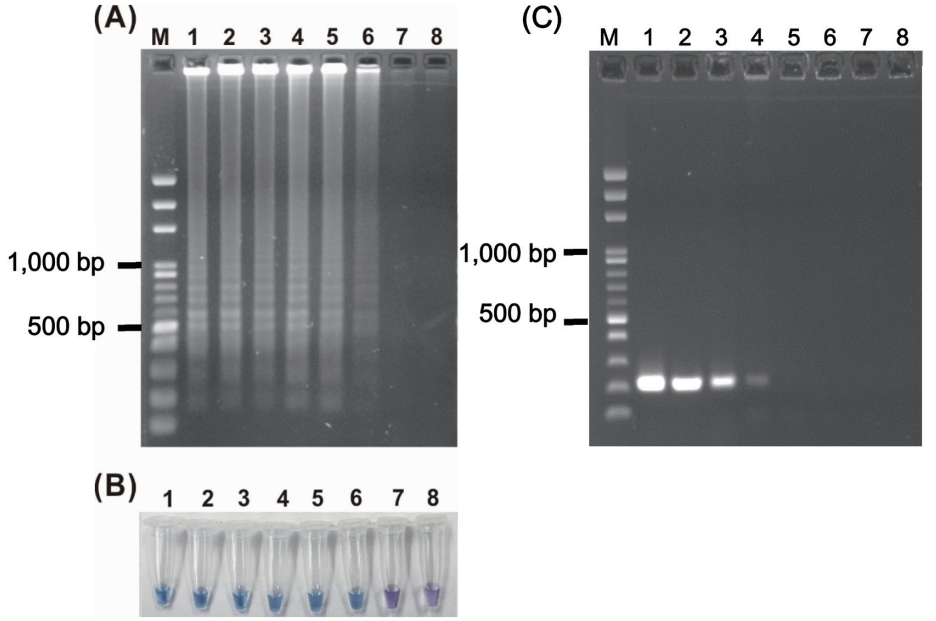

圖 3. RT-LAMP 與 RT-PCR 檢測 SPFMV 之靈敏度試驗。萃取 SPFMV 罹病株之 RNA，起始濃度自 237.9 ng μL^{-1} 以 10 倍系列稀釋方式稀釋至 237.9×10^{-6} ng μL^{-1} (1–7) 分別利用 (A) 1.5% 瓊脂凝膠電泳分析法與 (B) 指示染劑 (HNB) 呈色法測試 RT-LAMP 與 (C) RT-PCR 可偵測之最低濃度。M：100 bp DNA ladder；8：無核酸模板對照組。

Fig. 3. Sensitivity of reverse transcription loop-mediated isothermal amplification (RT-LAMP) and reverse transcription polymerase chain reaction (RT-PCR) assays. Serial 10-fold dilutions of the RNA of sweet potato feathery mottle virus (SPFMV)-infected plants ranging from 237.9 to 237.9×10^{-6} ng μL^{-1} (No. 1–7) were used to determine the minimum concentration that the (A and B) RT-LAMP and (C) RT-PCR was able to identify. (A) RT-LAMP identified by 1.5% agarose-gel electrophoresis and (B) RT-LAMP identified with indicator dye. M: 100 base pairs (bp) DNA ladder; and No. 8: non-template control.

健康無病毒之甘藷種苗與避免病毒媒介昆蟲大量滋生，得以減少病害蔓延。鑑於 SPFMV 為臺灣與其他國家甘藷生產區廣泛發生與常見之甘藷病毒，引起的病徵常隨甘藷品種、病毒株及環境而改變，且單獨感染甘藷時病徵輕微，不易直接診斷鑑定 (Untiveros *et al*. 2008)。因此，為早期預警病毒之發生，防堵病毒擴散並健全甘藷健康種苗生產體系，建立病毒快速篩檢技術甚為重要。本研究針對 SPFMV 開發之 RT-LAMP 檢測技術，具有靈敏度高於 RT-PCR、並能藉由肉眼直接判別結果的特點，可提供更為省時與簡便的檢測方法，作為協助甘藷健康種苗生產、田間病毒診斷及鑑定等工作之利器。

血清學法為常用之病毒檢測技術，然而甘藷富含澱粉與酚化物等抑制物質，往往使檢測精確度受到影響 (Kreuze & Fuentes 2008; Wanjala *et al*. 2021)，現今多應用核酸分子技術進行病毒檢測與鑑定。目前 SPFMV 檢測技術除了利用 RT-PCR 之外，近期 LAMP 技術亦被應用於此病毒檢測 (Jiang *et al*. 2018; Wanjala *et al*. 2021)。Jiang *et al*. (2018) 開發之 RT-LAMP 法，選擇 SPFMV 之 CP 基因，設計 2 個引子組，可專一性地偵測 SPFMV，此法反應時間需 70 min，靈敏度稀釋終點為 10^4 稀釋倍率，且靈敏度較 RT-PCR 檢測方法高 10 倍。本研究設計偵測 SPFMV 之 2 個引子組，以臺灣病毒株之序列為主，檢測的目標基因同樣為 CP 基因，但本研究建立之 RT-LAMP 方法，除可正確地檢測感染之 SPFMV，反應時間縮短為 45–60 min，可提供更快速的有效反應時間。靈敏度測試方面，電泳分析結果顯示

表 2. 利用反轉錄恆溫環狀擴增法 (RT-LAMP) 與反轉錄聚合酵素連鎖反應 (RT-PCR) 進行田間疑似感染 sweet potato feathery mottle virus (SPFMV) 之甘藷植株檢測結果。

Table 2. Detection of sweet potato feathery mottle virus (SPFMV) by reverse transcription loop-mediated isothermal amplification (RT-LAMP) and reverse transcription polymerase chain reaction (RT-PCR) for field sweet potato plants.

Field sample[z]	RT-LAMP[y]	RT-PCR[x]
A1	-	-
A2	+	+
A3	+	+
G1	+	+
G2	-	-
G3	+	+
G4	+	+
L1	+	+
L2	+	-
L3	+	-
L4	-	-
L5	-	-
L6	-	-
L7	+	+
SPFMV	+	+
H	-	-

[z] SPFMV: SPFMV infected sweet potato as positive control; H: healthy sweet potato as negative control.
[y] RT-LAMP results: + indicates a color change in the samples from purple to blue suggesting SPFMV infections; - indicates no color change in the samples suggesting negative reactions.
[x] RT-PCR results: + indicates a clear visible band in 1.5% agarose-gel electrophoresis; - indicates a negative reaction.

本研究之 RT-LAMP 法的稀釋終點靈敏度可達 10^5 稀釋倍率，相較 RT-PCR 法可提高靈敏度 100 倍。本研究開發之方法靈敏度較高，推測可能與使用之核酸萃取試劑組不同，使甘藷核酸樣本中含有較少的多酚等物質，減少反應中的干擾作用，有助提升靈敏度。此外，LAMP 生成之產物可利用多種方法檢視，如傳統之電泳分析、比色法 (colorimetric) (以螢光染劑或顏色指示劑加以顯色) 以及經由反應過程中產生不溶於水的焦磷酸鎂 (magnesium pyrophosphate) 白色沉澱物造成反應液濁度 (turbidity) 上升等。雖然 Wanjala *et al*. (2021) 開發的即時螢光定量 LAMP 法，選擇 SPFMV 之 CP 基因設計 3 個引子組，可於甘藷組織粗萃液樣本中檢測 SPFMV，依病毒量的高低不同，其反應時間約 5–30 min，但需購置相關螢光反應器材，本研究則利用比色法，藉 HNB 作為指示染劑辨別結果，此法的稀釋終點靈敏度與電泳分析法相當，顯示以 HNB 檢視反應結果，可提供快速與簡便的辨別方法，不須經儀器觀測反應結果，可降低檢測成本。

田間病毒檢測試驗顯示疑似病毒感染之甘藷植株中，以 RT-LAMP 檢測 SPFMV，其檢出率為 64.3%，而 RT-PCR 之檢出率為 50%，顯示本研究所建立之 RT-LAMP 可有效應用於檢測田間受 SPFMV 感染之甘藷植株，且與 RT-PCR 相較，本技術具有快速與高靈敏性。此外，亦可從檢出率發現臺灣田間甘藷栽培與其他甘藷栽培區如南韓、馬拉威等地相似，SPFMV 為普遍感染田間甘藷之病毒 (Ateka *et al*. 2004; Kwak *et al*. 2014; Mbewe *et al*. 2021)。於檢測植株中，部分樣本具有疑似病毒感染病徵，但仍未檢出 SPFMV，可能為植株受到其他甘藷病毒感染，如 SPCSV 亦可引起葉片黃化。此外，植物生理性障礙也可能引起與病毒黃化病徵相似之症狀，如甘藷缺鋅與缺鎂可導致葉脈間黃化、缺硫也會造成葉片黃化或葉脈透化的現象，其他如土壤水分過多與過度施肥也可能為植株出現黃化現象的原因之一 (O'Sullivan *et al*. 1997)，此部分需做進一步分析才能釐清。

本研究針對 SPFMV 建立之 RT-LAMP 檢測技術，兼具快速、專一性高及靈敏度優於 RT-PCR 等優點，並搭配可經肉眼直接判別結果之可視化技術，不需使用複雜的專業儀器設備即可操作，可提供檢測單位更為省時與簡便的 SPFMV 檢測方法。此外，為使健康種苗檢定工作更加健全，促使種苗產業升級，發展現場即時檢測 (on-site detection) 技術之需求大為提升。因此，本研究之 RT-LAMP 檢測技術，未來如配合植物核酸萃取技術進行簡化，或評估利用植物組織粗汁液作為檢測之反應模板的可行性，亦可開發 RT-LAMP 乾式檢測試劑套組與手持式的檢測裝置等，使種苗檢定人員可於檢查現場即時告知檢定結果，大幅縮短現行驗證檢定方法之結果等待期，未來也可提供不

具分子生物學背景的種苗業者能輕易自行進行種苗病毒檢測，更能落實早期預警病毒病之發生與提高健康種苗生產率。

誌謝

本研究承農業部農業試驗所嘉義農業試驗分所蔡佳達先生與林江美華小姐協助試驗進行，特此致謝。

引用文獻

Adikini, S., S. B. Mukasa, R. O. M. Mwanga, and R. W. Gibson. 2016. Effects of Sweet potato feathery mottle virus and Sweet potato chlorotic stunt virus on the yield of sweetpotato in Uganda. J. Phytopathol. 164:242–254. doi:10.1111/jph.12451

Ateka, E. M., R. W. Njeru, A. G. Kibaru, J. W. Kimenju, E. Barg, R. W. Gibson, and H. J. Vetten. 2004. Identification and distribution of viruses infecting sweet potato in Kenya. Ann. Appl. Biol. 144:371–379. doi:10.1111/j.1744-7348.2004.tb00353.x

Boonham, N., J. Kreuze, S. Winter, R. van der Vlugt, J. Bergervoet, J. Tomlinson, and R. Mumford. 2014. Methods in virus diagnostics: From ELISA to next generation sequencing. Virus Res. 186:20–31. doi:10.1016/j.virusres.2013.12.007

Cheng, Y. H., Y. C. Wang, L. Y. Wang, L. H. Huang, and T. C. Chen. 2020. First report of Sweet potato chlorotic stunt virus infecting sweetpotato in Taiwan. Plant Dis. 104:2535. doi:10.1094/PDIS-01-20-0122-PDN

Chiu, M. S. 2020. The first record of Sweet potato chlorotic fleck virus in Taiwan and the establishment of its detection system. Master Thesis. Department of Applied Chemistry, Chaoyang University of Technology. Taichung, Taiwan. 25 pp. (in Chinese with English abstract)

Chung, M. L., C. H. Liao, M. J. Chen, and R. J. Chiu. 1985. The isolation, transmission and host range of sweet potato leaf curl disease agent in Taiwan. Plant Prot. Bull. 27:333–341.

Clark, C. A., J. A. Davis, J. A. Abad, W. J. Cuellar, S. Fuentes, J. F. Kreuze, ... J. P. T. Valkonen. 2012. Sweet potato viruses: 15 years of progress on understanding and managing complex diseases. Plant Dis. 96:168–185. doi:10.1094/PDIS-07-11-0550

Domola, M. J., G. J. Thompson, T. A. S. Aveling, S. M. Laurie, H. Strydom, and A. A. Van den Berg. 2008. Sweet potato viruses in South Africa and the effect of viral infection on storage root yield. Afr. Plant Prot. 14:15–23.

Food and Agriculture Organization of the United Nations. 2022. FAOSTAT: Production: Crops and livestock products. https://www.fao.org/faostat/en/#data/QCL (visit on 11/14/2023)

Jiang, S. S., J. Feng, M. Zhang, S. J. Wang, Z. M. Xin, B. Wu, and X. Q. Xin. 2018. Development of RT-LAMP assay for rapid detection of Sweet potato feathery mottle virus (SPFMV). Sci. Agric. Sin. 51:1294–1302. (in Chinese with English abstract) doi:10.3864/j.issn.0578-1752.2018.07.007

Kreuze, J. and S. Fuentes. 2008. Sweetpotato viruses. p.659–669. *in*: Encyclopedia of Virology. 3rd ed. (Mahy, B. W. J. and M. H. V. Van Regenmortel, eds.) Academic Press. Amsterdam, The Netherlands. 3192 pp. doi:10.1016/B978-012374410-4.00647-6

Kwak, H. R., M. K. Kim, J. C. Shin, Y. J. Lee, J. K, Seo, H. U. Lee, ... H. S. Choi. 2014. The current incidence of viral disease in Korean sweet potatoes and development of multiplex RT-PCR assays for simultaneous detection of eight sweet potato viruses. Plant Pathol. J. 30:416−424. doi:10.5423/PPJ.OA.04.2014.0029

Li, F., R. Zuo, J. Abad, D. Xu, G. Bao, and R. Li. 2012. Simultaneous detection and differentiation of four closely related sweet potato potyviruses by a multiplex one-step RT-PCR. J. Virol. Methods 186:161–166. doi:10.1016/j.jviromet.2012.07.021

Liao, C. H., I. C. Chien, M. L. Chung, R. J. Chiu, and Y. H. Han. 1979. A study of sweet potato virus disease in Taiwan I. Sweet potato yellow spot virus disease. J. Agric. Res. China 28:127–137. (in Chinese with English abstract) doi:10.29951/JARC.197909.0001

Mbewe, W., A. Mtonga, M. Chiipanthenga, K. Masambaet, G. Chitedze, P. Pamkomera, ... F. Chipungu. 2021. Incidence and distribution of Sweetpotato viruses and their implication on sweetpotato seed system in Malawi. J. Plant Pathol. 103:961–968. doi:10.1007/s42161-021-00830-4

Notomi, T., H. Okayama, H. Masubuchi, T. Yonekawa, K. Watanabe, N. Amino, and T. Hase. 2000. Loop-mediated isothermal amplification of DNA. Nucleic Acids Res. 28:e63. doi:10.1093/nar/28.12.e63

Opiyo, S. A., E. M. Ateka, P. O. Owuor, L. O. A. Manguro, and D. W. Miano. 2010. Development of a multiplex PCR technique for simultaneous detection of Sweet potato feathery mottle virus and Sweet potato chlorotic stunt virus. J. Plant Pathol. 92:363–366.

O'Sullivan, J. N., C. J., Asher, and F. P. C., Blamey. 1997. Nutrient Disorders of Sweet Potato. ACIAR Monograph No. 48. Australian Centre for International Agricultural Research. Canberra, Australia. 136 pp.

Untiveros, M., S. Fuentes, and J. Kreuze. 2008. Molecular

variability of sweet potato feathery mottle virus and other potyviruses infecting sweet potato in Peru. Arch. Virol. 153:473–483. doi:10.1007/s00705-007-0019-0

Wang, L. Y., Y. H. Cheng, N. Y. Wang, K. C. Chen, and S. D. Yeh. 2013. First report of Sweet potato virus G infecting sweet potato in Taiwan. Plant Dis. 97:1260. doi:10.1094/PDIS-01-13-0111-PDN

Wang, L. Y., S. F. Lo, and Y. C. Lai. 2014. Assessment for the viral resistance of sweet potato varieties to three potyviruses by graft inoculation. Plant Pathol. Bull. 23:303–309. doi:10.6649/PPB.201409_23(3_4).0008

Wanjala, B. W., E. M. Ateka, D. W. Miano, S. Fuentes, A. Perez, J. W. Low, and J. F. Kreuze. 2021. Loop-mediated isothermal amplification assays for on-site detection of the main sweetpotato infecting viruses. J. Virol. Methods 298:114301. doi:10.1016/j.jviromet.2021.114301

Wanjala, B. W., E. M. Ateka, D. W. Miano, J. W. Low, and J. F. Kreuze. 2020. Storage root yield of sweetpotato as influenced by Sweetpotato leaf curl virus and its interaction with Sweetpotato feathery mottle virus and Sweetpotato chlorotic stunt virus in Kenya. Plant Dis. 104:1477–1486. doi:10.1094/PDIS-06-19-1196-RE

Establishment and Application of Reverse Transcription Loop-Mediated Isothermal Amplification Assay (RT-LAMP) for the Detection of Sweet Potato Feathery Mottle Virus in Sweet Potato

Ching-Yi Lin[1,*], Hui-Fang Ni[2], and Hui-Ju Lin[3]

Abstract

Lin, C. Y., H. F. Ni., and H. J. Lin. 2024. Establishment and application of reverse transcription loop-mediated isothermal amplification assay (RT-LAMP) for the detection of sweet potato feathery mottle virus in sweet potato. J. Taiwan Agric. Res. 73(2):113–122.

Viral diseases are a major constraint to sweet potato production. Sweet potato feathery mottle virus (SPFMV), a member of the genus *Potyvirus*, is the most widespread virus infecting sweet potato plants worldwide. The production of healthy sweet potato seedlings and the diagnosis of plant viruses at early stage rely on rapid and reliable viral detection technology, which is critical for effective viral prevention and control. In this study, a one-step reverse transcription loop-mediated isothermal amplification (RT-LAMP) assay was developed for detecting SPFMV. The RT-LAMP assay has been optimized to use hydroxy naphthol blue (HNB) for visual colorimetric distinction of positive and negative samples. Using total plant RNA of sweet potato as the template, the optimal reaction conditions were at 63℃ for 45–60 min. The detection limit of the RT-LAMP assay for SPFMV was 237.9×10^{-5} ng μL^{-1}, while that of reverse transcription polymerase chain reaction (RT-PCR) was 237.9×10^{-3} ng μL^{-1}, indicating that the RT-LAMP assay developed was 100 times more sensitive than RT-PCR. The RT-LAMP assay was also successfully applied to the detection of SPFMV in field samples. In conclusion, the RT-LAMP assay developed in this study was a rapid, specific and sensitive method for the detection of SPFMV in field samples of sweet potato.

Key words: Sweet potato feathery mottle virus, Reverse-transcription loop-mediated isothermal amplification, Sweet potato.

Received: November 27, 2023; Accepted: January 22, 2024.

* Corresponding author, e-mail: eris2024@tari.gov.tw

[1] Assistant Research Fellow, Plant Pathology Division, Taiwan Agricultural Research Institute, Taichung City, Taiwan, ROC.

[2] Associate Research Fellow and Division Director, Department of Plant Protection, Chiayi Agricultural Experiment Branch, Taiwan Agricultural Research Institute, Chiayi, Taiwan, ROC.

[3] Research Assistant, Department of Plant Protection, Chiayi Agricultural Experiment Branch, Taiwan Agricultural Research Institute, Chiayi, Taiwan, ROC.

台灣農業研究 (J. Taiwan Agric. Res.) 73(2):123–134 (2024)
https://doi.org/10.6156/JTAR.202406_73(2).0005

研究報告

文心蘭「檸檬綠」植體元素與花芽發育異常之探討

蔡東明[1,*] 錡虹汝[2] 吳承軒[3] 邱亭瑋[4] 莊耿彰[5] 戴廷恩[6]

摘要

蔡東明、錡虹汝、吳承軒、邱亭瑋、莊耿彰、戴廷恩。2024。文心蘭「檸檬綠」植體元素與花芽發育異常之探討。台灣農業研究 73(2):123–134。

本研究以 2 年生文心蘭「檸檬綠」(*Oncidesa* Gower Ramsey 'Honey Angel') 為試驗材料，在假球莖成熟其花芽或葉芽剛成長時，對其葉與假球莖進行植體元素分析，探討氮、磷、鉀、鈣、鎂、碳、碳氮比、鐵及錳等元素濃度與「檸檬綠」花芽發育異常之關係。嘉義大林與彰化大村發生僅長側芽 (跳花) 植株之葉中氮含量僅 1.64% 與 1.65%，遠低於開花正常的植株之葉中氮含量 2.15% 與 2.36%，且氮在植株體內含量高、波動大，推論氮可能與「檸檬綠」跳花有關。磷在植株體內含量低 (0.13%)、波動穩定，推論磷應與跳花相關性低，無促進開花效果。發生跳花的植株葉中鉀之含量 (2.18%) 遠低於開花正常的植株葉中鉀之含量 (3.12%)，且鉀在植株體內含量高、波動大，推論鉀可能與「檸檬綠」跳花有關。碳在文心蘭「檸檬綠」正常開花與跳花植株體內含量穩定，與跳花關係不大，碳氮比似乎不能完全解釋文心蘭開花的關係。鈣在正常開花與跳花植株體內波動大，應與植株缺氮有關、與跳花無關。鎂在植株體內波動較小、表現相對穩定，應與跳花無關。微量元素鐵、錳於植株中含量高或低都會造成跳花，顯示鐵、錳與跳花無關。經由植株元素分析與外表觀察及生理表現，總結嘉義大林與彰化大村兩處生產場域發生嚴重花芽異常發育應與植株氮缺乏有關。

關鍵詞：氮、鉀、碳氮比、文心蘭、跳花。

前言

文心蘭為複莖性蘭科植物，發育中的芽體與前幾個世代的基部相連，正在發育中的世代稱為當代莖，依其相連順序，距離當代莖最近者為前一代莖，再往前一代為前二代莖，以此類推 (Yong & Hew 1995)。一般以短縮莖上萌發假球莖處為第 0 節位，往上為正，往下為負，則第 0–1 節為假球莖，位於假球莖上方之葉片為上位葉 L1 與 L2，假球莖下方 (0 至 -1 節) 著生之葉片為下位葉 L3 與 L4 (Shyu 1997)。文心蘭「檸檬綠」L3 與 L4 葉片有大小區分 (圖 1)，通常在大葉 (L3) 節點 (0 節) 分化出的芽為花芽，小葉 (L4) 節點 (-1 節) 長出的芽為葉芽，除非大葉節點花芽遭外力破壞時，小葉節點有機會再分化長成花芽。因此，當假球莖成熟時，新芽由小葉節點抽出或是由 -2 至 -4 節點長出者 (Li & Chang 2023)，形成葉芽而不開花，此類花芽發育異常農民稱之為『跳花』(圖 2A)。

文心蘭「檸檬綠」切花以外銷日本為主要市場，特定季節需求量高、價格上揚，花農為獲得較高產量，常利用增加肥料用量與使用高磷鉀肥催花，或為了預防夏季軟腐病而降低氮肥使用等不當施肥處理，造成植株營養生長過

投稿日期：2023 年 12 月 19 日；接受日期：2024 年 2 月 29 日。
* 通訊作者：sdon@tari.gov.tw
[1] 農業部農業試驗所花卉試驗分所遺傳育種系副研究員。臺灣 雲林縣。
[2] 農業部農業試驗所花卉試驗分所產程開發系計畫助理。臺灣 雲林縣。
[3] 農業部農業試驗所花卉試驗分所產程開發系助理研究員。臺灣 雲林縣。
[4] 農業部農業試驗所花卉試驗分所遺傳育種系助理研究員。臺灣 雲林縣。
[5] 農業部農業試驗所花卉試驗分所遺傳育種系研究員兼系主任。臺灣 雲林縣。
[6] 農業部農業試驗所花卉試驗分所研究員兼分所長。臺灣 雲林縣。

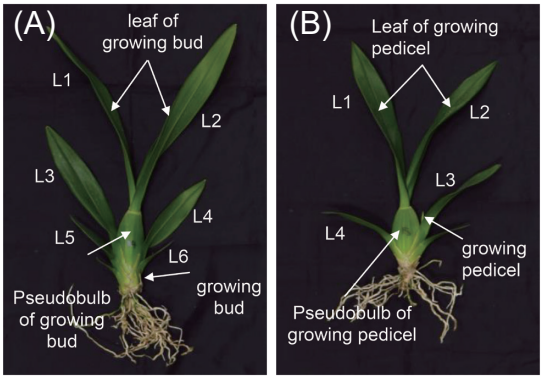

圖 1. 文心蘭植株 (A) 長側芽植株 (跳花)；(B) 長花芽植株 (正常開花)。

Fig. 1. Oncidium plant: (A) plant with lateral bud (abnormal flowering) and (B) plant with pedicel (normal flowering).

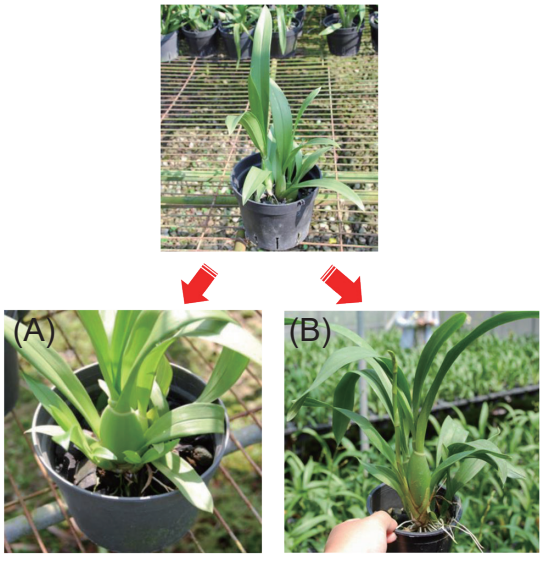

圖 2. 文心蘭植株生長情形：(A) 花芽異常發育 (跳花)；(B) 正常開花。

Fig. 2. Oncidium plant growth: (A) abnormal flowering and (B) normal flowering.

盛或不良，使得文心蘭跳花問題日趨嚴重，造成農民損失。為釐清文心蘭肥培管理與跳花發生之關係，本試驗希望藉由不同產區農民之植株採樣調查與植體元素分析來探討跳花發生之原因，並提出可能之改善建議。

材料與方法

試驗材料說明

取樣之植株部位分為花芽-葉 (leaf of growing pedicel)、花芽-假球莖 (pseudobulb of growing pedicel)、葉芽-葉 (leaf of growing bud)、葉芽-假球莖 (pseudobulb of growing bud)、L3 葉芽-葉 (leaf of L3 growing bud)、L3 葉芽-假球莖 (pseudobulb of L3 growing bud)、L4葉芽-葉 (leaf of L4 growing bud) 及 L4 葉芽-假球莖 (pseudobulb of L4 growing bud)。

(1) 花芽-葉：當代成熟假球莖其 L3 大葉節點剛抽花梗之植株，取其 L1 與 L2 葉子進行植體分析 (圖 1B)。

(2) 花芽-假球莖：當代成熟假球莖其 L3 大葉節點剛抽花梗之植株，取其假球莖進行植體分析 (圖 1B)。

(3) 葉芽-葉：當代成熟假球莖其 L4 小葉或 -2 至 -4 節點抽出葉芽之植株，取其 L1 與 L2 葉子進行植體分析 (圖 1A)。

(4) 葉芽-假球莖：當代成熟假球莖其 L4 小葉或 -2 至 -4 節點抽出葉芽之植株，取其假球莖進行植體分析 (圖 1A)。

(5) L3 葉芽-葉：當代成熟假球莖其 L3 大葉節點剛抽葉芽之植株，取其 L1 與 L2 葉子進行植體分析 (圖 3A)。

(6) L3 葉芽-假球莖：當代成熟假球莖其 L3 大葉節點剛抽葉芽之植株，取其假球莖進行植體分析 (圖 3A)。

(7) L4 葉芽-葉：當代成熟假球莖其 L4 小葉節點剛抽葉芽之植株，取其 L1 與 L2 葉子進行植體分析 (圖 3B)。

(8) L4 葉芽-假球莖：當代成熟假球莖其 L4 小葉節點剛抽葉芽之植株，取其假球莖進行植體分析 (圖 3B)。

植物材料

試驗一：臺中新社文心蘭「檸檬綠」95% 開花之植株元素分析

2019 年 1 月 31 日於臺中新社採樣植株，

圖 3. (A) 新芽-葉 (大葉 L3 長新芽)；(B) 新芽-葉 (小葉 L4 長新芽)。

Fig. 3. (A) Leaf (L3 growing bud) and (B) Leaf (L4 growing bud).

生產設施為具開頂與內循環風扇之塑膠布溫室，2 年生有 3 顆假球莖之 5 寸盆「檸檬綠」，第一次開花，慣行栽培 (介質上施用緩效性 N-P_2O_5-K_2O：20-20-20 的粒肥，及每星期噴灌 1−2 次 1,200−2,000 倍 N-P_2O_5-K_2O：14-14-14 的液肥，夏天會使用含氮低一點的液肥如 N-P_2O_5-K_2O：15-10-30)，園區植株抽梗率約 95% (每次調查 30 盆文心蘭植株，3 重複)。逢機選取 5 株成熟假球莖其 L3 大葉節點剛抽花梗之植株，另選取 5 株 L4 小葉或 -2 至 -4 節點抽出葉芽之植株，進行植株葉片與假球莖之植體元素分析 (圖 1)。

試驗二：臺中新社文心蘭「檸檬綠」75% 開花之植株元素分析

2019 年 1 月 18 日臺中新社採樣植株，生產設施為簡易黑色針織網，2 年生有 3 顆假球莖之 5 寸盆「檸檬綠」，第一次開花，慣行栽培，園區植株抽梗率約 75%。逢機選取 5 株成熟假球莖其 L3 大葉節點剛抽出花梗之植株，另選取 5 株 L4 小葉或 -2 至 -4 節點抽出葉芽之植株，進行植株葉片與假球莖之植體元素分析。

試驗三：嘉義大林文心蘭「檸檬綠」跳花之植株元素分析

2019 年 5 月 23 日於嘉義大林採樣植株，生產設施為簡易黑色針織網，2 年生有 3 顆假球莖之 5 寸盆「檸檬綠」，第一次開花，肥培方式：1 月起逐漸減少氮提供 (11、12 月文心蘭花期結束主要施用高氮水溶性速效肥料 N-P_2O_5-K_2O：30-10-10，1 月主要施用 N-P_2O_5-K_2O：20-10-20，2 月以後逐漸以 N-P_2O_5-K_2O：6-13-32 為主，液肥倍數約為 1,200 倍，electrical conductivity (EC) 值約為 0.7 mS cm^{-1})，園區植株發生嚴重跳花 (圖 4A)。逢機選取 5 株成熟假球莖其 L3 大葉節點剛抽花梗之植株，另選取 5 株 L4 小葉或 -2 至 -4 節點抽出葉芽之植株，進行植株葉片與假球莖之植體元素分析。

試驗四：彰化大村文心蘭「檸檬綠」跳花之植株元素分析

2020 年 11 月 11 日於彰化大村採樣植株，生產設施為簡易黑色針織網，2 年生有 3 顆假球莖之 5 寸盆「檸檬綠」，園區植株發生嚴重跳花，肥培方式：施用磷酸一鉀 (N-P_2O_5-K_2O：0-52-34) 與硫酸鉀催花，無施用其他含氮肥料。因全區幾乎無開花株，無法取得合適開花

圖 4. (A) 2019 年 5 月 23 日嘉義大林跳花嚴重；(B) 2020 年 4 月 15 日嘉義大林約 50% 開花；(C) 2020 年 4 月 15 日嘉義大林跳花植株老葉黃化；(D) 2020 年 11 月 11 日彰化大村跳花植株老葉黃化。

Fig. 4. (A) On May 23, 2020, serious abnormal flowering in Dalin, Chiayi; (B) on April 15, 2020, about 50% flowering in Dalin, Chiayi; (C) on April 15, 2020, the old leaves of abnormal flowering plants in Dalin, Chiayi turned yellow; and (D) on November 11, 2020, the old leaves of abnormal flowering plants in Dacun, Changhua turned yellow.

試驗植株，故逢機選取 5 株 L3 大葉節點抽出葉芽之植株，另選取 5 株 L4 小葉或 -2 至 -4 節點抽出葉芽之植株，進行植株葉片與假球莖之植體元素分析。

植體元素分析方法

將取樣之植株部位分為花芽-葉、花芽-假球莖、葉芽-葉、葉芽-假球莖、L3 葉芽-葉、L3 葉芽-假球莖、L4 葉芽-葉及 L4 葉芽-假球莖，秤其鮮重，經清洗表面髒汙與其他雜質後，再以 1% HCl 潤洗片刻，最後以去離子水潤洗 3 次，將表面乾擦後，裝入牛皮紙袋置於烘箱中，先以溫度 100℃ 1 h 殺菁以終止生化反應，後放置烘箱以溫度 70–80℃進行 48 h 以上烘乾，至植體完全乾燥為止，烘乾後將樣品秤重，使用小型高速粉碎機粉碎均質，再以硫酸紙袋包裝，存放於乾燥箱中。

取 0.5 g 乾粉為材料，以硝酸：過氯酸 = 4 : 1 之酸液 5 mL 進行消化分解，經常溫 8 h 以上之預分解後，再利用石墨爐加熱至 160℃，經 3 h 分解後取出冷卻。冷卻後材料加少許去離子水進行過濾，再定量成 50 mL 溶液。完成之液體樣品經稀釋與添加總量 5% 之釋放劑 (0.1% 氯化鍶) 後 (僅鉀、鈣及鎂樣品添加)，使用原子吸收儀 (Savant AA, GBC, Keysborough, Australia) 測量鉀、鈣、鎂、鐵及錳之元素含量；磷元素則在稀釋後添加鉬黃反應劑，反應 15–30 min 後以分光光度計 (V-630 BIO, Jasco, Tokyo, Japan) 測定。碳與氮含量則在乾粉秤重後，以錫囊包裹，透過固態碳氮硫分析儀 (Flash EA 1112 series, Thermo, Waltham, MA, USA) 測定。

試驗設計與統計分析

試驗採逢機取樣，每處理 5 重複，每重複 1 株。試驗數據以統計軟體 Costat 6.1 (CoHort Software, Minneapolis, MN, USA) 進行變方分析與最小顯著差異性測驗 (Fisher's protected least significant difference test; LSD test, $P < 0.05$)。

結果

試驗一：文心蘭「檸檬綠」臺中新社 (簡易塑膠布) 採樣植株分析數據 (表 1) 顯示，植株體內主要元素氮在葉片中含量高於假球莖，以葉芽-葉 2.36% 含量最高，開花株與不開花株間無顯著差異；磷在葉片中含量高於假球莖，以葉芽-葉 0.13% 含量最高，開花株與不開花株間無顯著差異；鉀在葉片中含量高於假球莖，以葉芽-葉 3.12% 含量最高，開花株與不開花株間無顯著差異；氮、磷、鉀在葉含量皆高於假球莖且具有顯著差異。鈣在葉片中含量高於假球莖，以葉芽-葉 0.91% 含量最高，葉片中鈣含量於開花株與不開花株間具顯著差異；鎂在葉片中含量高於假球莖，以葉芽-葉 0.31% 含量最高，葉片中鎂含量於開花株與不開花株間具顯著差異。碳在葉片中含量高於假球莖，以花芽-葉 46.06% 含量最高，開花株與不開花株間無顯著差異；碳氮比在假球莖比值高於葉，以花芽-假球莖 42.19 比值最高，假球莖中碳氮比於開花株與不開花株間具顯著差異。微量元素鐵在葉片中含量遠高於假球莖，以花芽-葉 248.8 mg L^{-1} 含量最高，開花株與不開花株間無顯著差異；錳在葉片中含量遠高於假球莖，以葉芽-葉 414.0 mg L^{-1} 含量最高，葉片中錳含量於開花株與不開花株間具顯著差異。

試驗二：文心蘭「檸檬綠」臺中新社 (黑網) 採樣植株分析數據 (表 2) 顯示，植株體內主要元素氮以葉芽-葉 2.15% 含量最高，其次為花芽-葉 1.87%，再其次為葉芽-假球莖 0.77%，最後為花芽-假球莖 0.59%；磷以葉芽-葉 0.3% 含量最高，其次為花芽-葉 0.22%，再其次為葉芽-假球莖 0.13%，最後為花芽-假球莖 0.11%；鉀以葉芽-葉 3.16% 含量最高，其次為花芽-葉 2.59%，再其次為葉芽-假球莖 1.28%，最後為花芽-假球莖 1.16%。氮、磷、鉀都以葉芽-葉含量最高，在葉芽-葉與花芽-葉間具有顯著差異，葉芽-假球莖與花芽-假球莖間無顯著差異，葉與假球莖間具顯著差異。鈣在葉片中含量顯示開花株高於不開花株，花芽-假球莖鈣含量 0.95% 與葉芽-假球莖 0.71% 具有顯著性差異。鎂在葉片中含量開花株與不開花株相同，花芽-假球莖鎂含量 0.25% 與葉芽-假球莖 0.23% 具有顯著性差異。碳在葉片中含量開花株與不開花株無顯著差異，葉與假球莖中碳含量有顯著差異，碳氮比以花芽-假球莖 74.39 比值最高，

開花株花芽-葉 25.55 與不開花株葉芽-葉 22.22 碳氮比無顯著差異，花芽-假球莖 74.39 與葉芽-假球莖 59.34 碳氮比有顯著差異。微量元素鐵以葉芽-葉 261.40 mg L^{-1} 含量最高，開花株與不開花株於葉片具有顯著差異。錳以花芽-葉 215.3 mg L^{-1} 含量最高，開花株與不開花株間無顯著差異。

試驗三：文心蘭「檸檬綠」嘉義大林 (黑網) 採樣植株分析數據 (表 3) 顯示，植株體內主要元素氮在葉片中含量高於假球莖，以葉芽-葉 1.64% 含量最高，開花株與不開花株間無顯著差異；磷在葉片中含量高於假球莖，以葉芽-葉與花芽-葉 0.22% 含量最高，開花株與不開花株間無顯著差異；鉀在葉片中含量高於假球莖，以葉芽-葉 2.31% 含量最高，葉片中鉀含量於開花株與不開花株間具顯著差異。鈣在假球莖中含量高於葉片，以花芽-假球莖 1.25% 含量最高，開花株與不開花株間無顯著差異；鎂在假球莖中含量高於葉片，以花芽-假球莖 0.35% 含量最高，開花株與不開花株間無顯著差異。碳在葉片中含量高於假球莖，以葉芽-葉 47.29% 含量最高，開花株與不開花株間無顯著差異；碳氮比在假球莖中比值高於葉片，以葉芽-假球莖 49.35 比值最高，假球莖中碳氮比比值於開花株與不開花株間具顯著差異。微量元素鐵在葉片中含量遠高於假球莖，以葉芽-葉 295.3 mg L^{-1} 含量最高，葉片中鐵含量於開花株與不開花株間具顯著差異；錳在假球莖中含量高於葉片，以葉芽-假球莖 825.5 mg L^{-1} 含量最高，假球莖中錳含量於開花株與不開花株間具顯著差異。

試驗四：文心蘭「檸檬綠」彰化大村 (黑網)

表 1. 溫室栽培文心蘭「檸檬綠」95% 開花之植株元素分析。

Table 1. Elemental analysis of 95% flowering *Oncidesa* Gower Ramsey 'Honey Angel' cultivated in greenhouse.

Item	N (%)	P (%)	K (%)	Ca (%)	Mg (%)	C (%)	C/N	Fe (mg L^{-1})	Mn (mg L^{-1})
Leaf of growing pedicel	2.16 a[z]	0.11 a	3.05 a	0.67 b	0.26 b	46.06 a	21.78 c	248.8 a	314.2 b
Pseudobulb of growing pedicel	1.08 b	0.09 b	1.96 b	0.29 c	0.22 b	44.31 b	42.19 a	72.3 b	87.7 c
Leaf of growing bud	2.36 a	0.13 a	3.12 a	0.91 a	0.31 a	45.90 a	19.88 c	245.1 a	414.0 a
Pseudobulb of growing bud	1.38 b	0.08 b	1.92 b	0.40 c	0.24 b	44.89 ab	32.70 b	82.4 b	118.4 c

[z] Mean separation within each column by Fisher's protected least significant difference test at $P \leq 0.05$, $n = 5$.

表 2. 網室栽培文心蘭「檸檬綠」75% 開花之植株元素分析。

Table 2. Elemental analysis of 75% flowering *Oncidesa* Gower Ramsey 'Honey Angel' cultivated in net house.

Item	N (%)	P (%)	K (%)	Ca (%)	Mg (%)	C (%)	C/N	Fe (mg L^{-1})	Mn (mg L^{-1})
Leaf of growing pedicel	1.87 b[z]	0.22 b	2.59 b	0.83 ab	0.19 c	47.59 a	25.55 c	211.40 b	215.3 a
Pseudobulb of growing pedicel	0.59 c	0.11 c	1.16 c	0.95 a	0.25 a	43.48 b	74.39 a	53.72 c	128.8 b
Leaf of growing bud	2.15 a	0.30 a	3.16 a	0.72 b	0.19 c	47.40 a	22.22 c	261.40 a	210.5 a
Pseudobulb of growing bud	0.77 c	0.13 c	1.28 c	0.71 b	0.23 b	43.63 b	59.34 b	58.10 c	121.6 b

[z] Mean separation within each column by Fisher's protected least significant difference test at $P \leq 0.05$, $n = 5$.

表 3. 嘉義大林文心蘭「檸檬綠」跳花之植株元素分析。

Table 3. Elemental analysis of abnormal flowering *Oncidesa* Gower Ramsey 'Honey Angel' in Dalin, Chiayi.

Item	N (%)	P (%)	K (%)	Ca (%)	Mg (%)	C (%)	C/N	Fe (mg L^{-1})	Mn (mg L^{-1})
Leaf of growing pedicel	1.60 a[z]	0.22 a	1.97 b	1.11 a	0.28 b	47.09 a	29.90 c	252.9 b	531.0 c
Pseudobulb of growing pedicel	1.10 b	0.18 a	1.56 c	1.25 a	0.35 a	44.22 b	41.64 b	79.6 c	655.0 b
Leaf of growing bud	1.64 a	0.22 a	2.31 a	1.11 a	0.29 ab	47.29 a	29.40 c	295.3 a	589.5 bc
Pseudobulb of growing bud	0.92 b	0.21 a	1.59 c	1.21 a	0.34 ab	44.83 b	49.35 a	109.2 c	825.5 a

[z] Mean separation within each column by Fisher's protected least significant difference test at $P \leq 0.05$, $n = 5$.

採樣植株分析數據 (表 4) 顯示，植株體內主要元素氮在葉片中含量高於假球莖，以 L4 小葉長新芽-葉 1.79% 含量最高，L3 大葉長新芽植株與 L4 小葉長新芽植株間無顯著差異；磷在葉片中含量高於假球莖，以 L3 大葉長新芽-葉 0.27% 含量最高，L3 大葉長新芽植株與 L4 小葉長新芽植株間無顯著差異；鉀在葉片中含量高於假球莖，以 L3 大葉長新芽-葉 2.32% 含量最高，假球莖中鉀含量於 L3 大葉長新芽植株與 L4 小葉長新芽植株間具顯著差異。鈣在假球莖中含量高於葉片，以 L3 大葉長新芽-假球莖 2.52% 含量最高，葉片中鈣含量於 L3 大葉長新芽植株與 L4 小葉長新芽植株間具顯著差異；鎂在假球莖中含量高於葉片，以 L4 小葉長新芽-假球莖 0.33% 含量最高，L3 大葉長新芽植株與 L4 小葉長新芽植株間無顯著差異。碳在葉片中含量高於假球莖，以 L4 小葉長新芽-葉 44.42% 含量最高，L3 大葉長新芽植株與 L4 小葉長新芽植株間無顯著差異；碳氮比在假球莖中比值高於葉片，以 L3 大葉長新芽-假球莖 46.81 比值最高，L3 大葉長新芽植株與 L4 小葉長新芽植株間無顯著差異。微量元素鐵在葉片中含量遠高於假球莖，以 L4 小葉長新芽-葉 482.5 mg L^{-1} 含量最高，L3 大葉長新芽植株與 L4 小葉長新芽植株間無顯著差異；錳在葉片中含量高於假球莖，以 L3 大葉長新芽-葉與 L4 小葉長新芽-葉 66.5 mg L^{-1} 含量最高，L3 大葉長新芽植株與 L4 小葉長新芽植株間無顯著差異。

總結文心蘭葉片與假球莖元素分析數據顯示，大量元素氮、磷、鉀在葉片中含量皆大於假球莖，其中氮與鉀元素含量具有顯著性差異。光合作用產物碳在葉片中含量大於假球莖，除了彰化大村數據無顯著差異外，其他 3 處皆顯示葉片與假球莖中碳含量具有顯著差異；葉片中碳氮比數據顯示皆小於假球莖，且具有顯著差異性。微量元素鐵在葉片中含量皆大於假球莖，具有顯著性差異。

討論

文心蘭為複莖性蘭科植物，通常在假球莖成熟後於 L3 大葉底端芽節處會花芽分化產生花梗，如果先萌動的芽是在 L4 小葉或更下層 (L5、L6……) 底端芽節，則會長出葉芽形成跳花，跳花會減少 1 次採收機會，尤其 4–6 月「檸檬綠」切花品質好、售價高時，常造成農民損失慘重。跳花常會發生在新定植之植株，一般文心蘭切花品種瓶苗出瓶後約 2 年會開第 1 支花，亦即瓶苗出瓶定植後，第 3 代假球莖成熟就具開花能力，本試驗所要討論的跳花是指栽種至第 2 年仍然無法全面開花，多數植株持續產生葉芽而非花芽。文心蘭生長主要可分為 2 階段，組培出瓶後 1–2 年為營養生長 (幼年期)，2 年之後進入生殖生長，Hew & Yong (1994) 認為文心蘭會因為植體本身的營養狀態選擇進行營養生長或生殖生長。本次試驗利用園區採樣正常開花的植株進行元素分析當對照組，與跳花嚴重園區採樣植株進行比較探討。

植物體內大量元素氮、磷、鉀與文心蘭「檸檬綠」跳花之關係

氮、磷、鉀在植物體內屬於移動快速的大

表 4. 彰化大村文心蘭「檸檬綠」跳花植株元素分析。

Table 4. Elemental analysis of abnormal flowering *Oncidesa* Gower Ramsey 'Honey Angel' in Dacun, Changhua.

Item	N (%)	P (%)	K (%)	Ca (%)	Mg (%)	C (%)	C/N	Fe (mg L^{-1})	Mn (mg L^{-1})
Leaf of L3 growing bud	1.65 a[z]	0.27 a	2.32 a	2.07 b	0.30 a	43.79 a	26.57 b	478.5 a	66.5 a
Pseudobulb of L3 growing bud	0.92 b	0.17 b	1.67 c	2.52 a	0.32 a	43.07 a	46.81 a	107.5 b	42.7 b
Leaf of L4 growing bud	1.79 a	0.25 a	2.18 a	1.86 c	0.28 a	44.42 a	24.83 b	482.5 a	66.5 a
Pseudobulb of L4 growing bud	1.03 b	0.20 b	1.96 b	2.48 a	0.33 a	44.29 a	43.17 a	101.5 b	41.1 b

[z] Mean separation within each column by Fisher's protected least significant difference test at $P \leq 0.05$, $n = 5$.

量元素，根部吸收後主要運往葉片，結合或協助光合作用的碳骨架形成蛋白質、核酸及脂肪等化合物。本試驗植體分析結果顯示，葉芽-葉中氮、磷、鉀元素含量最高，最能反映當時環境狀況與植物吸收情形，故本試驗在氮、磷、鉀的探討選擇以葉芽-葉的元素含量作為分析對象。一般花農會使用高磷鉀肥來促進開花，因此先由磷、鉀肥來探討與「檸檬綠」開花的關係。臺中新社開花率 75%「檸檬綠」之葉芽-葉磷含量為 0.30%，開花率 95% 之葉芽-葉磷含量為 0.13%，數據顯示磷含量較低者，文心蘭開花率較高；位於嘉義大林與彰化大村跳花場域植株抽樣分析，葉芽-葉中磷的含量分別為 0.22 與 0.27%，與臺中新社未跳花場域之磷含量未有顯著差異，園區卻出現嚴重跳花，顯示植株體內高磷並無促進開花效果，且磷在植株體內與氮、鉀比較含量偏低 (圖 5)，推論磷應與跳花關係不顯著。

新社開花率 75% 園區採樣植株之葉芽-葉中鉀含量為 3.16%；開花率 95% 園區採樣植株之葉芽-葉中鉀含量為 3.12%；嘉義大林跳花園區採樣植株之葉芽-葉中鉀含量為 2.31%；彰化大村跳花嚴重園區採樣植株之葉芽-葉中鉀含量為 2.32%，數據顯示發生跳花的園區其葉芽-葉中鉀含量遠低於開花正常的園區，且鉀在植株體內含量高、波動大 (圖 5)。鉀為植物生長必要元素之一，調控各種植物之生理反應如維持細胞體內之滲透壓、調控氣孔開閉與細胞中的酸鹼值等，鉀也與蛋白質合成有關如 ribulose-1,5-bisphosphate carboxylase 缺鉀時無法合成 (Peoples & Koch 1979)，推論鉀與文心蘭「檸檬綠」跳花可能有關係。又彰化大村跳花嚴重園區植株除了每週施用磷酸一鉀 ($N\text{-}P_2O_5\text{-}K_2O$ = 0-52-34) 外，隔 1 wk 會再加強施用硫酸鉀催花，園區植株在高鉀肥使用下，採樣植株元素分析卻顯示鉀肥含量偏低，推論氮肥不足可能會影響鉀的吸收。

蝴蝶蘭在肥料供應充足的情況下，花梗發育所用的氮 71% 來自根部所吸收的氮，29% 來自儲存於植體內的氮，若於花梗發育時期進行斷肥處理，則會影響花梗及花序發育，說明植體儲存的氮與環境所供應的氮多寡會影響植株之生長 (Peng 2008)。新社開花率 75% 園區採樣植株之葉芽-葉中氮含量為 2.15%；開花率 95% 園區採樣植株之葉芽-葉中氮含量為 2.36%；嘉義大林跳花園區採樣植株之葉芽-葉中氮含量僅 1.64%，主因花農為了降低 5、6 月軟腐病的高峰期，於 1 月起逐漸降低氮肥使

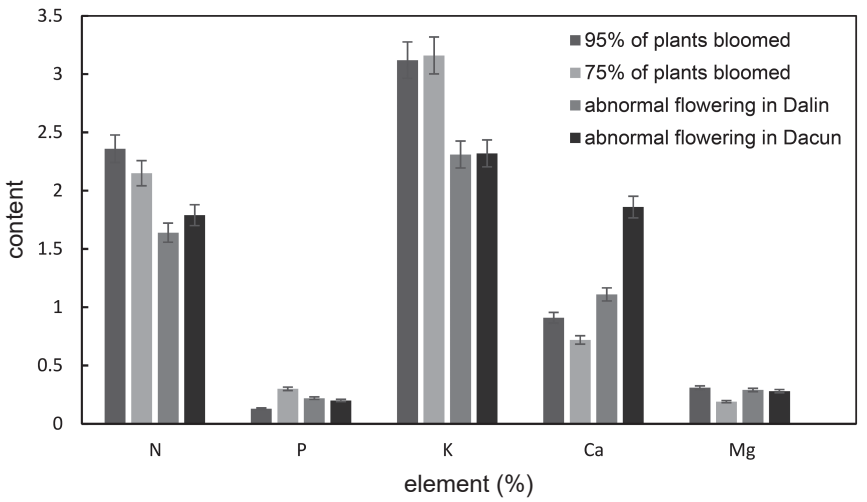

圖 5. 文心蘭「檸檬綠」不同地區葉芽-葉 N、P、K、Ca 及 Mg 元素分析。

Fig. 5. Elemental analysis of N, P, K, Ca, Mg in leaf of growing bud of *Oncidesa* Gower Ramsey 'Honey Angel' in different regions.

用；彰化大村跳花嚴重園區採樣植株之葉芽-葉中氮含量為 1.65%，花農僅用磷酸一鉀催花，數據顯示發生跳花之園區其葉芽-葉中氮含量遠低於開花正常的園區，且氮在植株體內含量高、波動大 (圖 5)，推論氮與文心蘭「檸檬綠」跳花可能有關係。

氮是植物生存所需的巨量元素之一，在植體內與碳和其他礦物元素合成核酸、胺基酸、色素及次級代謝物 (Inokuchi *et al*. 2002)，許多農藝作物如小麥、稻米等氮供應多寡，常是栽培上限制作物生長與產量的主要因子 (Lea & Azevedo 2006)。文心蘭新芽發育至假球莖膨大，前代假球莖的氮含量會下降，當代假球莖則提升了 1.5 倍的氮含量，說明前代假球莖提供當代新芽發育所需的氮素 (Hew & Ng 1996)。持續對嘉義大林園區監控發現，隔年 4 月園區約 50% 植株開花 (圖 4B–C)，前代植株老葉葉尖顏色變黃，推論因花梗發育需要大量的氮，但花農為了控制軟腐病降低氮肥供應，植株不得已只好降解前代假球莖與葉的胞器如葉綠體，提供花梗發育所需之含氮物質，顯示植株缺乏氮素。葉片衰老是植物資源管理必經過程，由於植物生長位置固定，無法逃離不良環境去尋找所需要的礦物營養，因此選擇了程序性細胞死亡與衰老，以應對它們遇到的零星營養缺乏 (Buchanan-Wollaston 1997; Lim *et al*. 2003; Guiboileau *et al*. 2010)。葉片衰老有助於擺脫低效與老化的光合作用器官，並在衰老過程中，葉綠體與蛋白質的降解提供了糖、脂類及氨基酸等營養物質的再利用 (Masclaux-Daubresse *et al*. 2006; Howarth *et al*. 2008; Hu *et al*. 2016)。植物在供源與積貯的關係中，葉片衰老對種子的肥大與作物產量增加具重要性 (Gregersenet *et al*. 2013)，葉綠體是葉片中蛋白質的主要來源，因此對葉片衰老過程中的蛋白質水解與氮再利用主要關鍵在葉綠體蛋白，尤其是 Rubisco 的再利用，這一點與葉綠體是最先被分解的細胞胞器事實非常吻合，亦即葉綠素降解引起的漸進性葉片變黃 (Peoples & Dalling 1988)。彰化大村園區詳細觀察發現，跳花植株前代老株下位葉黃化 (圖 4D)，且同一園區相同栽培模式下，另外一半所種植的老株卻正常開花。玫瑰在營養生長期會將大部分的氮運送至枝條內，除了供應枝條生長外，亦會將多餘的氮儲存起來，進入開花期，除了根部所吸收的氮會供應開花枝發育外，在營養生長期儲存於枝條內的氮亦會供應玫瑰開花所需的氮源 (Cabrera *et al*. 1995)。推論前代、前前代葉片及假球莖提供所需氮，補足了當代植株氮的缺乏，讓該區老株能執行生殖生長。

植物體內碳、碳氮比與文心蘭「檸檬綠」跳花之關係

植物經光合作用將環境中的二氧化碳與水固定合成碳水化合物儲存於植體內，依其功能可分為結構性碳水化合物與非結構性碳水化合物。結構性碳水化合物如纖維素、木質素等；非結構性碳水化合物如蔗糖、葡萄糖等，非結構性的碳水化合物除了供應植物生長所需的能量外，亦作為碳分子骨架，提供與其他元素結合成蛋白質、脂肪酸等 (Meier & Reid 1982)，故碳在植物體內非常重要。本試驗在不同地區蘭園採樣植株之碳元素分析數據顯示 (表 1–4)，同一園區開花與不開花之植株總碳含量非常接近，不同園區抽樣調查植株之碳元素含量亦相近，僅有彰化大村與其他地區有些微差異。作物的生長來自於植物對碳的累積，而氮的供應是影響植物對碳累積的主要因子 (Dickson 1989)，推估彰化大村碳含量較低可能與長時間僅提供高磷、鉀肥無氮肥供應，影響酶等含氮化合物生合成，進而影響光合作用之碳水化合物累積。總體歸納碳在正常開花與跳花植株體內含量穩定，不同園區採樣植株之假球莖中碳含量亦相近 (圖 6)，應與文心蘭「檸檬綠」跳花關係不大。其次碳氮比與跳花之關係，碳氮比可用來判斷植物生長與營養狀態的指標，植體內的碳水化合物含量增加，碳氮比提高可促進植株開花，而供應較多的氮，植株碳氮比下降則會促進植株進行營養生長 (Corbesier *et al*. 2002)。蘭科植物的假球莖具有貯藏水分、碳水化合物及礦物營養的功能，因此前人在研究文心蘭植體營養變化時，多以假球莖做為

分析對象 (Ng & Hew 2000)。表 2 資料顯示花芽-假球莖碳氮比高達 74.39，植株開花表現達 75%，符合 Corbesier (2002) 推論，但表 1 資料顯示花芽-假球莖碳氮比僅 42.19，植株開花率卻高達 95%，嘉義大林植株跳花，資料顯示花芽-假球莖碳氮比為 41.64 (表 3)，彰化大村植株嚴重跳花，葉芽-假球莖碳氮比為 46.81 (表 4)，碳氮比似乎不能完全解釋與文心蘭開花的關係 (圖 6)，推論可能影響碳氮比大小之因子，不在分子『碳』而是在分母『氮』。

植物體內鈣、鎂、鐵、錳與文心蘭「檸檬綠」跳花之關係

臺中新社 75% 開花園內採樣植株顯示，開花植株中鈣的含量大於不開花植株；新社 95% 開花園採樣植株顯示，開花植株中鈣的含量小於不開花植株；嘉義大林跳花園區採樣植株顯示，開花植株中鈣的含量約等於不開花植株，推論鈣與花芽分化應無相關。但臺中新社 75% 與 95% 開花園區葉芽-葉之鈣含量 0.72% 與 0.91%，比嘉義大林、彰化大村跳花園區葉芽-葉含量 1.11% 與 2.52% 低，嘉義大林與彰化大村園區並無對鈣加強施肥，僅降低氮使用，尤其彰化大村鈣高出一倍以上 (圖 5)，推論植體鈣含量較高與氮含量較低有關。可能因植株氮同化作用降低，減少植體糖類的消耗，導致合成細胞壁的大分子碳水化合物增加，鈣亦跟著增加。當植株吸收過多的氮，會因氮素之同化作用增加而持續消耗植體糖類與能量，導致構成細胞壁的大分子碳水化合物與澱粉聚集物減少，作物組織軟弱且易有病蟲害之發生 (Epstein & Bloom 2005)。鎂在 4 個採樣植株中含量低且呈現穩定，植株間差異不大，應與植株花芽分化無關 (圖 5)。鐵、錳主要分布在葉片，假球莖分布較少，嘉義大林跳花植株之鐵含量以葉芽-葉 295.3 mg L^{-1} 為最高、錳含量以葉芽-假球莖 825.5 mg L^{-1} 為最高；彰化大村植株之鐵含量以小葉長新芽-葉最高 482 mg L^{-1}、錳含量以小葉長新芽-葉 66.5 mg L^{-1} 最高，由表 3、4 比對分析及圖 7 顯示，不論鐵、錳含量高或低都會造成跳花，顯示微量元素鐵、錳與文心蘭「檸檬綠」跳花相關不明顯。

本試驗經由不同園區採樣植株元素分析與園區植株外表觀察及生理表現，推論嘉義大林與彰化大村園區嚴重跳花應與氮素缺乏有關。

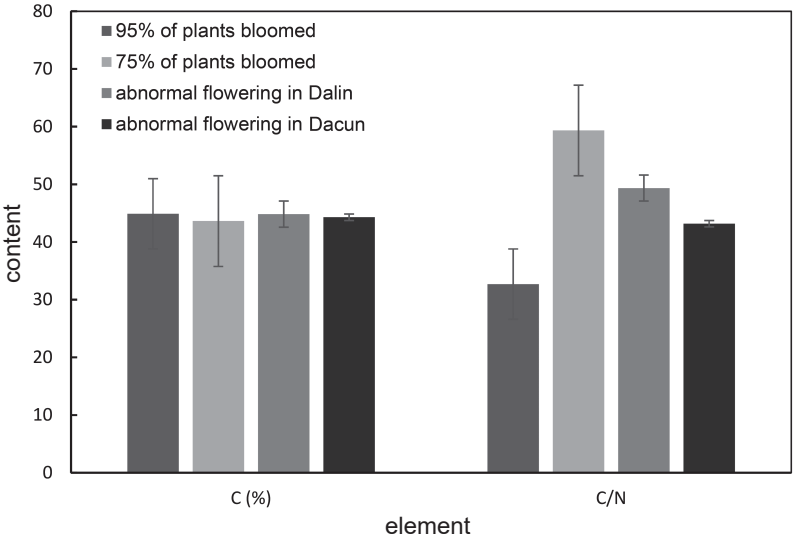

圖 6. 文心蘭「檸檬綠」不同地區葉芽-假球莖 C 與 C/N 元素分析。

Fig. 6. Elemental analysis of C and C/N in pseudobulb of growing bud of *Oncidesa* Gower Ramsey 'Honey Angel' in different regions.

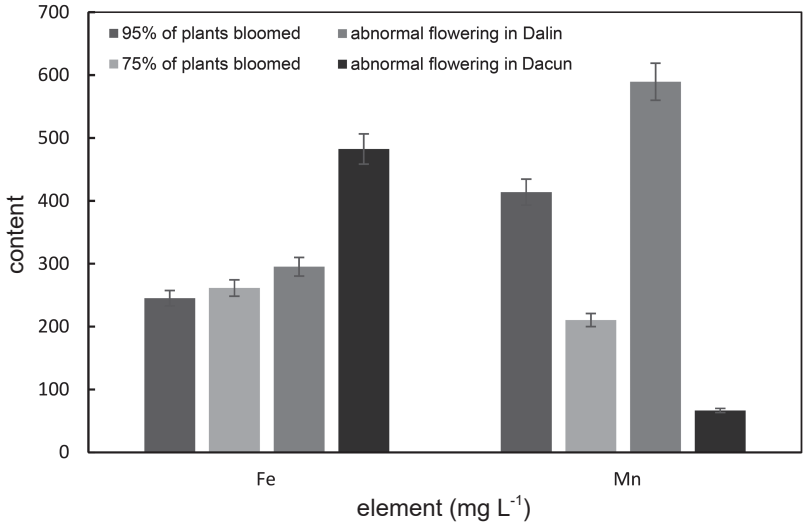

圖 7. 文心蘭「檸檬綠」不同地區葉芽-葉 Fe 與 Mn 元素分析。

Fig. 7. Elemental analysis of Fe and Mn in leaf of growing bud of *Oncidesa* Gower Ramsey 'Honey Angel' in different regions.

引用文獻

Buchanan-Wollaston, V. 1997. The molecular biology of leaf senescence. J. Exp. Bot. 48:181–199. doi:10.1093/jxb/48.2.181

Cabrera, R. I., R. Y. Evans, and J. L. Paul. 1995. Nitrogen partitioning in rose plants over a flowering cycle. Sci. Hortic. 63:67–76. doi:10.1016/0304-4238(95)00790-Z

Corbesier, L., G. Bernier, and C. Périlleux. 2002. C : N ratio increases in the phloem sap during floral transition of the long-day plants *Sinapis alba* and *Arabidopsis thaliana*. Plant Cell Physiol. 43:684–688. doi:10.1093/pcp/pcf071

Dickson, R. E. 1989. Carbon and nitrogen allocation in trees. Ann. Sci. For. 46:631s–647s. doi:10.1051/forest:198905ART0142

Epstein, E. and A. J. Bloom. 2005. Mineral Nutrition of Plants: Principles and Perspectives. 2nd ed. Sinauer Associates. Sunderland, MA. 380 pp.

Gregersen, P. L., A. Culetic, L. Boschian, and K. Krupinska. 2013. Plant senescence and crop productivity. Plant Mol. Biol. 82:603–622. doi:10.1007/s11103-013-0013-8

Guiboileau, A., R. Sormani, C. Meyer, and C. Masclaux-Daubresse. 2010. Senescence and death of plant organs: Nutrient recycling and developmental regulation. C. R. Biol. 333:382–391. doi:10.1016/j.crvi.2010.01.016

Hew, C. S. and C. K. Y. Ng. 1996. Changes in mineral and carbohydrate content in pseudobulbs of the C3 epephytic orchid hybrid *Oncidium* Goldiana at different growth stages. Lindleyana 11:125–134.

Hew, C. S. and J. W. H. Yong. 1994. Growth and photosynthesis of *Oncidium* 'Goldiana'. J. Hort. Sci. 69:809–819. doi:10.1080/14620316.1994.11516517

Howarth, J. R., S. Parmar, J. Jones, C. E. Shepherd, D. I. Corol, A. M. Galster, ... M. J. Hawkesford. 2008. Co-ordinated expression of amino acid metabolism in response to N and S deficiency during wheat grain filling. J. Exp. Bot. 59:3675–3689. doi:10.1093/jxb/ern218

Hu, C., B. K. Ham, H. M. El-Shabraw, D. Alexander, D. Zhang, J. Ryals, and W. J. Lucas. 2016. Proteomics and metabolomics analyses reveal the cucurbit sieve tube system as a complex metabolic space. Plant J. 87:442–454. doi:10.1111/tpj.13209

Inokuchi, R., K. I. Kuma, T. Miyata, and M. Okada. 2002. Nitrogen-assimilating enzymes in land plants and algae: Phylogenic and physiological perspectives. Physiol. Plant. 116:1–11. doi:10.1034/j.1399-3054.2002.1160101.x

Lea, P. J. and R. A. Azevedo. 2006. Nitrogen use efficiency. 1. Uptake of nitrogen from the soil. Ann. Appl. Biol. 149:243–247. doi:10.1111/j.1744-7348.2006.00101.x

Li, Y. T. and Y. C. A. Chang. 2023. Relationship between the growth of current shoot and the development of inflorescence and vegetative buds in *Oncidesa* Gow-

er Ramsey ‘Honey Angel’ leaf axils. HortScience 58:268–273. doi:10.21273/HORTSCI16960-22

Lim, P. O., H. R. Woo, and H. G. Nam. 2003. Molecular genetics of leaf senescence in *Arabidopsis*. Trends Plant Sci. 8:272–278. doi:10.1016/S1360-1385(03)00103-1

Masclaux-Daubresse, C., M. Reisdorf-Cren, K. Pageau, M. Lelandais, O. Grandjean, J. Kronenberger, ... A. Suzuki. 2006. Glutamine synthetase-glutamate synthase pathway and glutamate dehydrogenase play distinct roles in the sink-source nitrogen cycle in tobacco. Plant Physiol. 140:444–456. doi:10.1104/pp.105.071910

Meier, H. and J. S. G. Reid. 1982. Reserve polysamlharides other than starch in higher plants. p.418–471. *in*: Plant Carbohydrates I. (Loewus, F. A. and W. Tanner, eds.) Encyclopedia of Plant Physiology. Vol 13/A. Springer. Berlin, Germany. 918 pp. doi:10.1007/978-3-642-68275-9_11

Ng, C. K. Y. and C. S. Hew. 2000. Orchid pseudobulbs-‘false’ bulbs with a genuine importance in orchid growth and survival! Sci. Hort. 83:165–172. doi:10.1016/S0304-4238(99)00084-9

Peng, Y. C. 2008. The uptake, partitioning, and uses of nitrogen in *Phalaenopsis* Sogo Yukidian ‘V3’. Master Thesis. Department of Horticulture, National Taiwan University. Taipei, Taiwan. 131 pp. (in Chinese with English abstract) doi:10.6342/NTU.2008.02618

Peoples, M. B. and M. J. Dalling. 1988. The interplay between proteolysis and amino acid metabolism during senescence and nitrogen reallocation. p.181–217. *in*: Senescence and Aging in Plants (Noodén, L. D. and A. C. Leopold, eds.) Academic Press. San Diego, CA. 525 pp. doi:10.1016/b978-0-12-520920-5.50012-2

Peoples, T. R. and D. W. Koch. 1979. Role of potassium in carbon dioxide assimilation in *Medicago sativa* L. Plant Physiol. 63:878–881. doi:10.1104/pp.63.5.878

Shyu, H. E. 1997. Effect of light, nitrogen form ratio and flower stalks pruning on flowering of *Oncidium*. Master Thesis. Department of Horticulture, National Chung Hsing University. Taichung, Taiwan. 131 pp. (in Chinese with English abstract)

Yong, J. W. H. and C. S. Hew. 1995. The importance of photoassimilate contribution from the current shoot and connected back shoots to the inflorescence size in the thin-leaved sympodial orchid *Oncidium* Goldiana. Intl. J. Plant Sci. 156:450–459. doi:10.1086/297267

Study on the Correlation between Plant Elements and Abnormal Flower Bud Development in *Oncidesa* Gower Ramsey 'Honey Angel'

Tung-Ming Tsai[1,*], Hung-Ju Chi[2], Chen-Hsuan Wu[3], Ting-Wei Chiu[4], Keng-Chang Chuang[5], and Ting-En Dai[6]

Abstract

Tsai, T. M., H. J. Chi, C. H. Wu, T. W. Chiu, K. C. Chuang, and T. E. Dai. 2024. Study on the correlation between plant elements and abnormal flower bud development in *Oncidesa* Gower Ramsey 'Honey Angel'. J. Taiwan Agric. Res. 73(2):123–134.

In this study, 2-year-old *Oncidesa* Gower Ramsey 'Honey Angel' was used as the plant material to analyze the plant elements of its leaves and pseudobulbs to explore the ratio of nitrogen, phosphorus, potassium, calcium, magnesium, carbon, carbon to nitrogen ratio (C/N ratio), iron, manganese and other elements with the effects on abnormal flowering *O*. Gower Ramsey 'Honey Angel'. The nitrogen content in the leaves of the abnormal flowering plants collected from Dalin, Chiayi, and Dacun, Changhua Counties was only 1.64% and 1.65%, which was much lower than 2.15% and 2.36% in the leaves of plants with normal flowering, and the nitrogen content in the plant was high and fluctuated greatly. It was inferred that nitrogen might also be related to abnormal flowering. The content of phosphorus in the plant was around 0.13% and fluctuated stably. It showed that phosphorus had a low correlation with abnormal flowering and had no effect on promoting flowering. The potassium content of 2.18% in the leaves of abnormal flowering plants was much lower than the potassium content of 3.12% in the leaves of the normal flowering plants. Moreover, the potassium content in the plants was high and fluctuated greatly. It showed that potassium might be related to the *O*. Gower Ramsey 'Honey Angel' abnormal flowering. The content of carbon was stable both in normal and abnormal flowering *O*. Gower Ramsey 'Honey Angel', so it might not be related to the abnormal flowering, and the C/N ratio could not fully explain the flowering. Calcium content fluctuated greatly in normal flowering and abnormal flowering plants. It might be related to the plant nitrogen deficiency instead of the abnormal flowering. Magnesium content fluctuated less and was relatively stable in the plants, not relating to the abnormal flowering. Regardless of high or low content of iron and manganese trace elements in plants, all test plants had abnormal flowering, and it showed that iron and manganese were not related to abnormal flowering. Based on the elemental analysis, observation of plant growth, and physiological performance, it was concluded that severe abnormal flowering in these two production areas, Dalin, Chiayi, and Dacun, Changhua might be related to the nitrogen deficiency in plants.

Key word: Nitrogen, Potassium, C/N ratio, Oncidium, Abnormal flowering.

Received: December 19, 2023; Accepted: February 29, 2024.

* Corresponding author, e-mail: sdon@tari.gov.tw

[1] Associate Research Fellow, Department of Genetics and Breeding, Floricultural Experiment Branch, Taiwan Agricultural Research Institute, Yulin County, Taiwan, ROC.

[2] Project Assistant, Department of Production Process Development, Floricultural Experiment Branch, Taiwan Agricultural Research Institute, Yulin County, Taiwan, ROC.

[3] Assistant Research Fellow, Department of Production Process Development, Floricultural Experiment Branch, Taiwan Agricultural Research Institute, Yulin County, Taiwan, ROC.

[4] Assistant Research Fellow, Department of Genetics and Breeding, Floricultural Experiment Branch, Taiwan Agricultural Research Institute, Yulin County, Taiwan, ROC.

[5] Research Fellow and Division Director, Department of Genetics and Breeding, Floricultural Experiment Branch, Taiwan Agricultural Research Institute, Yulin County, Taiwan, ROC.

[6] Research Fellow and Director, Floricultural Experiment Branch, Taiwan Agricultural Research Institute, Yulin County, Taiwan, ROC.

台灣農業研究 (J. Taiwan Agric. Res.) 73(2):135–151 (2024)
https://doi.org/10.6156/JTAR.202406_73(2).0006

研究報告

利用數位土壤繪圖預測濁水溪流域土壤有機碳儲量

楊博鈞[1]　楊心如[1]　劉滄棪[2]　張翊庭[3]　許健輝[3,*]

摘要

楊博鈞、楊心如、劉滄棪、張翊庭、許健輝。2024。利用數位土壤繪圖預測濁水溪流域土壤有機碳儲量。台灣農業研究 73(2):135–151。

土壤碳庫為全球僅次於海洋的第二大自然碳庫，土壤碳固存 (carbon sequestration) 被認為在氣候變遷的調適與減緩過程，扮演著重要角色。同時，土壤有機碳 (soil organic carbon; SOC) 對於土壤物理、化學及生物特性具有正面的影響。因此，發展準確的繪圖技術對於預估區域尺度土壤有機碳儲量 (SOC stocks) 與量化土壤的功能是非常重要的。本研究目的為應用數位土壤繪圖 (digital soil mapping) 估算濁水溪流域表土 (0–30 cm) 與底土 (30–50 cm) 土壤有機碳儲量與繪製其空間分布預測圖及進行不確定分析，並且比較不同地形與土地覆蓋之土壤碳儲量差異。結果顯示，Regression Kriging (搭配 Cubist) 有最佳預測效果 (表土：R^2 = 0.46；底土：R^2 = 0.48)，其中土綱、高程及年均溫為表土與底土有機碳預測的重要環境參數。不確定度分析結果指出，因森林地區土壤調查樣點較少，導致模型預測範圍 (prediction range) 較大。不同土地覆蓋分類 (森林、水田、旱田、果園及其他) 結果發現，高山地區森林的表層土壤有機碳儲量最高 (11.2 kg m^{-2})，底土則是土地覆蓋類型間差異不明顯。根據預測結果指出，濁水溪流域內表土與底土的有機碳儲量約分為 28.22 與 15.14 百萬噸 (Tg)。本研究之結果可作為濁水溪流域土壤碳匯估算、生態系服務價值評估及碳農業 (carbon-farming) 規劃研究之參考依據。

關鍵詞：土壤有機碳儲量、數位土壤繪圖、濁水溪流域、機器學習。

前言

土壤有機碳 (soil organic carbon; SOC) 為全球碳循環的重要儲存庫 (Grace 2004)，會影響土壤肥力、化學及物理特性；其含量的微小變化也會顯著改變大氣中的碳濃度，對於局部或全球的碳循環具有很大的影響 (Johnston *et al*. 2004)。隨著大氣中二氧化碳濃度上升，農地土壤對於碳固存 (carbon sequestration) 的潛力更受到重視 (Singh *et al*. 2018)。在土壤有機碳的變化與量化，已有許多不同空間尺度與目的之研究成果，Viaud *et al*. (2010) 指出在景觀尺度 (landscape-scale) 下能夠同時考慮自然過程、人為操作及 SOC 動態變化的交互作用。因此，在該尺度下評估環境與農業生態系統的土壤有機碳變化較佳。

在評估土壤特性的空間分布方面，可以使用繪圖或建立預測模式的方法，建立預測模式屬於使用數學方程式模擬與預測真實的事件與過程，而繪圖則強調製作地圖或在地圖上進行描繪。數位土壤繪圖 (digital soil mapping; DSM) 是根據土壤觀測資料搭配與其相關的環境因子，透過不同統計方法或演算法建立的數值模型，進而預測未採樣區域土壤屬性的系統 (Grunwald 2009)。在繪製土壤特性的圖資時，需先建立目標區域內高密度的觀測數據 (Scull *et al*. 2003)，但在大規模的評估尺度下，由於時間與人力成本的限制，難以取得大量的數

投稿日期：2023 年 12 月 1 日；接受日期：2024 年 3 月 12 日。
* 通訊作者：chsyu@tari.gov.tw
[1] 農業部農業試驗所農業化學組計畫助理。臺灣 臺中市。
[2] 農業部農業試驗所農業化學組研究員兼組長。臺灣 臺中市。
[3] 農業部農業試驗所農業化學組副研究員。臺灣 臺中市。

據。因此，通常透過模型模擬的方式將分散點位數據繪製成土壤特性圖，在模擬過程中，土壤特性的空間變化為模型建構的要點 (Zhu & Lin 2010)。根據過去研究，有 2 種不同型式的通用模型，用於解決空間變化與預測未採樣點的土壤特性：(1) 非地理統計技術，基於 Jenny (1980) 與 McBratney *et al*. (2003) 所提出的 SCORPAN 模型，該模型旨在描述土壤形成過程之土壤特性與環境特性之間的關係，目的在於從詳盡的環境參數預測目標土壤特性，例如多元線性迴歸 (multiple linear regression; MLR) 與廣義加性模型 (generalized additive model; GAM)，隨著機器學習方法的發展，分類與迴歸樹 (classification and regression tree; CART) 也被應用於 DSM 上，其中以特徵分類的 Cubist Model (Quinlan 1992) 與集成學習方法 Random Forest (Breiman 2001) 為廣泛被使用的機器學習法；(2) 地理統計技術，即地理或純空間方法，明確考慮土壤特性在觀測點間的空間相關性，使土壤特性可以透過在土壤觀測位置之間插值，從空間位置進行預測，例如普通克利金法 (ordinary kriging; OK)、簡單克利金法 (simple kriging; SK) 以及通用克利金法 (universal kriging; UK) 等。此外，隨著相關研究的發展，亦有結合前述兩種方法的空間分析方法，該方法以非地理統計方法預測土壤特性，並以地理統計預測殘差的空間變異性，對於土壤特性的預測能夠達到更佳的表現，常見的方法為迴歸克利金法 (regression kriging; RK) (Keskin & Grunwald 2018)。在土壤特性的預測與繪製上，不同方法的預測表現會受到許多因素控制，例如空間尺度 (Poggio *et al*. 2010)、觀測點密度 (Tsui *et al*. 2016; Keskin & Grunwald 2018) 或是地形 (Zhu & Lin 2010) 等。

Lamichhane *et al*. (2019) 指出，土壤有機碳的空間預測模型包含多元線性迴歸、決策與迴歸樹、隨機森林 (random forest; RF)、神經網絡 (neural networks; NN) 以及迴歸克利金等。多元線性迴歸在前期為預測 SOC 的主要技術，如 Meersmans *et al*. (2008) 利用多元線性迴歸模型評估不同土地利用下 SOC 與土壤質地及地下水位間的關係；隨著 DSM 技術發展，RF 模型對於 SOC 的估算具有較佳的預測表現，Siewert (2018) 應用該模型於瑞典北部泥炭地 SOC 預測；Yang *et al*. (2016) 於青藏高原東北部的預測結果則顯示 RF 與提升決策樹 (boosted regression tree; BRT) 模型對於 SOC 空間分布皆有好的預測表現；Akpa *et al*. (2016) 則顯示在使用奈及利亞歷史數據預測 SOC 時，RF 的預測表現優於 BRT，並指出 RF 模型在高山生態系統中更能有效處理 SOC 與環境共變數間的非線性關係。除 MLR 與 RF 外，Cubist 模型亦為近年來常被使用於預測 SOC 的機器學習法之一，例如 Gray & Bishop (2016) 利用 Cubist 模型預測新南威爾士州在不同氣候模型下的 SOC 潛在變化，並比較氣候-母質-土地利用對於 SOC 的長期影響；Rudiyanto *et al*. (2018) 則運用該模型有效預測印尼廖內省泥炭地的厚度，估算研究區域內的有機碳儲量。近年來，迴歸克利金法則被認為是繪製土壤特性空間分布的重要方法之一 (Keskin & Grunwald 2018)，在此類混合模型中，模型用於評估目標變量與共變數間的確定性趨勢，而殘差則以克利金法進行分析；許多研究指出結合克利金的結果能夠對於模型預測結果進行優化，如 RF 模型 (Guo *et al*. 2015) 與 Cubist 模型 (Dorji *et al*. 2014; Ma *et al*. 2017)。然而，Vaysse & Lagacherie (2015) 於法國的研究中則指出加入克利金並不會提高 RF 模型的表現，而 Lamichhane *et al*. (2019) 則提出沒有能夠應用於所有地區的預測模型，由於採樣密度與共變數使用皆會影響預測能力，故建議需運用統合分析 (meta-analysis) 評估最具優勢的演算法。

過去以土壤分類估算臺灣耕地土壤深度 0–30 cm 與 0–100 cm 的有機碳儲量為 38.5 與 77.0 百萬噸 (Tg) (Jien *et al*. 2010)，森林土壤中則為 114 與 160 Tg (Tsai *et al*. 2010)。Tsui *et al*. (2013) 指出，臺灣耕地土壤從北向南由於溫度上升，平均 SOC 隨之降低，而森林土壤有機碳儲量受溫度與高程 (elevation) 變化影響，呈現高度相關。濁水溪位於臺灣中部，流域涵括彰化縣、南投縣、雲林縣及嘉義縣，為中部地區重要的農業生產區。流域內土壤有機碳含量不僅作為重要土壤品質指標，該指標也隨環境議題而日漸受到重視。因此，本研究的目的為利用數位土壤繪圖技術估算濁水溪流域

土壤 (0–30 cm 與 30–50 cm) 有機碳儲量並繪製該空間分布圖，並比較該流域範圍內不同土地覆蓋條件下土壤有機碳儲量之差異。

材料與方法

研究區域

濁水溪流域位於臺灣中部，流域範圍涵括彰化縣、南投縣、雲林縣及嘉義縣部分區域，以東經 120°13' 35.63" E 至 121°19' 45.9" E，北緯 23°28' 1.71" N 至 24°8' 20.94" N 為界，流域面積約為 3,156.9 km^2，海拔範圍由 0–3,844 m (圖 1A)，地形變化大，為呈現不同地形之土壤有機碳儲量差異，本研究以海拔作為分類的依據，區分種類包括高山 (海拔大於 1,000 m 之範圍，2,060.7 km^2，65.2%)、坡地 (海拔介於 100–1,000 m 之範圍，843.3 km^2，26.6%) 及平原 (海拔小於 100 m 之範圍，261.7 km^2，8.2%)；2011–2020 年平均溫度為 8.61–23.6℃ (圖 1B)、年累積雨量為 855–3,693 mm (圖 1C)，屬亞熱帶氣候；土壤特性方面，研究區上游以石質土為主，西部平原地區則以粘板沖積土為主。根據 2015 年土地覆蓋調查，流域上游多為森林 (forest)，下游緩坡與平原地區則多為水田 (paddy)、旱作 (upland) 及果園 (orchard) 為主 (圖 1D)。

土壤樣品與土壤分析

本研究使用農業部農業試驗所 (簡稱農試所) 土壤資源調查計畫 (2008–2020 年) 於濁水溪流域範圍內之調查數據，表土 (0–30 cm) 共 759 個、底土 (30–50 cm) 共 479 個，使用手持全球定位系統設備 (Garmin GPS Map 64 st, Garmin Corporation, Olathe, KS, USA) 記錄樣品位置。土壤樣品於室溫下風乾，以 35 目 (mesh) 篩網過篩並儲存於塑膠罐備用，而後以失重法 (Nelson & Sommers 1983) 分析土壤有機碳含量，並以土塊法或土環法測定總體密度 (Blake & Hartge 1986)，利用式 (1) 將有機碳含量與總體密度計算表土有機碳儲存量 (SOC_{stock})。一般而言，土壤中的含石量也是影響土壤有機碳儲量需要考量的重要參數，然而，考量取得總體密度數據 (含石量高之樣點無法採集土塊與土環樣本) 與含石量觀測變異較大，本研究選擇含石量為零之數據進行有機碳儲量計算。

$$SOC_{stock} = TOC \times \rho \times D/10 \quad (1)$$

其中 SOC_{stock} 為土壤有機碳儲存量 (kg m^{-2})，TOC 為有機碳含量 (%)，ρ 為土壤總體密度 (g cm^{-3})，D 為深度 (cm)。

環境共變數

本研究所使用的環境共變數可依資料類型與成土因子 (soil formation factor) 進行分類，包含數值高程模型 (digital elevation model; DEM)、衛星遙測影像、氣象、土地利用調查以及土綱 (soil order) 分布等空間分布資料 (表 1)，所有環境共變數皆以 R 4.0.5 重新取樣至 20 m 的空間解析度。

數值高程模型 (DEM) 取自內政部 20 m 網格資料，應用該資料結合 SagaGIS 8.0.1 產製相關地形屬性，包括坡度 (slope)、坡向 (aspect)、地形崎嶇指數 (terrain ruggedness index; TRI)、地形位置指數 (terrain position index; TPI)、地形濕度指數 (topographic wetness index; TWI)、多解析度谷底平坦度指數 (multiresolution index of valley bottom flatness; MrVBF)、多解析度脊頂平坦度指數 (multiresolution ridge top flatness; MrRTF)、曲度 (curvature)、匯流分析 (flow accumulation) 及逕流強度指數 (stream power index; SPI)，前列地形參數參考 Ma *et al*. (2017) 對於有機碳預測模型建立與繪圖之研究。

常態化差異植生指標 (normalized difference vegetation index; NDVI) 為利用衛星影像 (Sentinel 2) 2015–2020 年間紅外光 (b4) 與近紅外光 (b8) 影像資料所計算，用以判斷空間中綠色植物的覆蓋比例，根據 Mulder *et al*. (2011)，NDVI 能夠作為 DSM 中預測有機碳的有用共變數。

氣候為成土因子之一，Wiesmeier *et al*. (2019) 指出氣候為影響土壤有機碳儲存的指標之一，本研究使用 2011–2020 年的年平均溫度 (mean annual temperature; MAT) 與年累積降

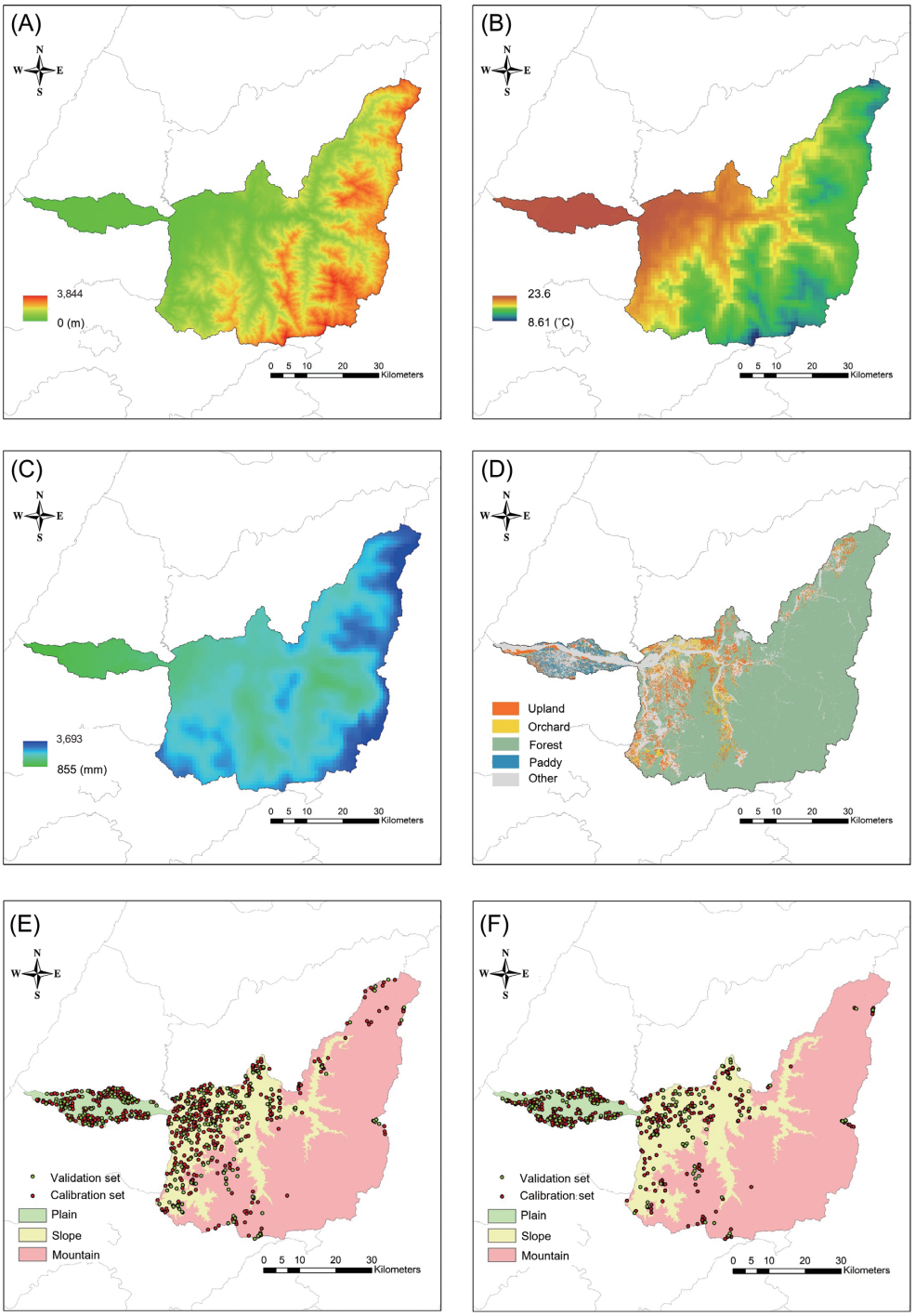

圖 1. (A) 濁水溪流域高程；(B) 2011–2020 年均溫；(C) 2011–2020 年累積雨量；(D) 土地覆蓋分布圖；(E) 表土樣本分布圖；(F) 底土樣本分布圖。

Fig. 1. (A) The distribution map of digital elevation model (DEM); (B) mean annual temperature during 2011–2020; (C) total annual precipitation during 2011–2020; (D) land cover; (E) sampling sites of topsoil; and (F) sampling sites of subsoil in Zhuoshui River basin.

表 1. 本研究環境共變數列表。

Table 1. List of the environmental covariates in this study.

Type of data	Environmental covariates	Soil forming factor[z]	Type[y]
Remote sensing	Normalized difference vegetation index (NDVI)	o; t	Q
Digital elevation model	Elevation	r	Q
	Slope	r	Q
	Aspect	r	Q
	Terrain ruggedness index (TRI)	r	Q
	Topographic wetness index (TWI)	r	Q
	Terrain position index (TPI)	r	Q
	Multiresolution index of valley bottom flatness (MrVBF)	r	Q
	Multiresolution ridge top flatness (MrRTF)	r	Q
	Stream power index (SPI)	r	Q
	Curvature	r	Q
	Flow accumulation	r	Q
Climate	Mean annual temperature (MAT)	c; t	Q
	Total annual precipitation (TAP)	c; t	Q
Land cover	Land cover	o; t	C
Soil	Soil order	s	C

[z] o: organism; t: time; r: relief; c: climate; s: soil.
[y] Q: quantitative; C: categorical.

水量 (total annual precipitation; TAP) 作為代表氣候的環境共變數。

本研究使用的土壤分類圖資為美國農業部所建立之土壤分類系統，六個分類綱目 (category) 中的最高級綱目『土綱』，該圖資為農試所產製。土綱能夠提供綜合性的土壤化育特徵、環境及時間等資訊，應有利於有機碳儲量之預測。在本研究區中，以弱育土 (inceptisols)、新成土 (entisols)、淋溶土 (alfisols) 及極育土 (ultisols) 為主，三者面積加總占研究區 90% 以上，另有少部分區域屬淋澱土 (spodosols)。

除以上因子外，土地覆蓋的種類也被認為會影響土壤有機碳儲存量 (Edmondson *et al*. 2014)。因此，使用 2015 年的土地覆蓋調查資料作為本研究環境共變數之一。為呈現不同土地覆蓋之土壤有機碳儲量差異，本文將研究區中的土地覆蓋分為水田、旱作 (包含雜糧、茶樹、檳榔以及竹林)、果園、森林 (人造林、原始森林以及高山箭竹林) 及其他 (雜地與河川地) 等 5 種類別，空間分布如圖 1D。水田、旱作、果園、森林及其他 5 個類別於研究區之面積占比分別為 2.8%、3.1%、0.94%、77% 及 16%。

預測模型

隨著相關研究發展，數位土壤繪圖技術已由簡單的線性模型發展至機器學習技術 (Minasny & McBratney 2016)，在本研究應用二項 (Cubist model 與 RF model) 廣泛被使用的數據挖掘模型之外，模型皆會再加入克利金法，成為結合地理與非地理統計效應的模型 RK with Cubist model 與 RK with RF model，並比較四者在有機碳儲量的空間分布預測能力差異。

Cubist model 為規則分類的演算法，由 Quinlan (1992) 所提出，基於 M5 樹狀模型所建立，根據 “if-then” 的模式，將數據區分數個子集合，並在各個子集合下找出目標變量與環境共變數的線性關係；本研究中使用 R 4.0.5 中的 Cubist 套件進行模型建立，其中 Cubist 模型需要的參數為 (1) rules，根據規則數對數據進

行分類；(2) extrapolations，決定模型對於數據的外推程度；以及 (3) committees，可以根據數量生成多個 committees 模型，可以用於修正前一個預測資料，並在最後輸出所有 committees 模型的結果；本研究不設定 rules 與 extrapolations，由 Cubist 預設，而 committees 利用 caret 套件計算，設定為 20。

RF model 為 Breiman (2001) 提出之學習集成方法，在模型訓練時利用隨機重複抽樣的方式將數據集重構為多個相同樣本大小的新數據集，並在每個數據集中隨機抽取環境共變數用以建立分類樹或迴歸樹，在連續變量中，模型預測值為所有迴歸樹所輸出之平均值，在 R 4.0.5 中使用 randomForest 套件進行模型建立，參數包括：(1) mtry，決定每個新數據集在建立迴歸樹時所需要抽取的環境共變數數量；(2) ntree，在隨機森林中迴歸樹的數量，本研究中參數利用 caret 套件計算，設定為 mtry = 7，ntree = 500。

模型訓練與驗證

在模型建立前，本研究利用 R 4.0.5 中 rpart 套件由數據集中抽取 70% 為訓練數據集 (calibration set) 利用其建立演算法；剩餘 30% 則設定為驗證數據集 (validation set)，用以驗證模型的預測效能；在模型表現上以驗證組的預測值與觀測值進行比較，使用誤差均方根 (root mean square error; RMSE) 與決定係數 (coefficient of determination, R^2) 作為模型評估指標。

不確定度分析

利用拔靴法 (自助抽樣法，bootstrap) 在訓練數據集裡，以取後放回的方式建立 50 個新數據集，並以新數據集建立模型與預測圖資，而後由以上預測圖資建立 90% 信賴區間圖資，以表示該預測模型的不確定度。

地理資訊與數據分析

本研究利用地理資訊軟體 ArcMap 10.7 進行圖資繪製與地理統計分析，而在數據處理上則利用 Excel 2016 與 R 4.0.5 進行數據的統計分析。

結果與討論

土壤有機碳儲量數據統計描述

採樣點位表土與底土的有機碳儲量分布顯示於圖 2，表土有機碳儲量分布範圍為 0.27–45.53 kg m^{-2}，平均 6.95 kg m^{-2}，變異係數為 73.86%；底土則為 0.44–16.19 kg m^{-2}，平均 3.76 kg m^{-2}，變異係數為 62.47%，兩個數據集偏度皆為 0.20，數據結構變異大並屬於正偏，為使數據符合模型建立上的統計前提，兩個數據集皆進行自然對數轉換，使其更接近常態分布，應用於模型建立。

預測模型選擇

本研究利用 Cubist model、RF model 以及 2 個模型的 RK 模型，以訓練數據集與環境共變數建立演算法，並利用不同指標檢驗模型在驗證數據集的預測表現，表土與底土的結果分別呈現於圖 3 與圖 4，兩層土壤皆以 RK with Cubist 模型有最好的有機碳儲存量預測能力 (表土 R^2 = 0.46、RMSE = 0.48；底土 R^2 = 0.48、RMSE = 0.50)，其他土壤有機碳的預測研究如 Adhikari *et al*. (2014) 以 RK 預測丹麥 0–5 cm 表土有機碳儲量之表現為 R^2 = 0.41、RMSE = 0.24；Lacoste *et al*. (2014) 以 Cubist 模型預測法國 0–7.5 cm 有機碳儲量的模型表現為 R^2 = 0.12、RMSE = 12.64，而 Ma *et al*. (2017) 利用 RK 預測中國 0–20 cm 土壤有機碳儲量之表現則為 R^2 = 0.25、RMSE = 0.12，本研究與其結果皆有相近或更高之預測表現，而後續會基於此模型進行預測圖資繪製。

環境共變數重要性

RK with Cubist model 會先建立 Cubist 的預測模型，再以各個預測點位的殘差繪製殘差的空間分布圖，而在建立 Cubist 模型時能夠計算環境共變數的使用比例，以得知環境共變數在預測土壤有機碳儲存量的重要性，環境共變數的貢獻比例顯示於圖 5。在環境共變數中，表土與底土都以土綱與高程作為數據區分的規則，表土分別使用 29% 與 80%、底土則分別為 18% 與 60%，表示土壤分類與地形都能有效作為建立分類的條件；而在分群下的

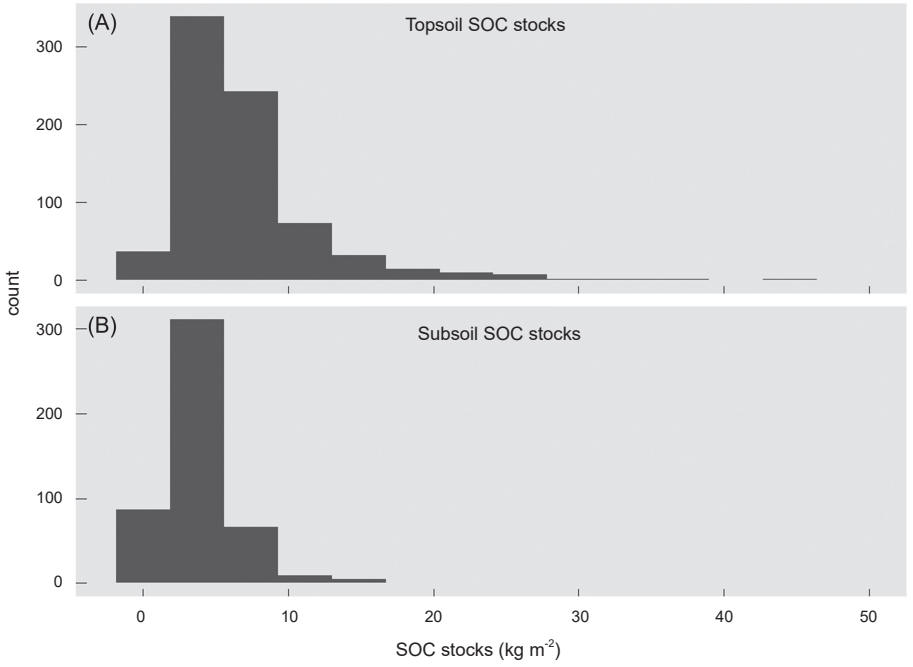

圖 2. 濁水溪流域 (A) 表土 (0–30 cm) 與 (B) 底土 (30–50 cm) 有機碳儲量直方圖。

Fig. 2. Histograms of soil organic carbon (SOC) stock in (A) topsoil (0–30 cm) and (B) subsoil (30–50 cm) in Zhuoshui River basin.

線性模型中，表土主要使用高程 (94%)、TRI (67%)、MAT (60%)、NDVI (47%) 及坡度 (43%)，而底土則以高程 (91%)、MAT (75%) 及坡度 (59%) 為主。TRI 與坡度代表地形崎嶇的程度，決定了該地點的太陽輻射強度與水分保留能力，對有機碳儲存產生影響；而 Rial *et al*. (2017) 指出溫度與 SOC 含量呈現負相關，較高的海拔與緯度會降低 SOC 的分解速度。儘管高程所造成的影響歸因於溫度，但由於溫度圖資原始解析度為 1 km，仍需由高解析度的高程圖資建立更細緻的 SOC 空間分布。NDVI 為表土主要使用的環境共變數，作為植被覆蓋的指標之一，而越高的植被覆蓋也會影響 SOC 的累積。

有機碳儲存量預測圖

圖 6 為濁水溪流域表土與底土有機碳儲量預測圖，結果顯示，大部分區域表土有機碳儲量高於底土，預測後的表土有機碳儲量範圍 0.21–29.52 kg m^{-2}，平均值為 9.01 kg m^{-2}；底土有機碳儲量範圍 1.12–12.2 kg m^{-2}，平均值為 4.82 kg m^{-2}。由於表層土壤累積大部分來自於地表植生之殘體，土壤有機碳含量通常高於底土 (Jien *et al*. 2010; Tsai *et al*. 2010; Adhikari *et al*. 2014; Chen *et al*. 2018; Wadoux *et al*. 2023)。Adhikari *et al*. (2014) 指出丹麥表土 0–30 cm 的有機碳儲量平均約為 72 Mg ha^{-1}，深度 0–100 cm 土壤有機碳儲量約為 120 Mg ha^{-1}，該結果顯示 1 m 的土壤剖面，表層土壤 (0–30 cm) 占了 60% 的土壤有機碳；Jien *et al*. (2010) 與 Tsai *et al*. (2010) 也指出臺灣耕地與林地 0–30 cm 土壤有機碳儲量約占 0–100 cm 土壤有機碳儲量的 50% 與 71%。表土與底土有機碳儲量分布圖呈現濁水溪流域上游較下游高的趨勢，推測是因為流域上游多為森林且溫度較低，利於土壤有機碳累積；然而，下游平坦處為農業區，高溫多雨與頻繁耕犁導致土壤有機碳容易被分解，故有機碳儲量較低。由環境共變數重要性結果也指出，高程、年均溫及 NDVI 均為本研究土壤有機碳儲量重要之預測

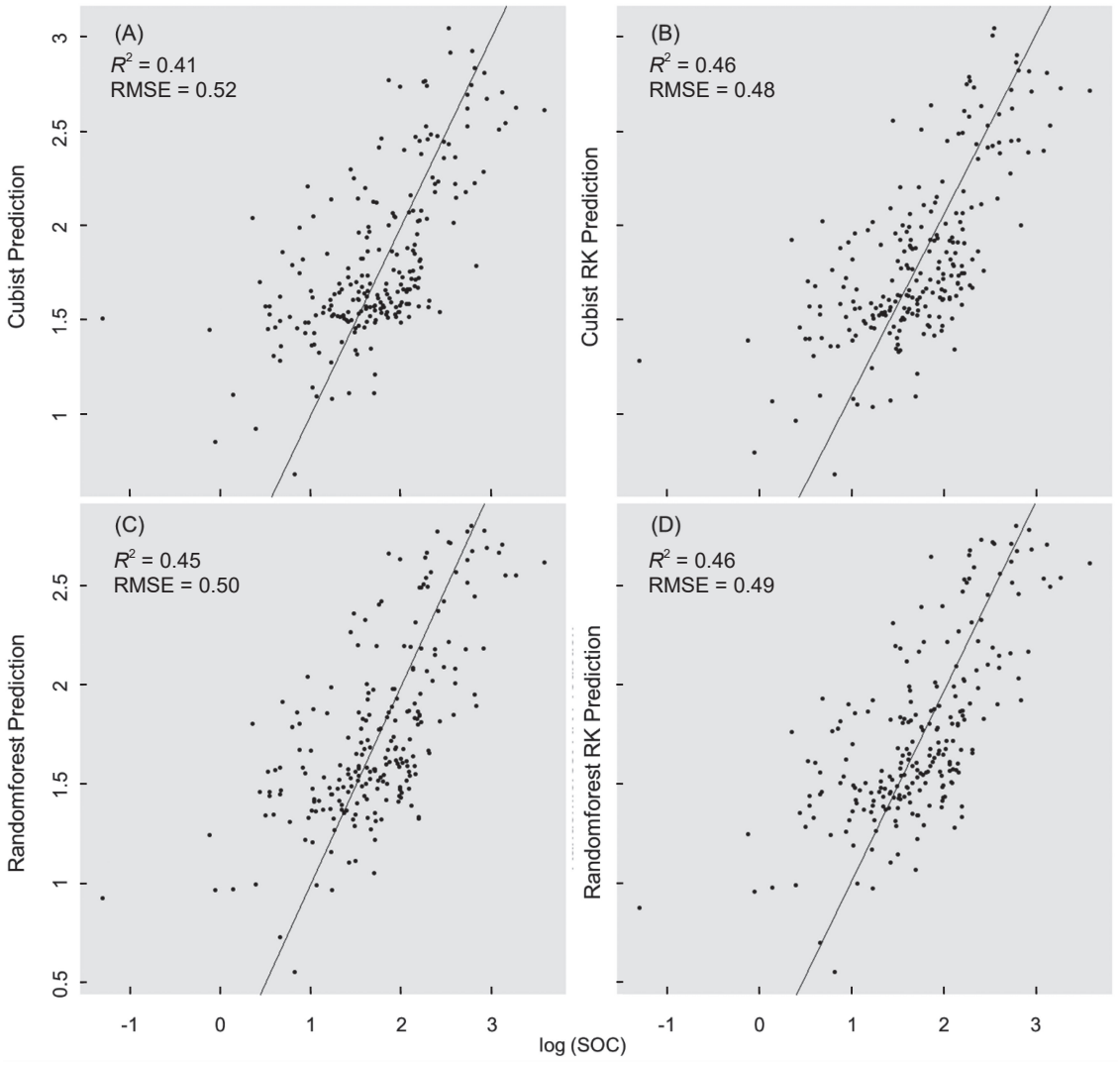

圖 3. 表土 (0–30 cm) 有機碳儲量驗證數據集在 (A) Cubist、(B) Regression kriging with Cubist、(C) Random forest 及 (D) Regression kriging with Random forest 模型之散布圖，橫軸表示觀測值，縱軸表示預測值，實線表示擬合線。

Fig. 3. Scatter plots of soil organic carbon (SOC) stock for topsoil (0–30 cm) of (A) Cubist, (B) Regression kriging (RK) with Cubist, (C) Random forest and (D) Regression kriging with Random forest models based on validation dataset. The x-axis is observed value and the y-axis is predicted value, the solid line is fitted line.

參數 (圖 5)，該結果支持土壤有機碳儲量之空間分布趨勢。此外，土壤有機碳儲量分布結果也指出，河道鄰近處有機碳儲量較低，推測在山谷處高程較低而 TWI 較高，因河流沖刷或更頻繁的水分移動導致有機碳流失；同時，由於河道鄰近處土壤以粗質地居多，也導致有機碳不易長時間累積於土壤中。Guillaume *et al*. (2022) 的研究指出土壤粒徑為評估土壤持久固碳的關鍵，因細顆粒土壤 (黏粒與坋粒) 所保存的有機碳能避免受微生物分解。Tsui *et al*. (2013) 在陽明山的研究結果指出，不同深度範圍 (0–30 cm、0–50 cm 及 0–100 cm) 之土壤有

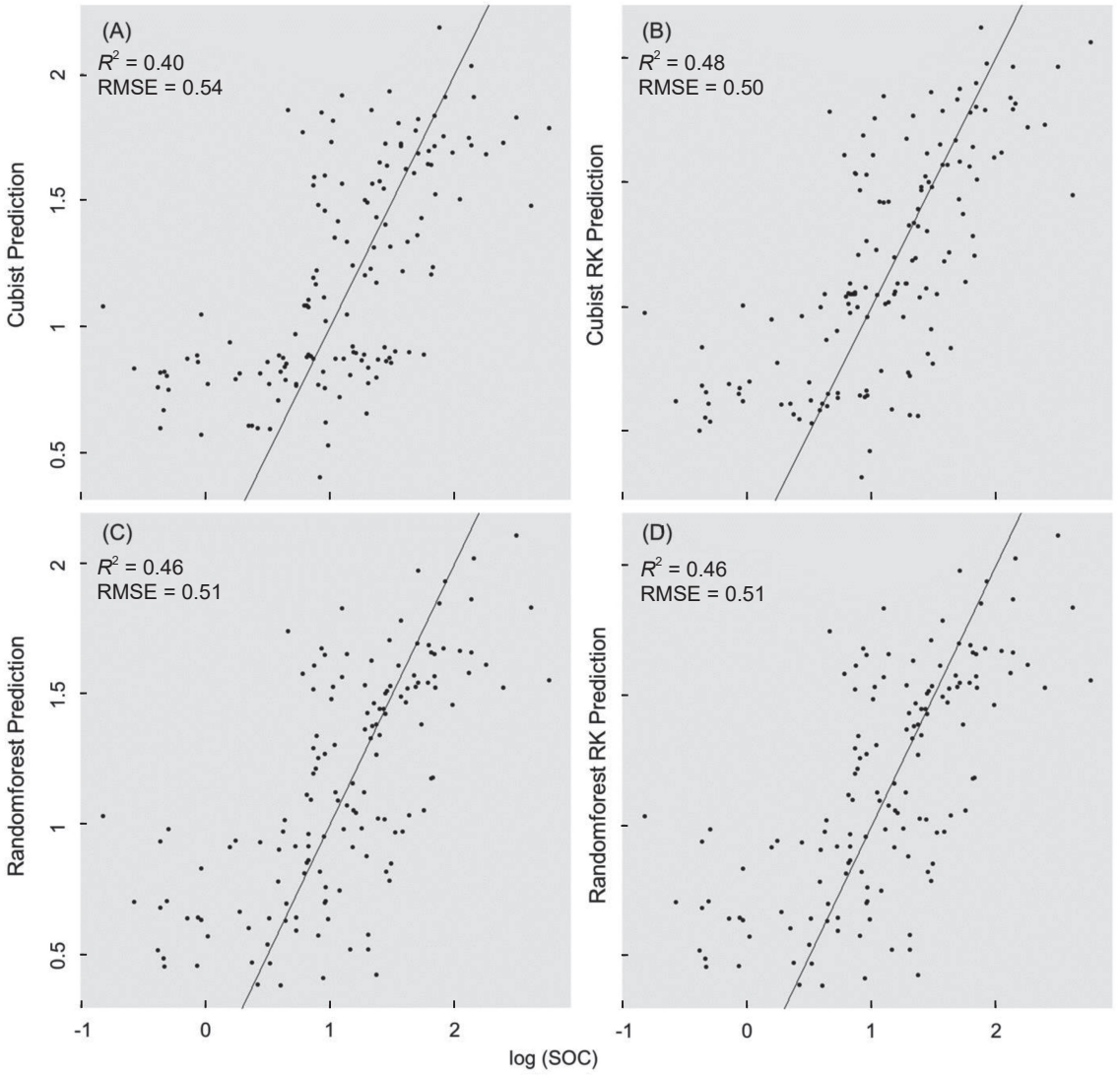

圖 4. 底土 (30–50 cm) 有機碳儲量驗證數據集在 (A) Cubist、(B) Regression kriging with Cubist、(C) Random forest 及 (D) Regression kriging with Random forest 模型之散布圖，橫軸表示觀測值，縱軸表示預測值，實線表示擬合線。

Fig. 4. Scatter plots of soil organic carbon (SOC) stock for subsoil (30–50 cm) of (A) Cubist, (B) Regression kriging (RK) with Cubist, (C) Random forest and (D) Regression kriging with Random forest models based on validation dataset. The x-axis is observed value and the y-axis is predicted value, the solid line is fitted line.

機碳儲量與高程具有高度的線性相關，本研究繪製之有機碳分布亦有相同之趨勢 (圖 6)。最後，利用數值計算求得濁水溪流域表土與底土的總碳儲量分別為 28.22 與 15.14 Tg。由於本研究未將含石量納入土壤有機碳儲量之計算，因此，可能導致山坡地與高山地區土壤有機碳儲量之預測呈現高估的情形，進而高估總碳儲量之結果，未來將納入合理的土壤含石量觀測結果，優化土壤有機碳儲量之估算。

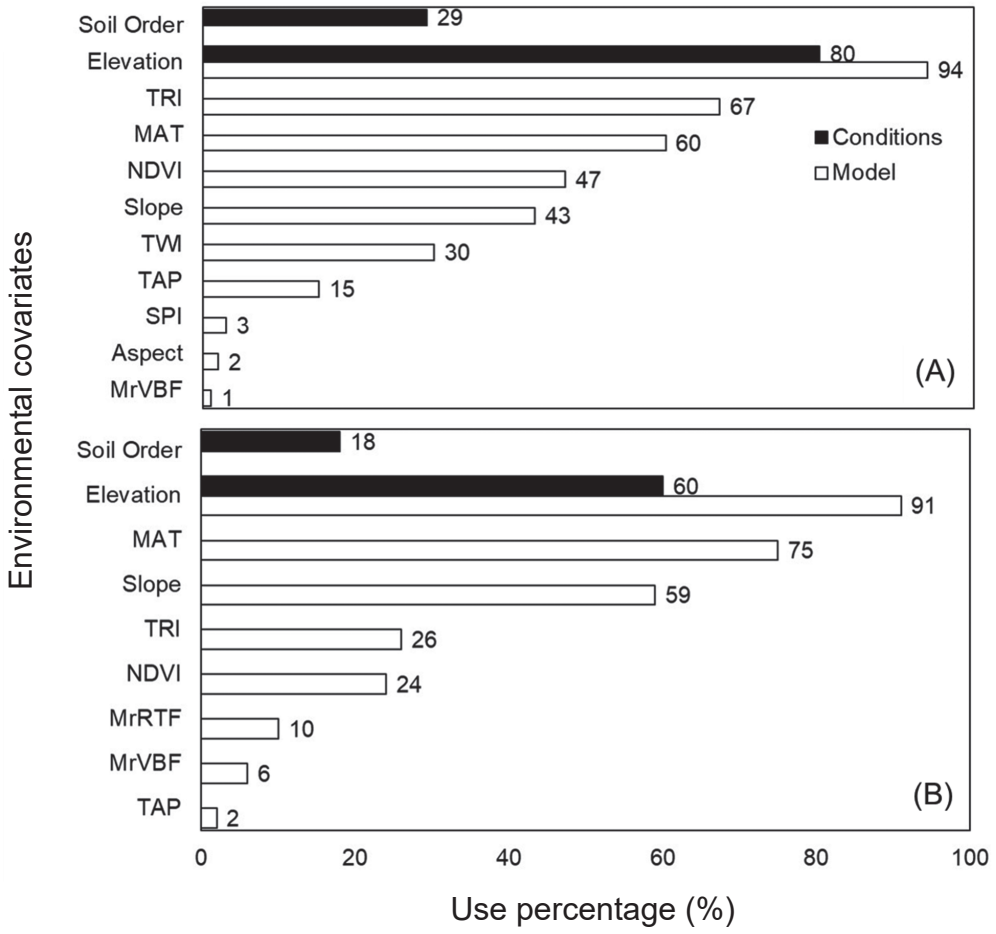

圖 5. (A) 表土與 (B) 底土 Cubist 模型中環境共變數預測之重要性。

Fig. 5. Importance of the environmental covariates predictors in Cubist model for (A) topsoil and (B) subsoil. TRI: terrain ruggedness index; MAT: mean annual temperature; NDVI: normalized difference vegetation index; TWI: topographic wetness index; TAP: total annual precipitation; SPI: stream power index; MrVBF: multiresolution index of valley bottom flatness; MrRTF: multiresolution ridge top flatness.

地形與土地覆蓋對土壤有機碳儲存量的影響

圖 7 為濁水溪流域不同地形與土地覆蓋條件下有機碳儲量之差異，結果顯示在同一種土地覆蓋條件下，高山表層土壤 (0–30 cm) 的有機碳儲量明顯大於坡地與平地，其中森林與其他類型的差異分別可高達 1.9–3.1 倍與 1.7–2.4 倍，該結果再次驗證海拔高度、氣溫及雨量為影響土壤有機碳儲量的主要環境參數 (圖 5)。底土 (30–50 cm) 的結果顯示，在同一種土地覆蓋條件下，高山與坡地範圍的底土有機碳儲量無明顯差異，這兩種地形範圍之底土有機碳儲量皆顯著大於平原地區，在不同土地覆蓋間皆大於 2 倍以上 (圖 8)。不同土地覆蓋表層土壤有機碳儲量結果顯示，高山地區以森林土壤 (11.2 kg m^{-2}) 明顯高於其他土地覆蓋類型；在坡地與平原地區，平均碳儲量最高的類型分別為森林土壤 (5.86 kg m^{-2}) 與水田土壤 (4.38 kg m^{-2})。Tsai *et al*. (2009) 在臺灣北部地區人工林土壤調查結果指出，在海拔範圍 230−1,950 m 下，闊葉樹人工林與針葉樹人工林 0–30 cm 土壤有

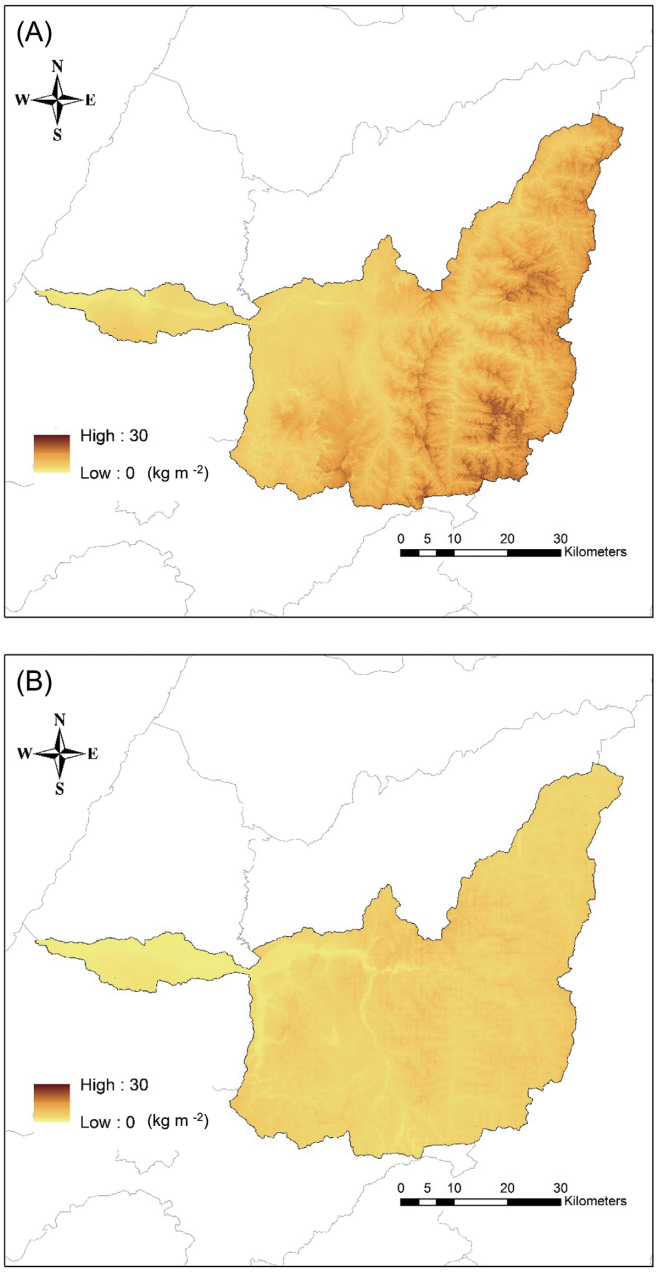

圖 6. 濁水溪流域 (A) 表土 (0–30 cm) 與 (B) 底土 (30–50 cm) 有機碳儲量預測圖。

Fig. 6. (A) Topsoil (0–30 cm) and (B) subsoil (30–50 cm) soil organic carbon (SOC) stock predicted maps in Zhuoshui River basin.

機碳儲量平均值分別為 6.5 kg m^{-2} 與 7.4 kg m^{-2}，該結果與本研究不同的原因可能為氣候條件、樹種及調查方法 (如採樣密度與含石量估算等) 不同所導致。Tsai *et al.* (2010) 的研究指出，全臺森林土壤 (0–30 cm)，除了有機質土 (histosols，36.9 kg m^{-2}) 與淋溶土 (29.5 kg m^{-2})

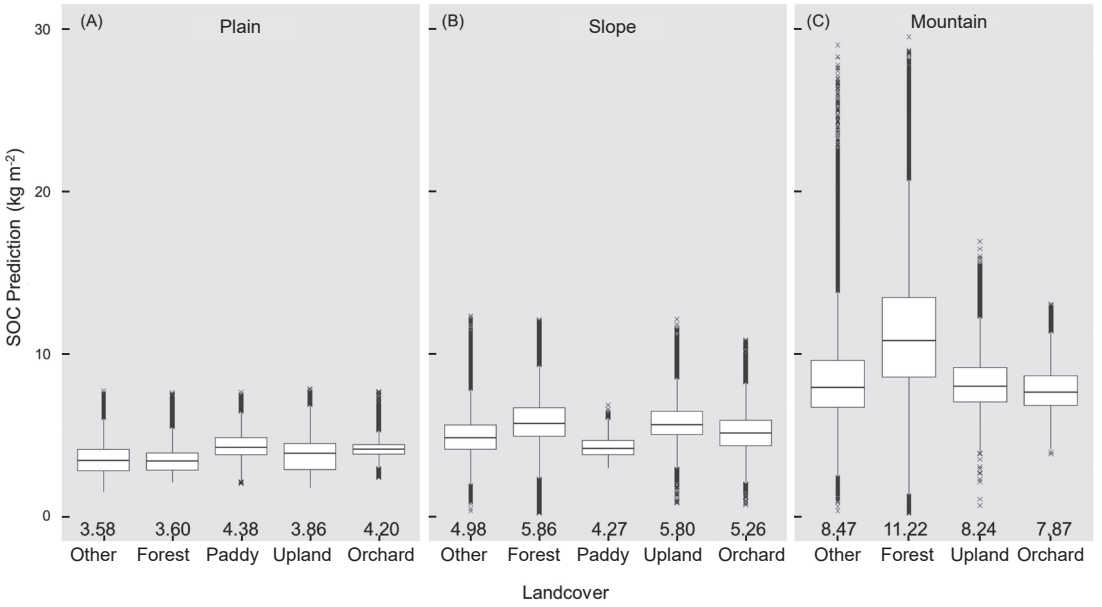

圖 7. 濁水溪流域 (A) 平原、(B) 坡地及 (C) 高山地區不同土地覆蓋之表土 (0–30 cm) 有機碳儲量盒鬚圖。

Fig. 7. Boxplots of topsoil (0–30 cm) soil organic carbon (SOC) stock under different landcover in (A) plain, (B) slope and (C) mountain areas of Zhuoshui River basin.

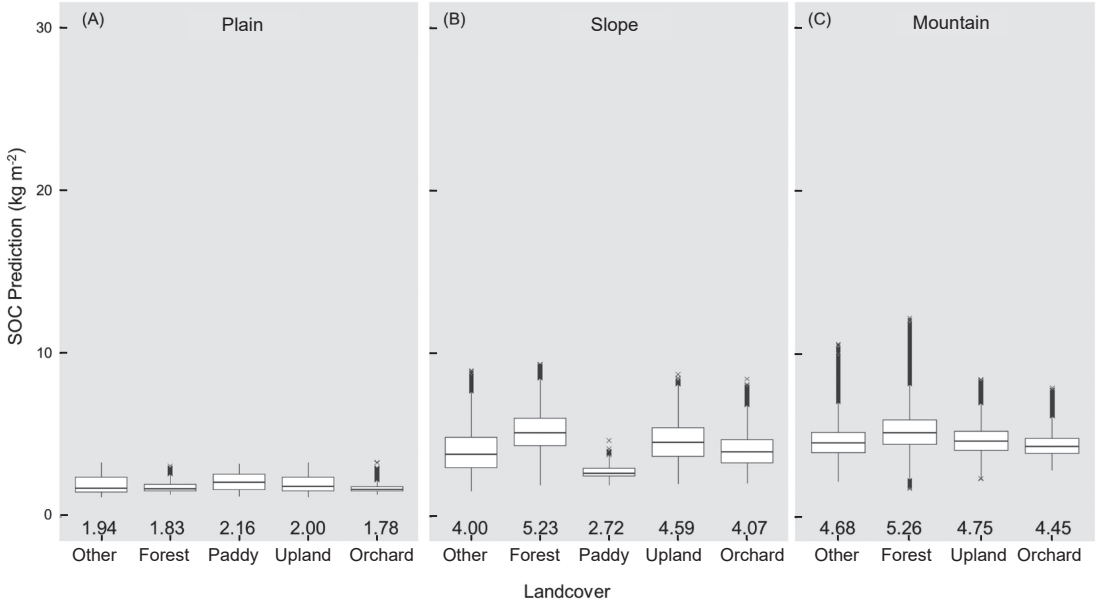

圖 8. 濁水溪流域 (A) 平原、(B) 坡地及 (C) 高山地區不同土地覆蓋之底土 (30–50 cm) 有機碳儲量盒鬚圖。

Fig. 8. Boxplots of subsoil (30–50 cm) soil organic carbon (SOC) stock under different landcover in (A) plain, (B) slope and (C) mountain areas of Zhuoshui River basin.

以外，其他土綱之土壤的平均值為10.1 kg m^{-2}。本研究結果顯示，以研究區內分布最廣的弱育土為例，高山與坡地地區表層土壤 (0–30 cm) 有機碳儲量平均值約為 12.3 kg m^{-2} (數據未顯示)。有關水田土壤有機碳儲量，Liu *et al*. (2021) 的研究指出，水稻栽培有助於提高土壤碳儲量，並說明水田狀態下雖然會有甲烷排放發生，但碳儲存量往往大於該排放量，因此建議水稻田管理可抵減人為造成的溫室氣體排放。此外，該研究也指出全球水稻田土壤 (0–30 cm) 的碳儲存量約為 51 Mg ha^{-1} (相當於 5.1 kg m^{-2})，本研究的水田土壤平均值 (4.38 kg m^{-2}) 略低於該研究之結果，推測是由於研究區水稻田位於亞熱帶區域，高溫與頻繁耕犁 (普遍一年兩期作) 導致土壤中的有機碳容易分解。儘管如此，相較於旱田與果園土壤，水田的浸水條件仍有助於有機碳的儲存。最後，利用數值計算求得濁水溪流域水田、旱地、果園、森林及其他類型表土 (0–30 cm) 有機碳儲量分別為 0.32 Tg (1.12%)、1.18 Tg (4.19%)、0.34 Tg (1.19%)、23.72 Tg (84.04%) 及 2.67 Tg (9.45%)；底土 (30–50 cm) 有機碳儲量則分別為 0.16 Tg (1.05%)、0.83 Tg (5.47%)、0.24 Tg (1.61%)、12.09 Tg (79.83%) 及 1.82 Tg (12.03%)。

不確定度分析

數位土壤繪圖除了可用來預測土壤性質，也可提供預測上界、預測下界及預測限制範圍 (prediction limit range)，呈現模型預測的不確定度與其空間分布 (Xiong *et al*. 2015)。圖 9 為利用拔靴法產製之表層土壤 (0–30 cm) 有機碳儲量預測限制區間、90% 預測上限及 90% 預測下限分布圖，Malone *et al*. (2014) 指出在大多數情況下，90% 的觀測值都符合其定義的預測區間。圖 6A 顯示濁水溪流域表層土壤預測之有機碳儲量平均為 9.01 kg m^{-2}，預測上界與下界平均分別為 23.55 kg m^{-2} 與 3.41 kg m^{-2} (圖 9B 與圖 9C)，這代表本研究試驗區有機碳儲量總體預測範圍。由預測限制區間圖顯示，高山地區相較於坡地與平原地區，具有較大的預測範圍 (平均 24.81 kg m^{-2})，代表其不確性度較高 (圖 9A)。不確定度高的原因為高山的採樣點較少 (圖 1E)，導致模型無法準確預測高山有機碳儲量分布情形；反之，淺山與平原地區，因為調查樣點較密集，因此模型預測的不確定度較低。由不確定度分析結果指出濁水溪流域表層土壤的預測範圍與誤差，該資訊除了提供模型的預測能力外，也可作為未來調查規劃的參考依據，進而提升模型的預測準確度與降低誤差。

結論

本研究利用數位土壤繪圖預測濁水溪流域表土 (0–30 cm) 與底土 (30–50 cm) 有機碳儲量，兩層土壤皆以 RK with Cubist 模型具有最好的預測能力 (表土 R^2 = 0.46、底土 R^2 = 0.48)，環境共變數中以土綱、高程及年均溫為重要的預測參數。於有機碳儲量預測圖顯示，濁水溪流域土壤有機碳儲量上游較下游高，主要是因為流域上游海拔高且溫度較低，土地覆蓋以不常變動的森林為主，利於土壤有機碳累積；流域下游處 (淺山坡地與平原) 則因高溫多雨，土地覆蓋又以頻繁耕犁的農業用地 (旱田、水田及果園) 為主，易導致土壤有機碳被分解，故有機碳儲量普遍較低。此外，本研究結果也指出表土碳儲量大於底土，經由數值計算得知表土與底土的有機碳儲量分別為 28.22 與 15.14 Tg。不確定度分析結果指出，高山地區由於樣點較少，模型預測的不確定度較高。

引用文獻

Adhikari, K., A. E. Hartemink, B. Minasny, R. Bou Kheir, M. B. Greven, and M. H. Greve. 2014. Digital mapping of soil organic carbon contents and stocks in Denmark. PloS One 9:e105519. doi:10.1371/journal.pone.0105519

Akpa, S. I. C., I. O. A. Odeh, T. F. A. Bishop, A. E. Hartemink, and I. Y. Amapu. 2016. Total soil organic carbon and carbon sequestration potential in Nigeria. Geoderma 271:202–215. doi:10.1016/j.geoderma.2016.02.021

Blake, G. R. and K. H. Hartge. 1986. Bulk density. p.363–375. *in*: Methods of Soil Analysis, Part 1: Physical and Mineralogical Methods. 2nd ed. (Klute, A. ed.) American Society of Agronomy, Soil Science Society of America. Madison, WI. 1188 pp.

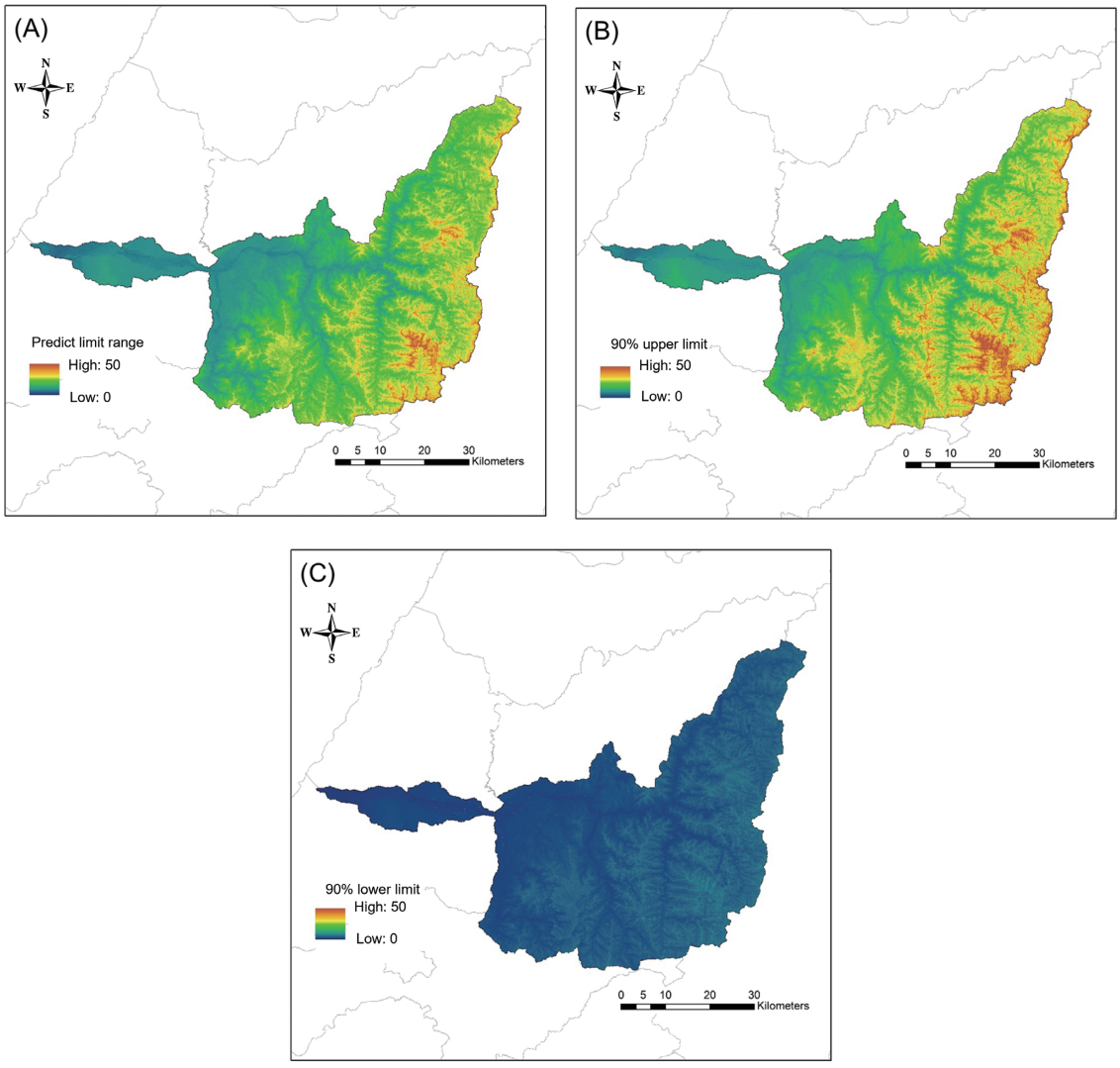

圖 9. 利用拔靴法產製之表土 (0–30 cm) 有機碳儲量 (A) 預測限制區間、(B) 90% 預測上限及 (C) 90% 預測下限圖。

Fig. 9. Topsoil (0–30 cm) soil organic carbon (SOC) stock maps of (A) prediction limit range, (B) 90% upper prediction limit and (C) 90% lower prediction limit derived using bootstrapping.

doi:10.2136/sssabookser5.1.2ed.c13

Breiman, L. 2001. Random forests. Mach. Learn. 45:5–32. doi:10.1023/A:1010933404324

Chen, S., M. P. Martin, N. P. A. Saby, C. Walter, D. A. Angers, and D. Arrouays. 2018. Fine resolution map of top- and subsoil carbon sequestration potential in France. Sci. Total Environ. 630:389–400. doi:10.1016/j.scitotenv.2018.02.209

Dorji, T., I. O. A. Odeh, D. J. Field, and I. C. Baillie. 2014. Digital soil mapping of soil organic carbon stocks under different land use and land cover types in montane ecosystems, Eastern Himalayas. For. Ecol. Manag. 318:91–102. doi:10.1016/j.foreco.2014.01.003

Edmondson, J. L., Z. G. Davies, S. A. McCormack, K. J. Gaston, and J. R. Leake. 2014. Land-cover effects on soil organic carbon stocks in a European city. Sci. Total Environ. 472:444–453. doi:10.1016/j.scitotenv.2013.11.025

Grace, J. 2004. Understanding and managing the global carbon cycle. J. Ecol. 92:189–202. doi:10.1111/j.0022-0477.2004.00874.x

Gray, J. M. and T. F. A. Bishop. 2016. Change in soil organic carbon stocks under 12 climate change projections over New South Wales, Australia. Soil Sci. Soc. Amer. J. 80:1296–1307. doi:10.2136/sssaj2016.02.0038

Grunwald, S. 2009. Multi-criteria characterization of recent digital soil mapping and modeling approaches. Geoderma 152:195–207. doi:10.1016/j.geoderma.2009.06.003

Guillaume, T., D. Makowski, Z. Libohova, L. Bragazza, F. Sallaku, and S. Sinaj. 2022. Soil organic carbon saturation in cropland-grassland systems: Storage potential and soil quality. Geoderma 406:115529. doi:10.1016/j.geoderma.2021.115529

Guo, P. T., M. F. Li, W. Luo, Q. F. Tang, Z. W. Liu, and Z. M. Lin. 2015. Digital mapping of soil organic matter for rubber plantation at regional scale: An application of random forest plus residuals kriging approach. Geoderma 237:49–59. doi:10.1016/j.geoderma.2014.08.009

Jenny, H. 1980. The Soil Resource: Origin and Behavior. Ecological Studies. Vol. 37. Springer. New York, NY. 377 pp. doi:10.1007/978-1-4612-6112-4

Jien, S. H., Z. Y. Hseu, H. Y. Guo, C. C. Tsai, and Z. S. Chen. 2010. Organic carbon storage and management strategies of the rural soils on the basis of soil information system in Taiwan. p.125–137. *in*: Proceedings of International Workshop on Evaluation and Sustainable Management of Soil Carbon Sequestration in Asian Countries. Bogor, Indonesia, September 28–29, 2010. (Chen, Z. S. and F. Agus, eds.) Food and Fertilizer Technology Center (FFTC) for the Asian and Pacific Region. Taipei, Taiwan.

Johnston, C. A., P. Groffman, D. D. Breshears, Z. G. Cardon, W. Currie, W. Emanuel, ... L. Wielopolski. 2004. Carbon cycling in soil. Front. Ecol. Environ. 2:522–528. doi:10.1890/1540-9295(2004)002[0522:CCIS]2.0.CO;2

Keskin, H. and S. Grunwald. 2018. Regression kriging as a workhorse in the digital soil mapper's toolbox. Geoderma 326:22–41. doi:10.1016/j.geoderma.2018.04.004

Lacoste, M., B. Minasny, A. McBratney, D. Michot, V. Viaud, and C. Walter. 2014. High resolution 3D mapping of soil organic carbon in a heterogeneous agricultural landscape. Geoderma 213:296–311. doi:10.1016/j.geoderma.2013.07.002

Lamichhane, S., L. Kumar, and B. Wilson. 2019. Digital soil mapping algorithms and covariates for soil organic carbon mapping and their implications: A review. Geoderma 352:395–413. doi:10.1016/j.geoderma.2019.05.031

Liu, Y., T. Ge, K. J. van Groenigen, Y. Yang, P. Wang, K. Cheng, ... Y. Kuzyakov. 2021. Rice paddy soils are a quantitatively important carbon store according to a global synthesis. Commun. Earth Environ. 2:154. doi:10.1038/s43247-021-00229-0

Ma, Y., B. Minasny, and C. Wu. 2017. Mapping key soil properties to support agricultural production in Eastern China. Geoderma Reg. 10:144–153. doi:10.1016/j.geodrs.2017.06.002

Malone, B. P., B. Minasny, N. P. Odgers, and A. B. McBratney. 2014. Using model averaging to combine soil property rasters from legacy soil maps and from point data. Geoderma 232:34–44. doi:10.1016/j.geoderma.2014.04.033

McBratney, A. B., M. L. M. Santos, and B. Minasny. 2003. On digital soil mapping. Geoderma 117:3–52. doi:10.1016/S0016-7061(03)00223-4

Meersmans, J., F. De Ridder, F. Canters, S. De Baets, and M. Van Molle. 2008. A multiple regression approach to assess the spatial distribution of Soil Organic Carbon (SOC) at the regional scale (Flanders, Belgium). Geoderma 143:1–13. doi:10.1016/j.geoderma.2007.08.025

Minasny, B. and A. B. McBratney. 2016. Digital soil mapping: A brief history and some lessons. Geoderma 264:301–311. doi:10.1016/j.geoderma.2015.07.017

Mulder, V. L., S. de Bruin, M. E. Schaepman, and T. R. Mayr. 2011. The use of remote sensing in soil and terrain mapping- A review. Geoderma 162:1–19. doi:10.1016/j.geoderma.2010.12.018

Nelson, D. W. and L. E. Sommers. 1983. Total carbon, organic carbon, and organic matter. p.539–579. *in*: Methods of Soil Analysis, Part 2: Chemical and Microbiological Properties. (Page, A. L, ed.) American Society of Agronomy, Soil Science Society of America. Madison, WI. 1159 pp. doi:10.2134/agronmonogr9.2.2ed.c29

Poggio, L., A. Gimona, I. Brown, and M. Castellazzi. 2010. Soil available water capacity interpolation and spatial uncertainty modelling at multiple geographical extents. Geoderma 160:175–188. doi:10.1016/j.geoderma.2010.09.015

Quinlan, J. R. 1992. Learning with continuous classes. p.343–348. *in*: Proceedings of the 5th Australian Joint Conference on Artificial Intelligence. (Adams, A. and L. Sterling, eds.) World Scientific. Singapore. 410 pp.

Rial, M., A. Martínez Cortizas, and L. Rodríguez-Lado. 2017. Understanding the spatial distribution of fac-

tors controlling topsoil organic carbon content in European soils. Sci. Total Environ. 609:1411–1422. doi:10.1016/j.scitotenv.2017.08.012

Rudiyanto, B. Minasny, B. I. Setiawan, S. K. Saptomo, and A. B. McBratney. 2018. Open digital mapping as a cost-effective method for mapping peat thickness and assessing the carbon stock of tropical peatlands. Geoderma 313:25–40. doi:10.1016/j.geoderma.2017.10.018

Scull, P., J. Franklin, O. A. Chadwick, and D. McArthur. 2003. Predictive soil mapping: A review. Prog. Phys. Geog. 27:171–197. doi:10.1191/0309133303pp366ra

Siewert, M. B. 2018. High-resolution digital mapping of soil organic carbon in permafrost terrain using machine learning: A case study in a sub-Arctic peatland environment. Biogeosciences 15:1663–1682. doi:10.5194/bg-15-1663-2018

Singh, B. P., R. Setia, M. Wiesmeier, and A. Kunhikrishnan. 2018. Agricultural management practices and soil organic carbon storage. p.207–244. *in*: Soil Carbon Storage: Modulators, Mechanisms and Modeling. (Singh, B. K., ed.) Academic Press. Cambridge, MA. 340 pp. doi:10.1016/B978-0-12-812766-7.00007-X

Tsai, C. C., Z. S. Chen, Z. Y. Hseu, C. T. Duh, and H. Y. Guo. 2010. Organic carbon storage and management strategies of the forest soils based on the Forest Soil Survey Database in Taiwan. p.85–102. *in*: Proceedings of International Workshop on Evaluation and Sustainable Management of Soil Carbon Sequestration in Asian Countries. Bogor, Indonesia, September 28–29, 2010. (Chen, Z. S. and F. Agus, eds.) Food and Fertilizer Technology Center (FFTC) for the Asian and Pacific Region. Taipei, Taiwan.

Tsai, C. C., T. E. Hu, K. C. Lin, and Z. S. Chen. 2009. Estimation of soil organic carbon stocks in plantation forest soils of Northern Taiwan. Taiwan J. For. Sci. 24:103–115. doi:10.7075/TJFS.200906.0103

Tsui, C. C., X. N. Liu, H. Y. Guo, and Z. S. Chen. 2016. Effect of sampling density on estimation of regional soil organic carbon stock for rural soils in Taiwan. p.35–53. *in*: Geospatial Technology-Environmental and Social Applications. (Imperatore, P. and A. Pepe, eds.) InTech. London, UK. 260 pp. doi:10.5772/64210

Tsui, C. C., C. C. Tsai, and Z. S. Chen. 2013. Soil organic carbon stocks in relation to elevation gradients in volcanic ash soils of Taiwan. Geoderma 209:119–127. doi:10.1016/j.geoderma.2013.06.013

Vaysse, K. and P. Lagacherie. 2015. Evaluating digital soil mapping approaches for mapping GlobalSoilMap soil properties from legacy data in Languedoc-Roussillon (France). Geoderma Reg. 4:20–30. doi:10.1016/j.geodrs.2014.11.003

Viaud, V., D. A. Angers, and C. Walter. 2010. Toward landscape-scale modeling of soil organic matter dynamics in agroecosystems. Soil Sci. Soc. Amer. J. 74:1847–1860. doi:10.2136/sssaj2009.0412

Wadoux, A. M. J. C., M. Román Dobarco, B. Malone, B. Minasny, A. B. McBratney, and R. Searle. 2023. Baseline high-resolution maps of organic carbon content in Australian soils. Sci. Data 10:181. doi:10.1038/s41597-023-02056-8

Wiesmeier, M., L. Urbanski, E. Hobley, B. Lang, M. von Lützow, E. Marin-Spiotta, ... I. Kögel-Knabner. 2019. Soil organic carbon storage as a key function of soils- A review of drivers and indicators at various scales. Geoderma 333:149–162. doi:10.1016/j.geoderma.2018.07.026

Xiong, X., S. Grunwald, D. B. Myers, J. Kim, W. G. Harris, and N. Bliznyuk. 2015. Assessing uncertainty in soil organic carbon modelling across a highly heterogeneous landscape. Geoderma 251–252:105–116. doi:10.1016/j.geoderma.2015.03.028

Yang, R. M., G. L. Zhang, F. Liu, Y. Y. Lu, F. Yang, F. Yang, ... D. C. Li. 2016. Comparison of boosted regression tree and random forest models for mapping topsoil organic carbon concentration in an alpine ecosystem. Ecol. Indic. 60:870–878. doi:10.1016/j.ecolind.2015.08.036

Zhu, Q. and H. S. Lin. 2010. Comparing ordinary kriging and regression kriging for soil properties in contrasting landscapes. Pedosphere 20:594–606. doi:10.1016/S1002-0160(10)60049-5

Using Digital Soil Mapping to Predict Soil Organic Carbon Stocks in Zhuoshui River Basin

Bo-Jiun Yang[1], Hsin-Ju Yang[1], Tsang-Sen Liu[2], Yi-Ting Zhang[3], and Chien-Hui Syu [3,*]

Abstract

Yang, B. J., H. J. Yang, T. S. Liu, Y. T. Zhang, and C. H. Syu. 2024. Using digital soil mapping to predict soil organic carbon stocks in Zhuoshui River basin. J. Taiwan Agric. Res. 73(2):135–151.

Soil carbon sink is the second-largest natural carbon sink globally, surpassed only by the ocean. Soil carbon sequestration is recognized as playing a crucial role in climate change adaptation and mitigation. Simultaneously, soil organic carbon (SOC) has positive effects on the physical, chemical, and biological properties of soil. Therefore, the development of accurate mapping techniques is essential for estimating SOC stocks and quantifying soil functions at a regional scale. The objective of this study is to apply digital soil mapping to estimate the SOC stocks in the surface soil (0–30 cm) and subsoil (30–50 cm) of the Zhuoshui River basin. This involves creating spatial distribution prediction maps and conducting uncertainty analysis. Additionally, the study also aims to compare the differences in soil carbon stocks under different topography and land cover. The results show that Regression Kriging (combined with Cubist) has the best predictive performance (surface soil: R^2 = 0.46; subsurface soil: R^2 = 0.48), with soil order, elevation, and mean annual temperature (MAT) identified as crucial environmental parameters for predicting SOC stocks in both layers. Uncertainty analysis indicates a higher prediction range in forested areas due to fewer soil survey points. In terms of different land cover types (forest, paddy, upland, orchard, other), the study reveals that the surface soil organic carbon stock is highest in mountainous forested areas (11.2 kg m^{-2}), while no significant differences are observed in subsoil among land cover types. According to the prediction results, the estimated organic carbon stocks in the surface and subsurface soils of the Zhuoshui River basin are approximately 28.22 and 15.14 million tons (Tg), respectively. The findings of this study can serve as a reference for soil carbon sink estimation, ecosystem services value assessment, and carbon-farming planning in the Zhuoshui River basin.

Key words: Soil organic carbon stocks, Digital soil mapping, Zhuoshui River basin, Machine learning.

Received: December 1, 2023; Accepted: March 12, 2024.
* Corresponding author, e-mail: chsyu@tari.gov.tw
[1] Project Assistants, Agricultural Chemistry Division, Taiwan Agricultural Research Institute, Taichung City, Taiwan, ROC.
[2] Research Fellow and Division Director, Agricultural Chemistry Division, Taiwan Agricultural Research Institute, Taichung City, Taiwan, ROC.
[3] Associate Research Fellows, Agricultural Chemistry Division, Taiwan Agricultural Research Institute, Taichung City, Taiwan, ROC.

Editorial Board

JOURNAL OF TAIWAN AGRICULTURAL RESEARCH

Vol. 73 No. 2 June 30, 2024

Published by Taiwan Agricultural Research Institute, Ministry of Agriculture

Publisher	Hsueh-Shih Lin
Editor-in-Chief	Hsien-Tzung Shih
Address	No.189, Zhongzheng Rd., Wufeng Dist., Taichung City 413008, Taiwan, ROC
Website	https://www.tari.gov.tw/jtar; E-mail: jtar@tari.gov.tw; Tel: +886-4-2331-7236
Submission	https://www.ipress.tw/J0042
	Complete instructions to authors are available on Journal of Taiwan Agricultural Research website: https://www.tari.gov.tw/jtar/
Press	Ainosco Press
Address	18F, No.80, Sec.1, Chenggong Rd., Yonghe Dist., New Taipei City 234634, Taiwan, ROC
Tel	+886-2-2926-6006
E-mail	press@airiti.com
Price	NT$ 175 (per copy)
Distributor	1. GB Books / 1F., No.209, Songjiang Rd., Taipei City 104472, Taiwan, ROC GB Website: http://www.govbooks.com.tw; Tel: +886-2-2518-0207 2. Wunan Books / No.6, Zhongshan Rd., Taichung City 400002, Taiwan, ROC; Tel: +886-4-2226-0330